UNIVERSITY *of the*
WESTERN CAPE

PETROPHYSICAL EVALUATION OF FOUR WELLS WITHIN CRETACEOUS GAS-BEARING SANDSTONE RESERVOIRS, IN BLOCK 4 AND 5 ORANGE BASIN, SOUTH AFRICA.

By

THIERRY KAMGANG

A Thesis submitted in partial fulfillment

For the Master degree in the faculty of science, Earth sciences Department,University of the Western Cape, Bellville, South Africa

Supervisor: Dr. Opuwari Mimonitu

Co-supervisor: Prof. Jan Van Bever Donker

ABSTRACT

Petrophysical evaluation of four wells within Cretaceous gas-bearing sandstone reservoirs in blocks 4 and 5 Orange Basin, South Africa.

Thierry Kamgang

The present research work evaluates the petrophysical characteristics of the Cretaceous gas-bearing sandstone units within Blocks 4 and 5 offshore South Africa. Data used to carry out this study include: wireline logs (LAS format), base maps, well completion reports, petrography reports, conventional core analysis report and tabulated interpretative age reports from four wells (O-A1, A-N1, P-A1 and P-F1). The zones of interest range between 1410.0m-4100.3m depending on the position of the wells.

The research work is carried out in two phases:

The first phase corresponds to the interpretation of reservoir lithologies based on wireline logs. This consists of evaluating the type of rocks (clean or tight sandstones) forming the reservoir intervals and their distribution in order to quantify gross zones, by relating the behavior of wireline logs signature based on horizontal routine. Extensively, a vertical routine is used to estimate their distribution by correlating the gamma-ray logs of the corresponding wells, but also to identify their depositional environments (shallow to deep marine).Sedlog software is used to digitize the results.

The second phase is conducted with the help of Interactive Petrophysics (version 4) software, and results to the evaluation of eight petrophysical parameters range as follow: effective porosity (4.3% - 25.4%), bulk volume of water (2.7% – 31.8%), irreducible water saturation (0.2%-8.8%), hydrocarbon saturation (9.9% - 43.9%), predicted permeability (0.09mD – 1.60mD), volume of shale (8.4% - 33.6%), porosity (5.5% - 26.2%) and water saturation (56.1% -

90.1%). Three predefined petrophysical properties (volume of shale, porosity and water saturation)are used for reservoir characterization. The volume of shale is estimated in all the wells using corrected Steiber method. The porosity is determined from the density logs using the appropriate equations in wells O-A1 and P-A1, while sonic model is applied in well A-N1 and neutron-density relationship in well P-F1. Formation water resistivity (Rw) is determined through the following equation: Rw = (Rmf × Rt) / Rxo, and water saturation is calculated based on Simandoux relation. Furthermore, a predicted permeability function is obtained from the crossplot of core porosity against core permeability, and it results match best with the core permeability of well O-A1. This equation is used to predict the permeability in the other wells.

The results obtained reveal that average volumes of shale decrease from the west of the field towards the east; while average porosities and water saturations increase from the south-west through the east despite the decreasing average water saturation in well P-A1.

A corroboration of reference physical properties selected for reservoir characterization, with predefined cut-off values result to no net pay zones identified within the reservoir intervals studied.

Consequently, it is suggested that further exploration prospects should be done between well O-A1 and A-N1.

Keywords: Orange Basin, petrophysical analysis, reservoir, wireline log, volume of shale, porosity, water saturation.

DECLARATION

I declare that *"Petrophysical evaluation of four wells within Cretaceous gas-bearing sandstone reservoirs in blocks 4 and 5 Orange Basin, South Africa"* is my own work, that it has not been submitted before for any degree or examination in any other University, and that all the sources I have used or quoted have been indicated and acknowledged by means of complete references.

THIERRY KAMGANG

_____

Signature March 2013

DEDICATION

This research project is dedicated to

The

ALMIGHTY GOD

For his limitless grace that was more than expected for me.

ACKNOLEDGMENTS

Several persons have contributed throughout the completion of this project and deserve particular attention.

To my supervisors, Dr. Opuwari Mimonitu and Prof. Jan Van Bever Donker, who were always available and grateful to respond my queries, even during weekends. You developed my knowledge of Interactive Petrophysics and guide me all the way from the beginning till the end of this project. I am deeply grateful for your time, your disposition and your care. You motivated me during critical stages of this study and I thank you a lot.

This research could not have been completed without the financial support of INKABA *ye* AFRICA, supervised by Professor Jan Van Bever Donker. I am really grateful for such an opportunity. I am also thankful to Petroleum Agency of South Africa for their professionalism in helping me choosing the right data and to Schlumberger for their technical support.

To the department of earth sciences, University of the Western Cape, Cape Town, South Africa. The Head of department Prof. Charles Okujeni, I would like to thank you for your professionalism and your support during my studies. To the department staff and fellow students Emmanuel, Achu, Chris, Eric, Stephane, Fadipe, Vala and James.

I am particularly grateful to my family, Mrs. Rosalie Wegang, Mrs. Marceline Boudjekeu, Mrs. Julienne Kamgang and Mrs. Jeannette Kamgang for all their prayers and financial support. All my other family members are equally gratefully acknowledged.

TABLE OF CONTENTS

LIST OF FIGURES

LIST OF TABLES

TABLE OF APPENDICES

CHAPTER 1: INTRODUCTION AND BASICS

1.1. Introduction

In recent years, discovery of new technology in petroleum exploration has caused enhancement of former non-economic fields. Current oil reserves are rapidly becoming depleted due to an increase in global demand for hydrocarbons as primary source of energy. This is a consequence of the fact that new petroleum plays are becoming increasingly complex, important and arduous to deal with. This state of affairs has prompted the oil industry to be very accurate, consistent and efficient to augment production from the estimated recoverable hydrocarbon reserves within minimal time.

In petroleum reservoir characterization, it is crucial to understand the mineralogy and the shape of the hydrocarbon-bearing rocks which are usually sandstones or fractured limestones. The importance of petrophysical studies is based on the need to evaluate porosity from the grain size of the rock, but also permeability from the throw thickness of sands and the clays contained within the rock. This is the case in Southern Africa where petrophysics are extensively used at the first stage of exploration, to predict physical properties of reservoir zones.

The Orange Basin in the south western margin of the Atlantic Ocean shows variable reservoir rock qualities (Macdonald et al., 2003). These Cretaceous (Barremian-Santonian) clastic sediments marked by regional unconformities 6At1-15At1 (Brown et al., 1996), have not been widely studied to ascertain the reasons for the variable reservoir qualities as reported by Macdonald et al. (2003). The southern section of the basin was characterized by drifting, and the resulting grabens were filled with predominantly siliciclastic rocks mixed with volcanic formations (Brown et al., 1996). In the basin, a total of 45 wells have been drilled with only one oil discovery and a number of gas discoveries to date (PASA, 2003a).

This study will be focused on evaluating the physical properties of sandstone rocks forming the shallow to deep water reservoirs within the Orange Basin, using petrophysical analysis.

1.2. Thesis outline

The thesis is organized as follows:

- Chapter one gives a general overview of the basics by presenting the framework, the aims, the objectives, and the methodology used to achieve this research.
- Chapter two deals with regional geology of the Orange Basin, outlining the stratigraphy of the successions wherein the petroleum systems are developed.
- Chapter three describes the basic formation evaluation concepts.
- Chapter four explains the lithology interpretation of reservoir zones based on wireline logs description. Furthermore, a basic analysis of their depositional environments is developed.
- Chapter five presents the results of petrophysical analysis carried out within the targeted reservoirs and comprises volume of shale, permeability, porosity, effective porosity, water saturation, hydrocarbon saturation, irreducible water saturation and bulk volume of water.
- Chapter six summarizes the main observations and interpretations made during the study, and gives a few recommendations for further exploration.

1.3. Objectives of the research

This research is aimed at exploring the petroleum resources within the sandstone units of Cretaceous age in the Orange Basin, utilizing the broad expertise of qualitative and quantitative interpretation of wireline logs.

Lithology interpretation aims to determine the reservoir rock type and the under petrophysical analysis through the shape of the wireline log curves.

Petrophysical evaluation aims to calculate the physical properties of reservoir rocks and their fluids content. It consists of formation evaluation and application of predefined cut-off values to selected reference parameters, which will lead to the identification of net pay zones.

Furthermore, the strategic aims of this research are:

- To correlate the studied wireline logs, for a better understanding of sandstone units distribution.
- To present comprehensive net pay zones of selected reservoir sands from petrophysical analysis.
- To give suggestions for further explorations.

Hence, this research project will be the first to evaluate the petrophysical properties of reservoir zones within wells O-A1, A-N1, P-A1 and P-F1 using wireline logs.

1.4. Scope of the work

The data set for this research are basically geophysical logs and technical reports. Interactive Petrophysics software is being used to process, analyze, interpret and model the available digitized data.

Data collected from Petroleum Agency of South Africa for this research work are:

- Base maps
- Geological well completion reports
- Well completion reports
- Petrography reports
- Digitized wireline logs
- Tabulated interpretative age reports.

The research starts with the review of previous work done in the field, followed by the geological background of the Orange basin. This gives an overview of sedimentology, structural evolution and petroleum system of the offshore fields in the West coast of South Africa.

The next step consists of analyzing and describing wireline logs for lithology and depositional environments interpretations. Subsequently, they are correlated to understand the distribution of reservoir rocks.

The final step focuses on the petrophysical evaluation of the reservoir zones, using Interactive Petrophysics software. Figure 1.2 gives a concise illustration of the steps taken in carrying out this study.

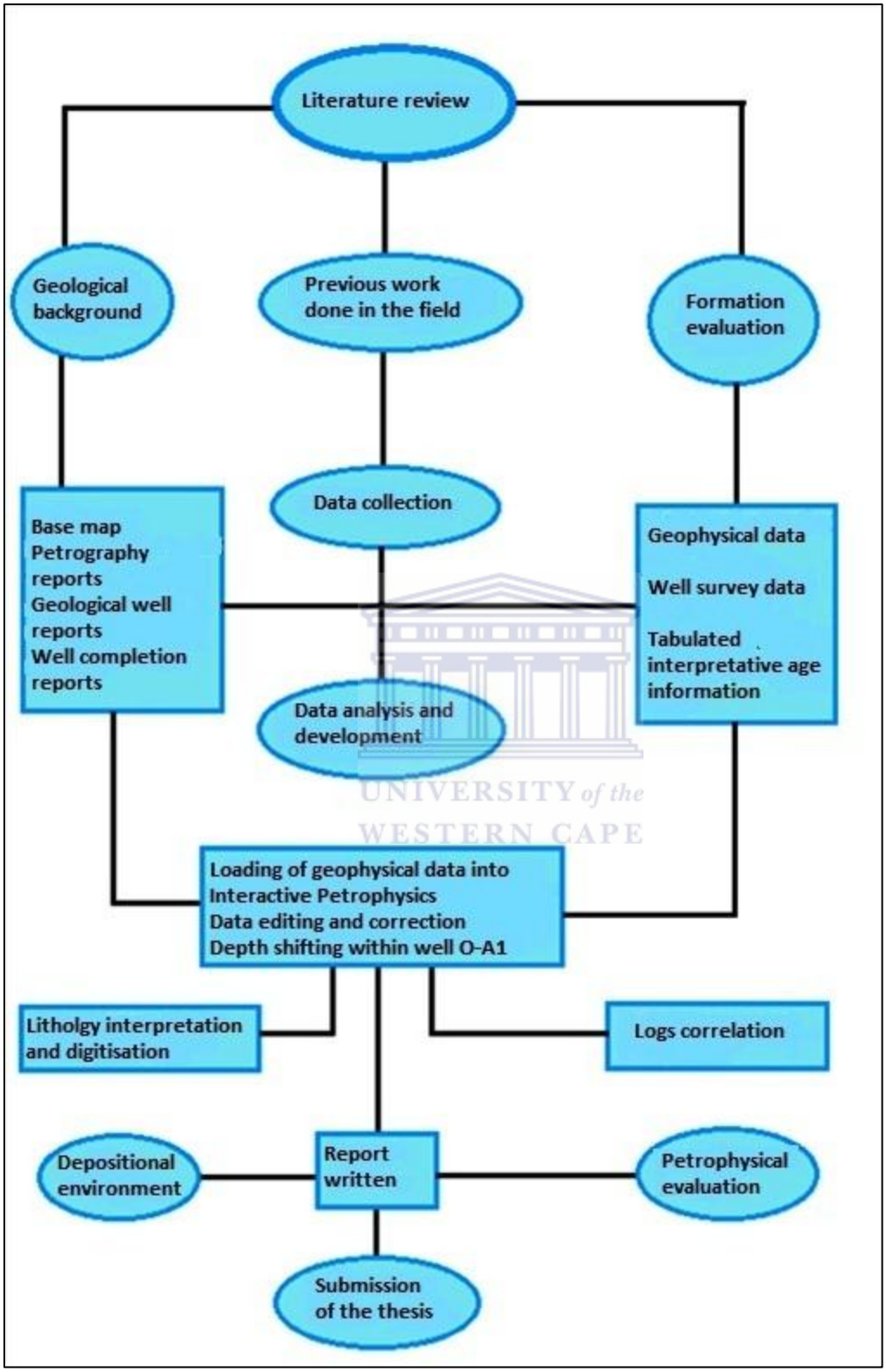

Figure 1.1: Chart flow of the thesis.

1.5. Study area

The Orange Basin is located offshore off the western coast of South Africa (figure 1.3), which underlies the Atlantic Ocean and extends 50 km offshore between Cape Town and the South Africa-Namibia coast border, with water depths that range between 200 m at the continental shelf to 2000 m in the deep marine environment (PASA, 2003a).

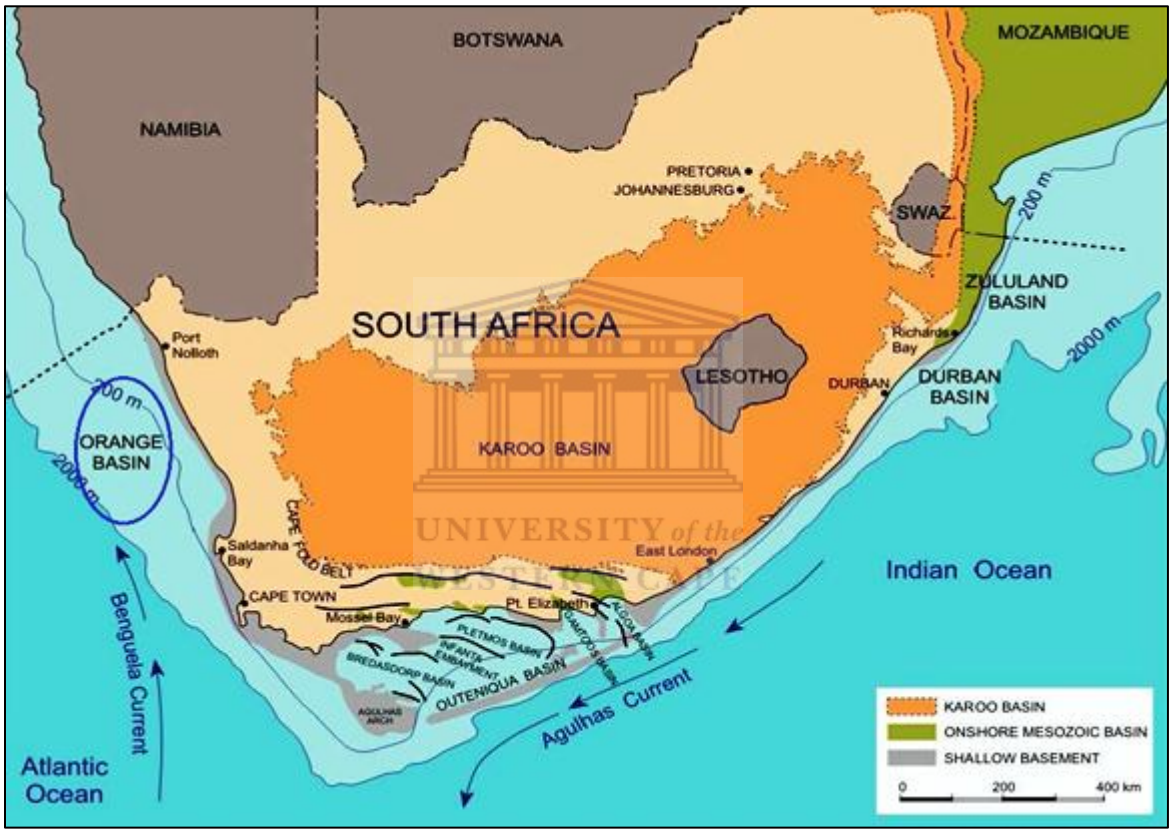

Figure 1.2: Location map of the Orange Basin (modified from PASA, 2003a).

It is a volcanic continental margin which covers an area of approximately 145 000 km^2, bounded to the North by the Kudu Arch and in the southwestern region by the Agulhas Columbine Arch. These arches are basement composed of volcanic, metamorphic and sedimentary rocks (De wit and Ransome 1992).

The basin is divided into:

- The northern Orange Basin that reaches the coast of Namibia and hosts the Kudu gas field.
- The southern Orange Basin along the Western coastline of South Africa which hosts the Ibhubesi gas field, area of interest (figure 1.4).

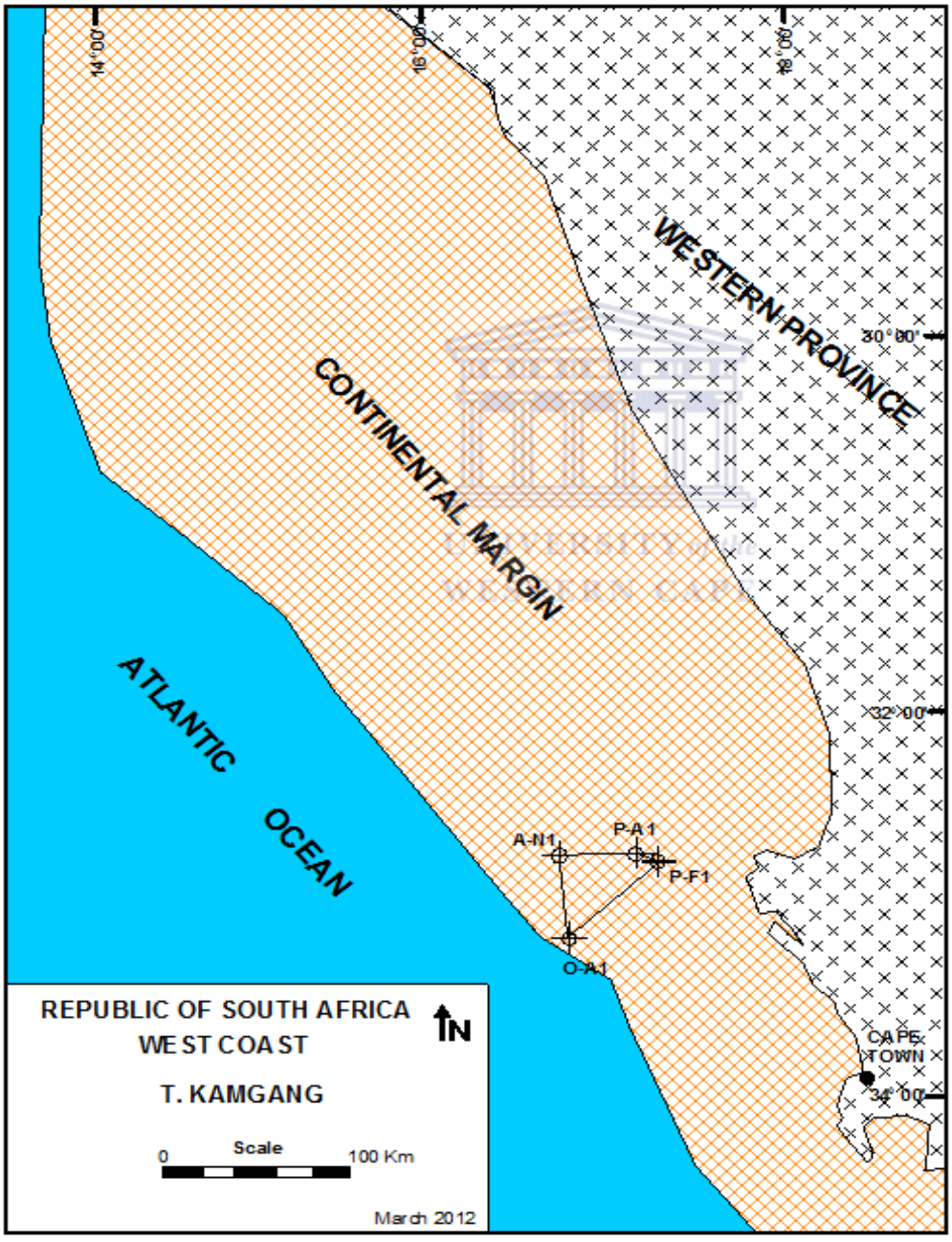

Figure 1.3: Location map showing the distribution of wells in this study.

The wells studied are located within blocks 4 and 5, and have not been extensively explored. This research will focus on wells A-N1, P-A1, P-F1 and O-A1. Table 1.1 below summarizes the geographical co-ordinate and wireline depths of the corresponding wells.

Table 1.1: Geographical co-ordinate of the wells.

Well names	Locations	Depths (m)
A-N1	Latitude: 32° 43' 27.00'' Longitude: 16° 47' 24.22''	3005
P-A1	Latitude: 32 ° 41' 21.88'' Longitude: 17 ° 13' 59.27''	3272
P-F1	Latitude: 32 ° 44' 52.38'' Longitude: 17 ° 24' 15.96''	1492
O-A1	Latitude: 33 ° 09' 40.64'' Longitude: 16 ° 49' 23.46''	4398

1.6. Previous work done on the orange basin

Various exploration techniques have been applied to understand hydrocarbon potential of reservoir rocks within the Orange Basin; nevertheless much work still needs to be done in terms of geology, stratigraphy, paleo-geography and structural features. Therefore, oil companies are encouraged to invest more on academic research to minimize expenses and numerical errors during oilfield appraisal.

Gerald and Smith (1982) delineated four major seismic sequence boundaries that range in age from Mesozoic to Cenozoic, using seismic and sequence stratigraphy concepts. From their interpretation, seismic horizon T was regarded as the rift-onset unconformity and horizon R as the drift-onset unconformity, with dipping reflections beneath it considered to be the boundary

between the continental shelf and the ocean floor. The P to L interval is formed by a thick sedimentary succession and encompasses a number of seismic sequences.

Muntingh and Brown (1993) reported on the lowstand petroleum plays and fairways within post-lower Aptian-Cretaceous deposits, underlying 90 000km^2 of the Orange Basin using the same concepts. They identified twenty-three fundamental third-order type 1 depositional sequences, and five composite third-order type 1 sequences comprising 12 fourth-order sequences which were provisional dated, correlated and mapped. They focused their interest on a lowstand system tract within highly progradational third-order sequence sets, because of its potential for supplying a large volume of reservoir-quality sands to basin-floor fans during lowstand fluvial entrenchment of the third order highstand fluvial/deltaic system; consequently it is likely to form the most favored petroleum play and fairways. It comprised a third order incised valley fill, deltaic prograding wedge and basin floor prospects which shifted far into the basin during progradational supercycles.

According to Brown et al. (1995), the initial definition of sequences in the Orange Basin was done using major unconformities as recognised on seismic sections and they were assigned numbers 1 to 22. This study was based on acoustic impedance contrast. The depositional system tracts exhibited distinct seismic expressions and were delineated using truncation and lap -out relationships.

Jikelo (1999) investigated the petroleum prospectivity of the deep-water Orange Basin, using 2D seismic data which allows a more complete understanding of the hydrocarbon potential of the area, and therefore predicted sandstone reservoirs in the Lower Cretaceous.

Based on multichannel seismic profiles, Ben-Avraham et al. (2002) detected a widespread occurrence of bottom simulating reflectors along the upper continental slope in the Southern periphery of the Orange River delta, probably indicating the presence of large quantities of gas hydrates in the area.

Macdonald et al. (2003) used new palinspatic paleofacies reconstructions of southwest Gondwana, to demonstrate that the regional hydrocarbon potential of the southern south Atlantic has been constrained by the tectonic evolution of the area.

Prospectivity of the Northern Orange Basin shows sediments ranging in age from the late Jurassic to the Hauterivian synrift graben fill, to drift sediments dating from the early Cretaceous to the present. Three major play types are present in the area: a rift play represented by possible lacustrine sandstones, trapping oil from organic rich claystones as encountered in the A-J graben to the South; a synrift play where sediments are pinching out against basement to the West of the hinge line; a drift play including the early Cretaceous Aeolian sandstones play, the Albian incised valley play and structural plays in younger shelf sediments, and deeper water plays comprising roll-over anticlines in growth fault zones and turbiditic fans (Van der Spuy, 2005).

Paton et al. (2007) demonstrated that the tectonic evolution of the Southern part of the Orange Basin margin has a significant effect on the hydrocarbon system of the area. They predicted that it increased the hydrocarbon potential of the area by integrating a seismic-stratigraphic investigation with a structural modeling of the field.

1.7. General overview of subsurface studies

Subsurface exploration has evolved tremendously over the years with the use of geophysical methods. For example, measurements within an acre are used to determine the physical properties that reflect the distinguishing characteristics of the local subsurface geology. Once these methods have been used to locate favourable geological conditions for likely hydrocarbon accumulation and thus possible reservoir zone, an exploratory well will be drilled through the prospective structure, to facilitate various techniques of evaluating the resources.

Most of the oil and gas that are currently produced come from hydrocarbon accumulations in the pore spaces of reservoir rocks such as sandstones, limestones or dolomites. In order to have an idea of the commerciality of a reservoir, some basic petrophysical parameters need to be generated. These include porosity, permeability, hydrocarbon saturation, thickness and areal

extent of the reservoir formation. These parameters can be derived or inferred primarily from electrical, nuclear and acoustic logs as well as other well data.

Well logging is the process of recording various physical, chemical, electrical or other properties of the rock/fluid mixture penetrated by drilling a well into the earth's crust (Crain, 2004).

The actual running of a log (figure 1.5) involves the tool on the end of the logging cable, the cable itself, and the surface electronics. A sensor and its associated electronics are housed in a sonde, which is suspended in the hole by an armoured electric cable. The sensor is separated from the virgin formation by drilling mud, mud-cake, and often an invaded zone in the formation. The signals from the sensor are conditioned by down-hole electronics for transmission up the cable to the surface electronics which in turn, conditions the signals for output and recording (Ellis and Singer, 2008).

As the cable is raised or lowered, it activates a depth measuring device which provides depth information to the surface electronics and recording device. The data is recorded on digital tape, film, and paper.

Petrophysics encompasses standard log analyses and various techniques of characterizing reservoir rocks through derivation of conventional reservoir parameters. In standard log analyses, large volumes of log data are reduced to more manageable results. Petrophysics is the most important and useful field of science available to a petroleum geologist.

Alongside field development from its initial discovery is generation of large volume of well log, seismic and production data. These are used to get an estimate of possible productive acres, which in combination with an estimated recovery factor will give an estimate of total recoverable oil in Barrel (bbl) and gas in Million Cubic Feet per Acre Foot (Mcf/acre-ft) from the reservoir if it happens that one exist.

In the early stages of planning exploration and development in a new area, surface seismic surveys are used extensively to delineate prospective structural or stratigraphic traps. Improvements in digital filtering have led to high quality results under favourable conditions.

When wells are drilled, opportunities exist to overcome the limitation in seismic data through the use of well logs in verifying reflection events in a seismic section and relating seismic features to geological structures.

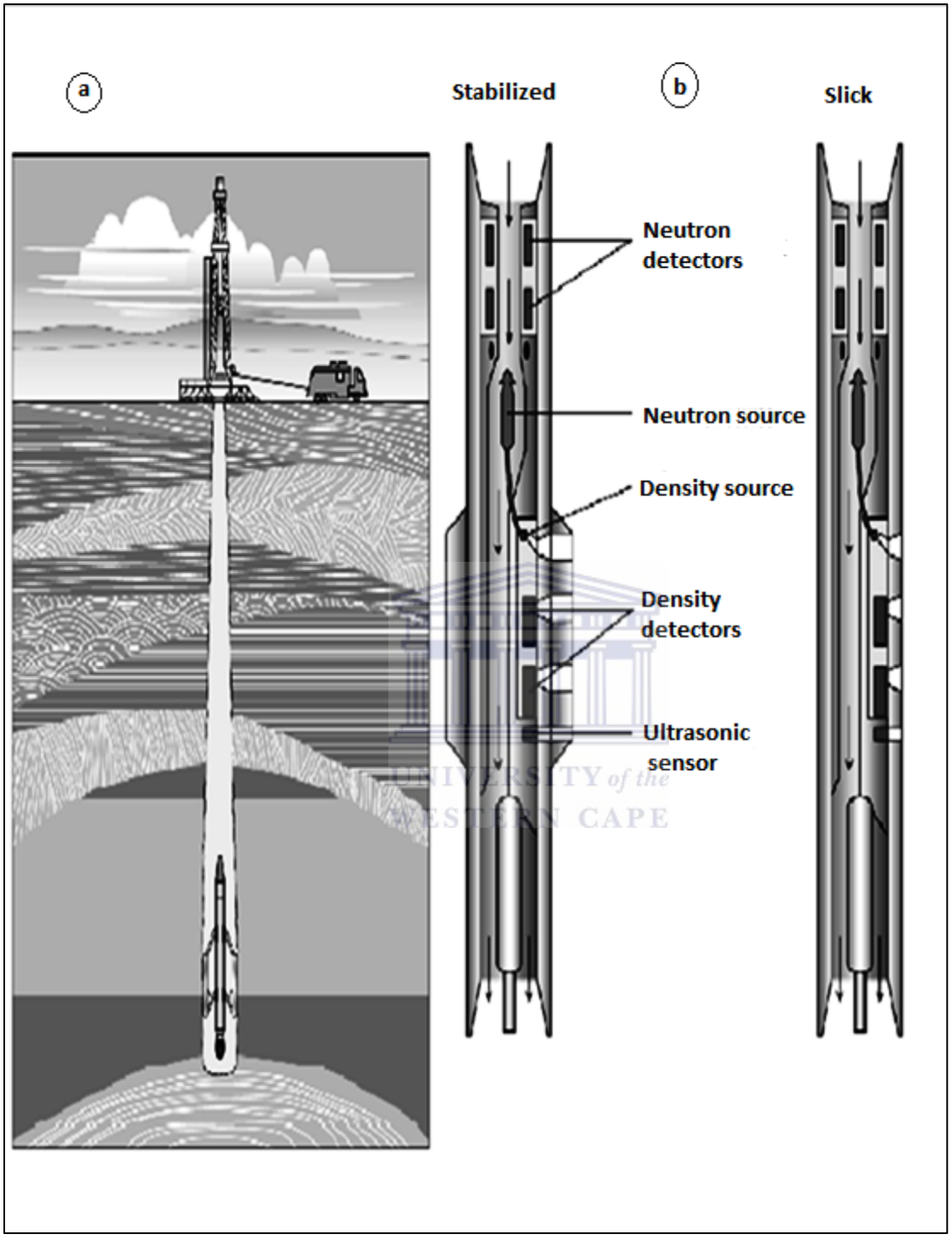

Figure 1.4.a: The elements of well logging: a measurement sonde in a borehole, the wireline and a mobile laboratory. b. An LWD device containing a neutron and density measurements (modified from Ellis and Singer, 2008).

CHAPTER 2: GEOLOGICAL BACKGROUND OF THE ORANGE BASIN

South Africa coastline has a total length of 3000 Km. It comprises the western coast, from the Orange River to Cape Point is about 900 Km long and the remainder from Cape Point further round the southern coast, up along the eastern coast through Durban and Zululand Basins, to the Mozambique border is more than 2000 Km (PASA, 2010).

Beyond the coastline is the continental shelf, where the wells selected for this work are located. It constitutes South Africa offshore environment and is 20-160 Km wide off the west coast, 50-200 Km wide off the south coast, but less than 30 Km wide off the east coast, except along the Durban Basin. As defines by figure 2.1, the continental slope connects the shelf area with the deep marine environment. It follows a similar trend in width and fairly wide on the west and south coasts but become narrower to the eastern coast.

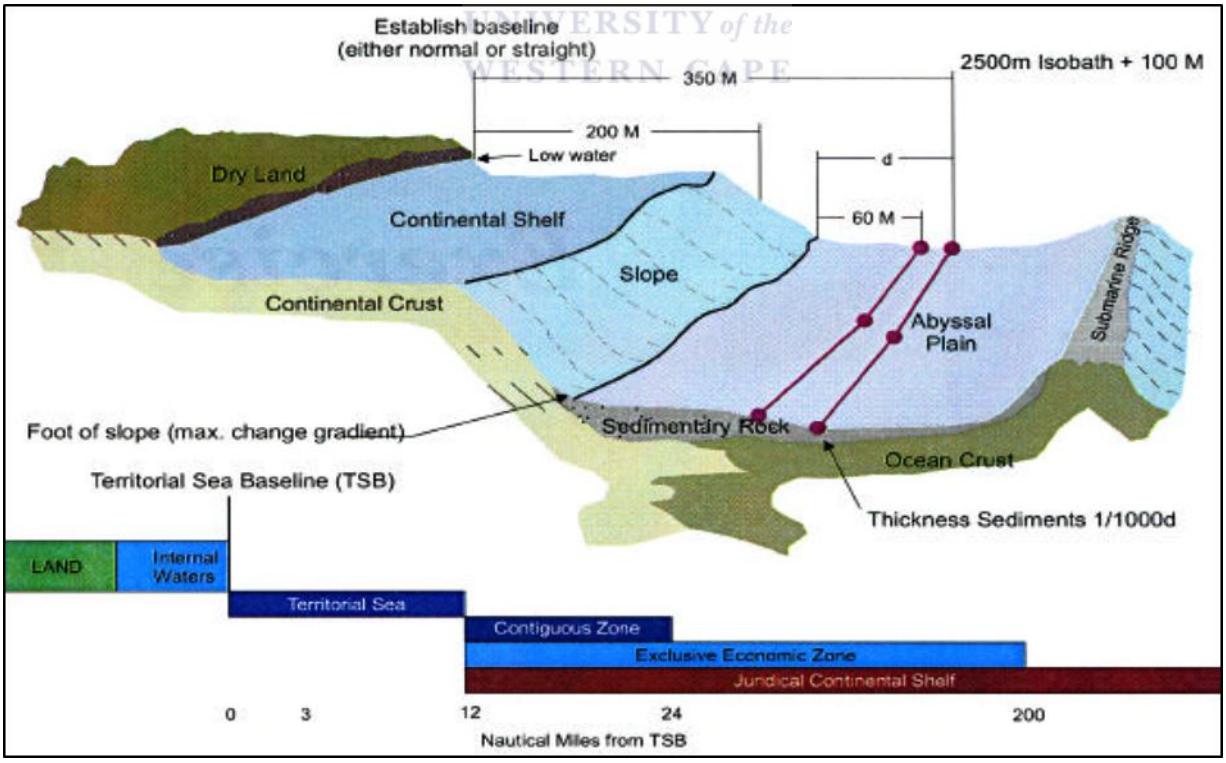

Figure 2.1: South Africa continental margin and crust (modified from Broad, 2004).

2.1. Tectonic setting of the orange basin

The Orange Basin results from the breakup of the Gondwana during the Late Jurassic-Early Cretaceous, followed by a succession of rifting and drifting apart of the African and South-American plates. Before this major geological event, some tectonic activities were emplaced along this area, leading to the development of the Kalahari shield approximately 1Ga ago when ocean-like crust was formed over the Kaapvaal Craton. Likewise, a large network of Proterozoic to early Paleozoic Belts established ensuing through the Damara Orogeny, and part of it evolves to the Saldanha belts in South Africa (Hirsch et al., 2010).

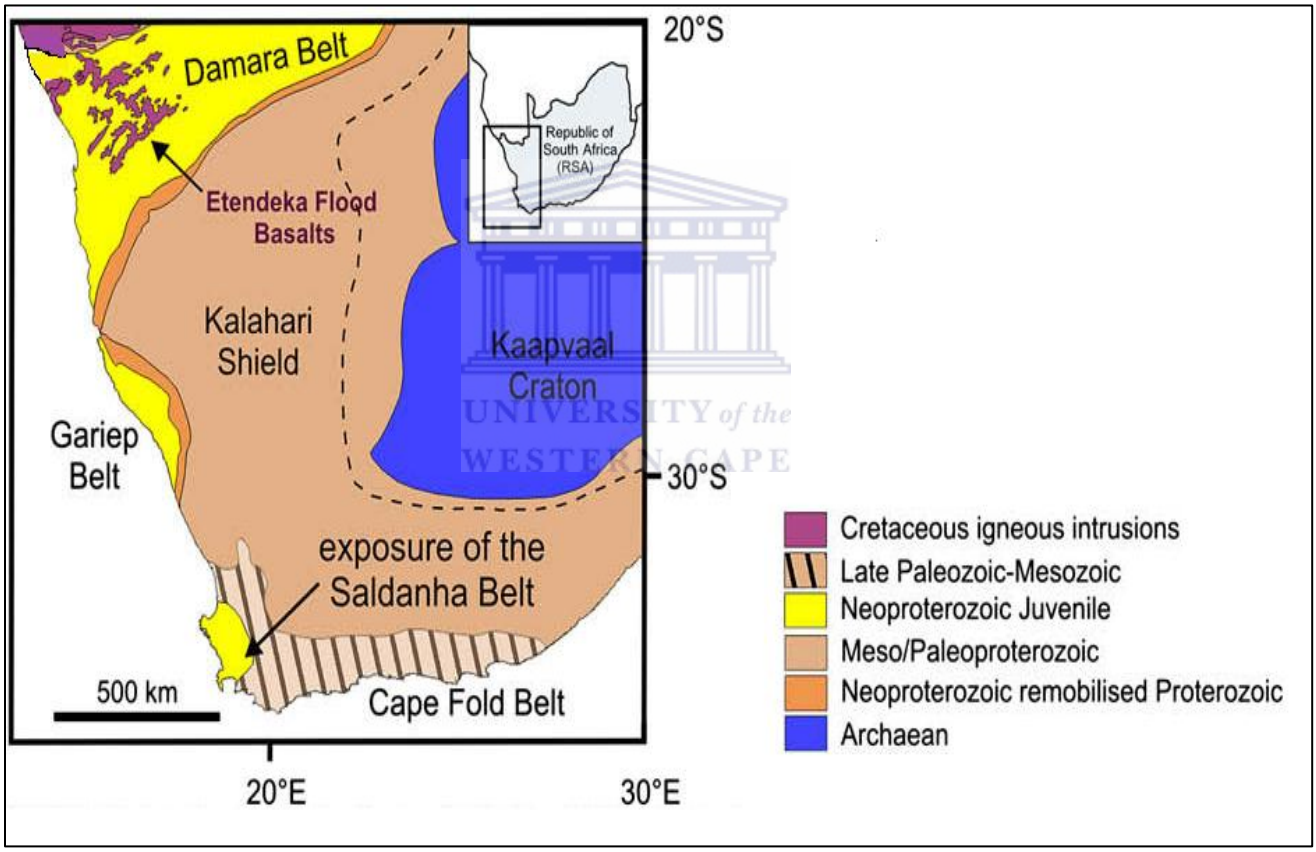

Figure 2.2: Geological map of the southwest Africa (modified after De wit and Stankiewitz, 2007).

The Orange Basin underwent two phases of synrift which were part of the Gondowana breakup:

- The first phase involved normal faulting during initial rifting of the Atlantic margin. These faults show progressive rotation and displacement through time and produce typical half-graben structures (figure 2.3), with the rift depositional section progressively on-lapping his basement towards the rift hinge (PetroSA Report, 2003).

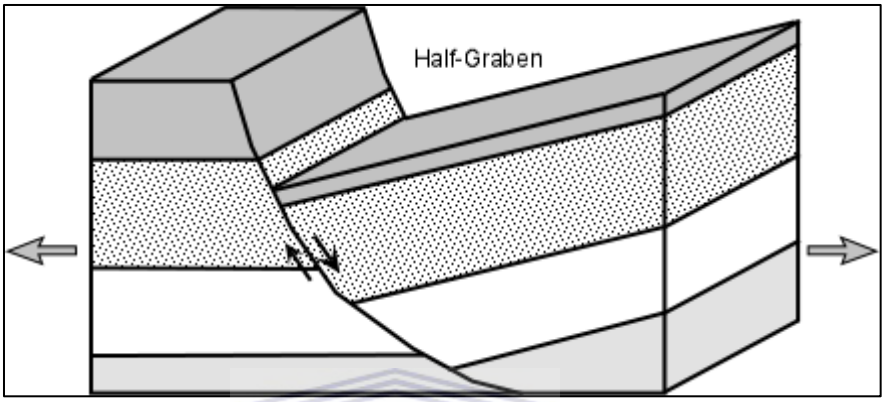

Figure 2.3: Formation of a half-graben (after Leeder and Gawthorpe, 1987).

- The second episode of deformation was driven by extension of drift phase sediments across the shelf. PASA (2008) has delineated two types of drifting on seismic.
    - Basement involved normal faults predominantly active during Aptian-Late Paleogene.
    - Neogene to recent gravity driven detachment faults, which are largely super-imposed on earlier rift faults.

New higher angle faults are also observed within detachement faults. They result from the thermal subsidence of the cold brittle transitional crust. They also extend the Upper Mesozoic-Lower Paleogene with a relatively constant displacement, with offset decreasing in the Upper Paleogene section. However, faults associated with the western flank of the main rift graben show Neogene reactivation and displacement.

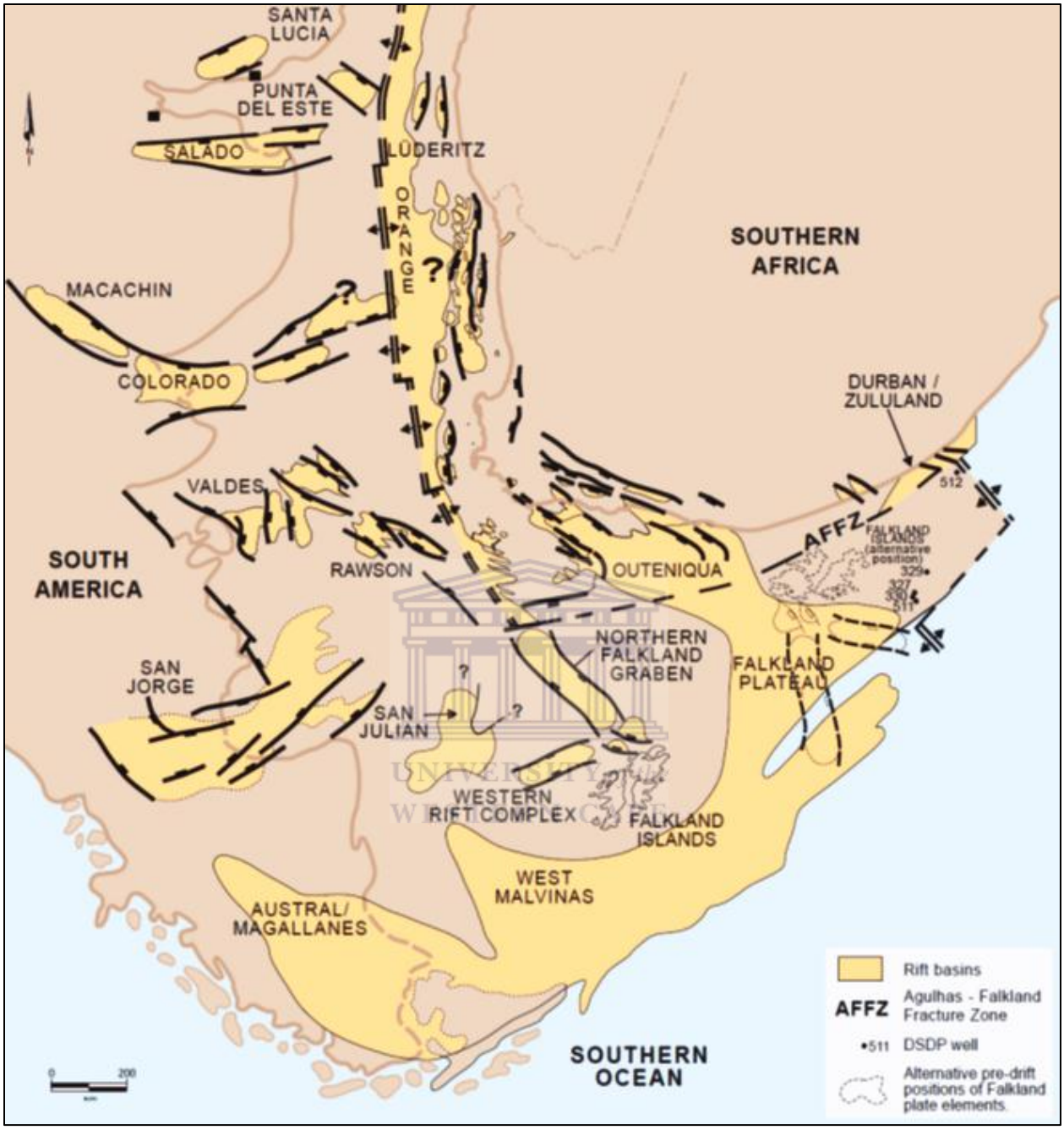

Figure 2.4: Pre-breakup distribution of rift Basins within southwest Gondwana (after Jungslager, 1999).

2.2. Regional geology of the Orange Basin

The Orange Basin offshore southwest Africa is located within the passive continental margin (Jungslager, 1999) of the South Atlantic Ocean between 31^{o} and 33.3^{o} latitude. It is areally and volumetrically the largest of South Africa's offshore Basins, but is relatively unexplored with one well per 4000 Km^2 (PASA, 2006).

The sedimentary system to the Basin was obtained from the Orange River drainage system, with a rivaling delta to the North of the Basin. However, the Olifant and Berg River systems have also contributed to the sedimentation of the Basin; although their influence is confined to the South (PASA, 2007). The underlying synrift succession comprises generally isolated, truncated remnants of half-graben to the east of the medial hinge (figure 2.5). Sedimentary rocks maybe as old as Jurassic but the oldest dated sediments are back to Hauterivian in the Basin. All the penetrated sediments are from the continent and are embedded with igneous lithologies. Along the west side, subareal flood-basalts thought to have poured rapidly onto the attenuated continental crust during the closing of the active rifting phase (figure 2.2). These coeval basalts are interbedded with continental to shallow marine sediments mostly found in the transgressive ramp-like succession. Therefore, the western margin is for the divergent volcanic type (PASA, 2010).

The Orange Basin is one of the few examples where margin deformation mechanisms were not active throughout most of the Basin history (Hirsch et al. 2010). However, the margin was divided into a number of crustal segments, with the southern segment probably of the rifted margin type (figure 2.4). Rather than be a strictly structurally confined area, Orange Basin is defined by the extend and thickness of post-rift sedimentary siliciclastic successions deposited during the Cretaceous, and progressively ranging from continental in the east to deep marine in the west (PASA, 2007).

The Tertiary succession mainly comprised calcareous oozes and chemical sediments. The wedge of drift sediments underwent repeated deformation of the paleo-shelf edges and paleo-slopes

due to sediment loading and slope instability, especially during Early Cretaceous. The shelfal portion of the drift succession is largely unstructured because most of the sedimentary

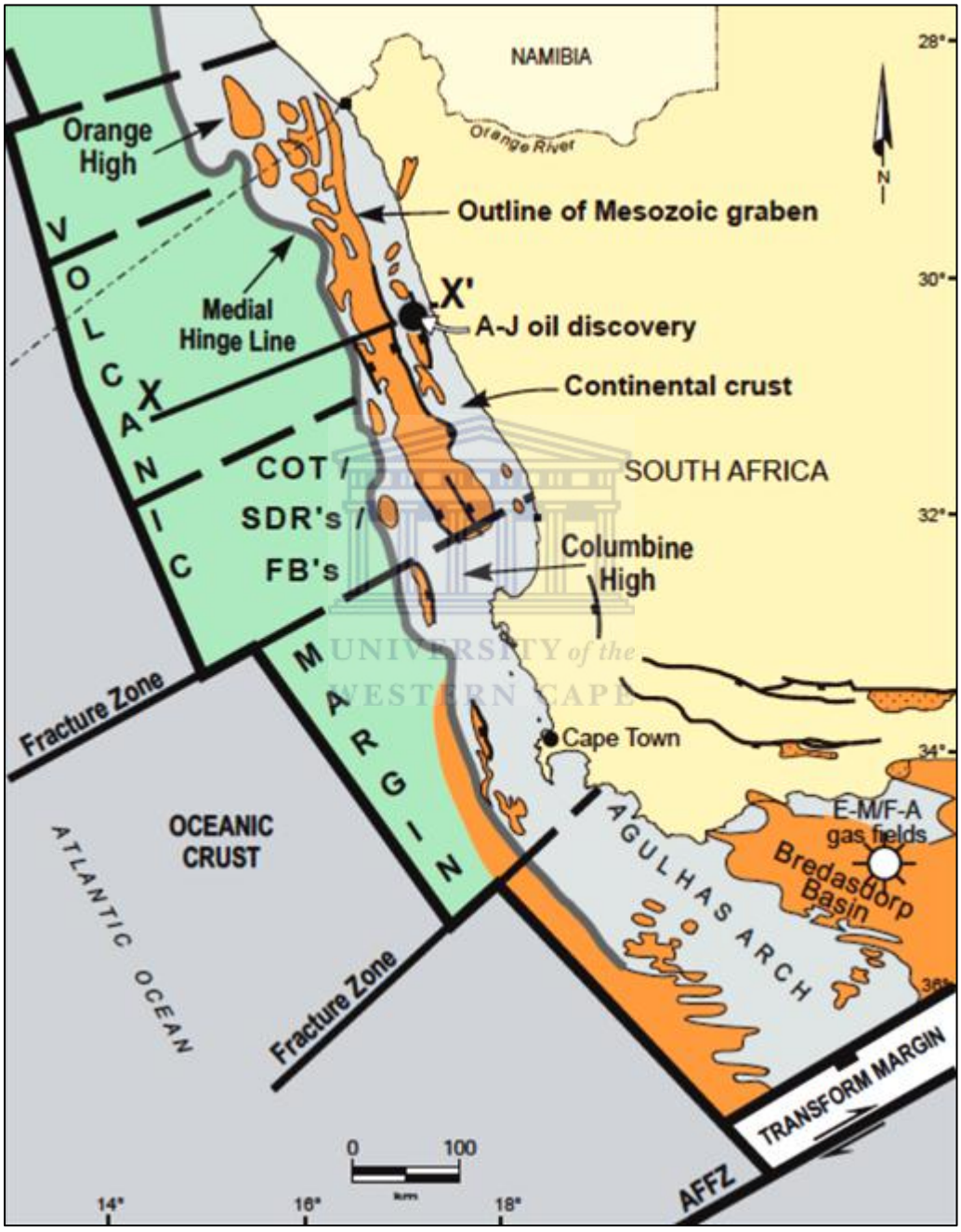

Figure 2.5:Major tectonics elements and crustal segments of the rifted volcanic margin (after Jungslager, 1999).

tectonic features comprise extensional gravity faults and folds up-dip, compressional toe-thrust faults and folds down-dip, detachement glide plane in overpressured shales (PASA 2006).

2.3. Sequence stratigraphy

2.3.1. Overview of the fundamentals of sequence stratigraphy

Sequence stratigraphy is the study of genetically related facies within a framework of chronostratigraphycally significant surfaces (Van Wagoner et al., 1990). It is a concept that integrates geological time with the vertical and lateral variations of sedimentary successions in terms of relative seal level changes.

According to Vail et al., (1977) a sequence is the fundamental stratal unit of sequence stratigraphy. It is composed of a succession of system tracts and is interpreted to be deposited between eustatic fall inflection points. Furthermore, the sequence of strata is also deposited under the same regime of sediment input and dispersal, its boundary representing a geometrically manifested change in the pattern of sedimentation (Schlager, 1992).

In a vertical succession, a sequence (figure 2.6.a) is arranged in the following order: sequence boundary (SB), lowstand systems tract (LST), transgressive surface (TS), transgressive systems tract (TST), maximum flooding surface (MFS) and highstand systems tract (HST).

- **Sequence boundary (SB)**

A sequence boundary defines the beginning and the end of a depositional sequence. It can be identified as significant erosional unconformity and its correlative conformities. It is the product of a fall in sea level that erodes the sub-aerially exposed sediment surface of the earlier sequence. According to Catuneanu (2002), a sequence boundary is diachronous because it caps the previous highstand systems tracts and erodes the surface of the downstepping sediments which are usually deposited in coarsening-up, prograding shoreline successions of the so-called regression.

❖ Lowstand systems tract (LST)

The lowstand systems tract represents sediments deposited after the onset of relative sea-level rise. It develops above the formation of a sequence boundary and because of relatively limited shallow water area available for sedimentation; sediment production is reduced on rimmed shelves.

When the sea-level falls sufficiently and a distinct shelf-slope break exists, lowstand systems tract comprised two distinct parts:

- The lowstand wedge which consists of progradational set of parasequences shaped out from the pre-existing continental slope. The slow rise in sea level subsequent to its fall and the production of a sequence boundary brings in a slow rate of accommodation coupled with a comparatively high supply of sediments and, results in the progradational stacking of the sediment typically of lowstand wedge.
- The lowstand fan represents a basin-floor submarine fan which typically displays aggradational stacking and is overlain by the lowstand wedge. The river incises into the exposed shelf during the time of the lowest relative sea level and sediments get shunted directly off the shelf edge to feed submarine fans.

When the system lacks a distinct shelf-slope break and the sea level does not fall sufficiently, only a lowstand wedge may form.

❖ Transgressive surface (TS)

The transgressive surface is the first marine flooding surface following maximum regression and in shallower areas of the shelf, where it is associated with erosion and marks the passage from non-marine to marine sedimentation (Nummedal and Swift, 1987). It separates the underlying lowstand systems tract from the overlying transgressive systems tract. Sediments resulting from transgressive surface erosion are mostly lags, minerals, especially glauconite concentrations and cementation of the underlying surface (Baum and Vail, 1988).

❖ Transgressive systems tract (TST)

This systems tract lies directly on the transgressive surface and is overlain by the maximum flooding surface (figure 2.6.b). It is made up of retrogradational sets of parasequences and comprises deposits that accumulated from the onset of coastal transgression, until the time of maximum transgression of the coast just prior to the renewed regression of the highstand systems tract. However, in case where there is high sediment supply the parasequences maybe aggradational.

❖ Maximum flooding surface (MFS)

It is a marine flooding surface that separates the underlying transgressive systems tract from the overlying highstand systems tract. The surface marks the deepest water facies within a sequence and commonly represents a change from retrogradational to progradational parasequences. The process of deposition in this surface is slow and may displays evidence of condensation, which will result to abundant burrowing, hardgrounds and fossils accumulation.

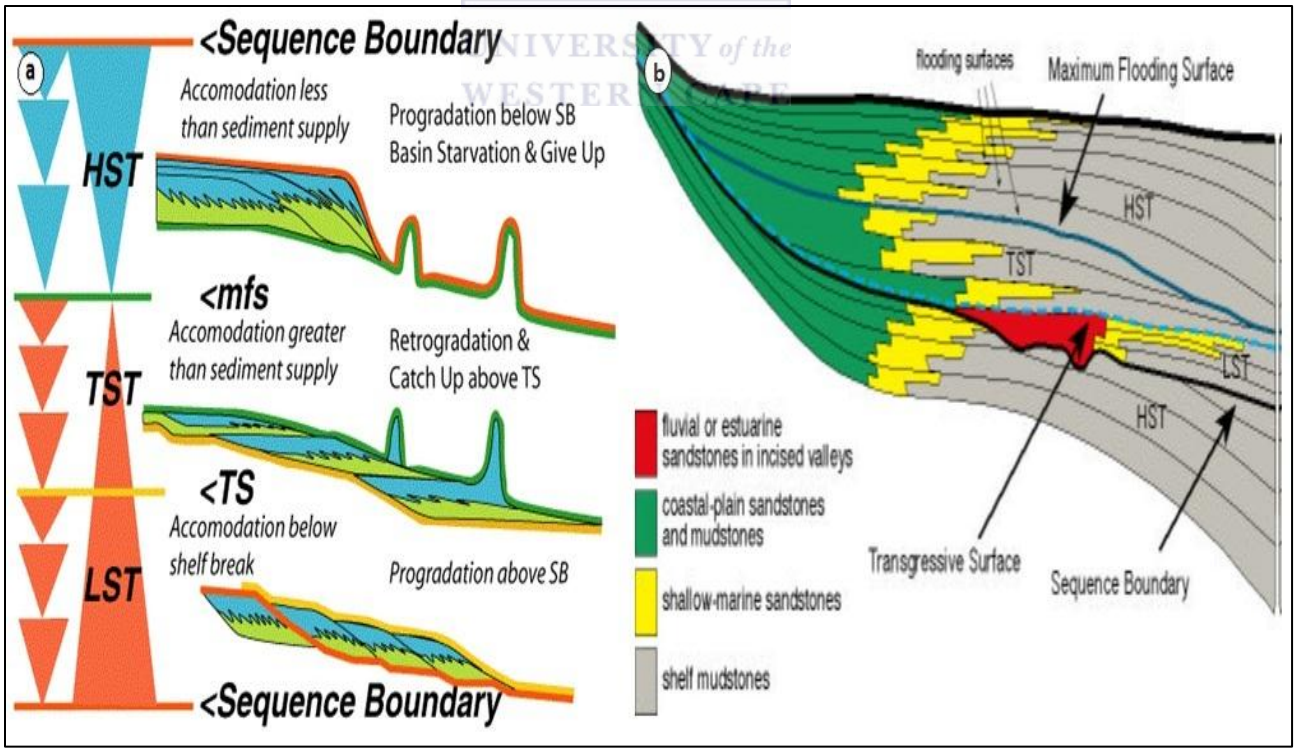

Figure 2.2.a.: Illustration of different depositional systems tracts. b. Sequence systems tracts (modified from Van Wagoner et al. 1990).

❖ Highstand systems tract (HST)

A highstand systems tract constitutes the upper systems tract of a sequence stratigraphy and overlies the maximum flooding surface. It consists of aggradational to progradational set of parasequences stacking patterns thinning upward, and is terminated at the top by the next sequence boundary.

2.3.2. Tectonic Evolution of the Orange Basin

The presence of major deltaic depocentres found to the mouth of the Orange and Olifant Rivers is tangible evidence that they are sediment providers of the Orange Basin (Dingle et al., 1983). However, the Olifant River only contributed to filling the Basin and for approximately 13.5 Ma (Brown et al., 1995), after which the Orange River stayed the sole provider (Van der Spuy, 2003).

Four main depositional events are observable along the sequence stratigraphic framework of the Orange Basin (figure 2.7):

- The pre-rift phase constituted of basement rocks of Pre-Jurassic age, comprises high to low grade metamorphites in the southern part, granitic plutons and alkaline intrusive towards the north (Broad et al., 2006). It may also include possible Karoo, Cape, Nama and Mamelsbury rocks.
- The Pre-Barremian synrift phase has overlain and formed a hinge line towards the basement. It is composed of synrift I containing volcanic and alluvial rocks followed by the synrift II with volcanic, alluvial and lagoonal rocks.
- The Transitional phase overlies the Pre-Barremian synrift phase and represents the first marine incursions. It was buildup by flood basalts covered by alternating fluvial and marine deposits, resulting from successive transgression and regression of the sea-level.
- Finally, the drifting phase was developed between the Early Aptian and the present, and can be subdivide in three depositional episodes (figure 2.7):
    - Early Aptian-Late Cenomanian was a period of important sedimentation. The Basin underwent a regional drowning and a thermal subsidence or eustatic

effects. Sediments deposited during this episode are formed by continental red beds occasionally interbedded with organic rich shales, and fluvio-deltaic sandstones.

- Cenomanian-Turonian period corresponds to an aggradational deposition which dominated a short progradational parasequence.

The last depositional episode represents a succession of organic and chemical sediments containing terrigenous materials.

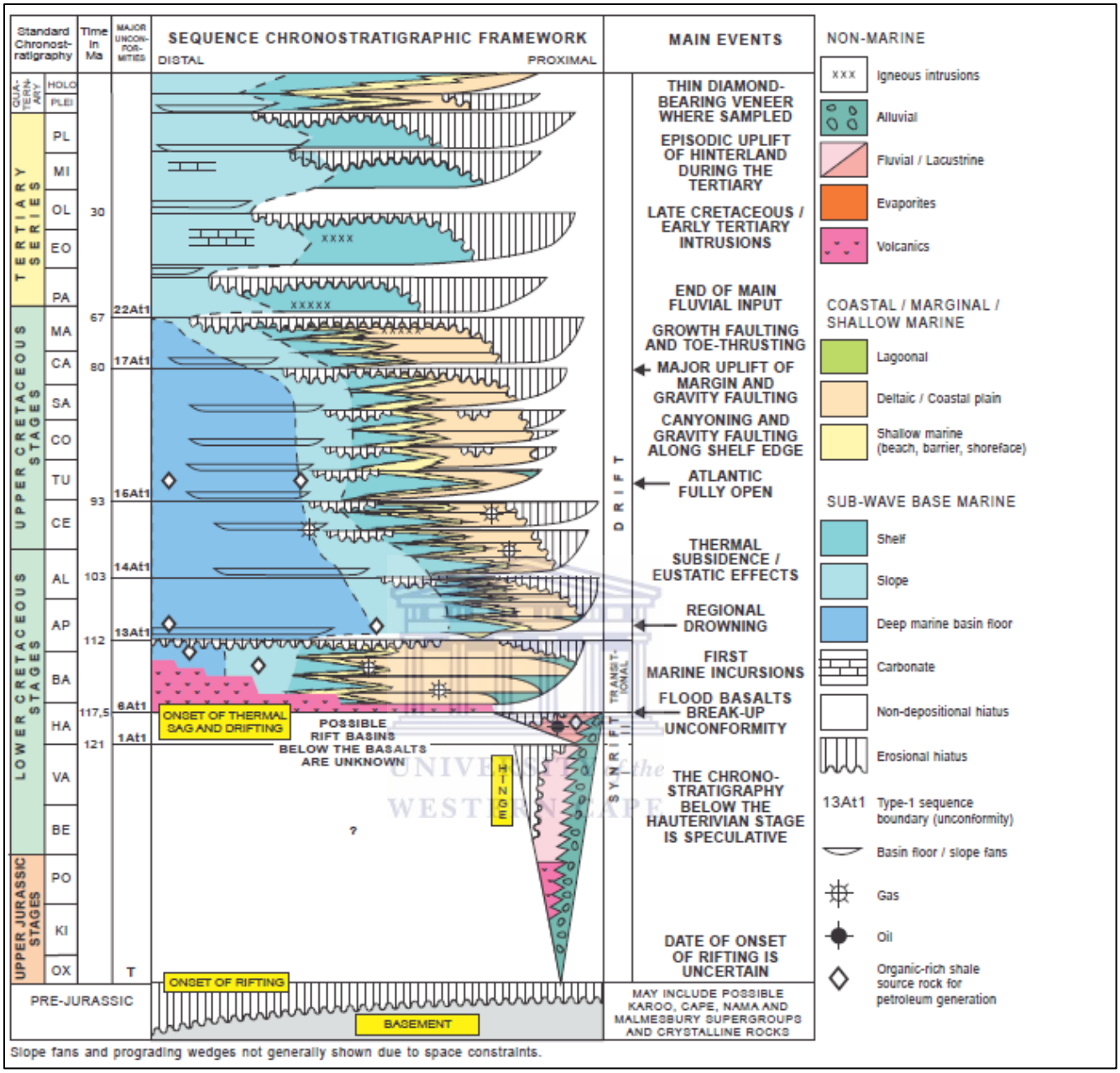

Figure 2.3: Sequence stratigraphic framework of the Orange Basin (PetroSA Report, 2003).

These geological events were marked by majors second order tectonically enhanced sequence boundaries, which indicated the end of each sequence stratigraphy within the basin (figure 2.7).

2.4. Petroleum system

2.4.1. Basics

A petroleum system is a dynamic petroleum generating and concentrating physiochemical system, functioning in a geologic space and time scale (Demaison and Huizinga, 1994). It requires the timely convergence of certain geologic elements and events essential to the formation of petroleum deposits:

- Mature and organic-rich source rocks.
- Porous and permeable reservoir rocks to store the accumulated oil and gas.
- A system of retention composed of trap and seal, to prevent oil and gas from leaking away.

❖ **Source rock**

A source rock is a fine-grained sediment containing an important amount of organic matter, which has generated and released enough hydrocarbons to form commercial accumulation of petroleum.

The formation of a good oil and gas source rock depends of sufficient biological productivity to create organic matter, and suitable depositional conditions and preservations. Therefore, the quality of petroleum generated will be determined by the maturity of sediments or kerogen type.

Common petroleum source rocks are shales and carbonate muds.

❖ **Reservoir rock**

It is a porous and permeable rock capable of bearing commercial accumulation of oil and gas. Reservoir rocks are commonly coarse-grained sandstones, but they can also be fractured fine-grained rocks (shales, limestones, dolomites).

❖ Trap

A trap is any geometric arrangement of rock that prevents migration of hydrocarbons. It must include a reservoir rock in which to store oil and gas, and a seal or set of seals that impede or stop petroleum leakage.

Different types of traps exist:

- Structural traps such as anticlines and faults, formed by the formation of rock layer. This type of trap is usually associated with the shifting of fault layers along the fault plane.
- Stratigraphic traps such as pinch-out are formed when a reservoir rock is cut-off by a horizontal layer of impermeable rock.
- A combination of structural and stratigraphic traps.

2.4.2. Petroleum system of the Orange Basin

The Orange Basin is one of the most underexplored passive margins in the world with 160 000 km^2 acre to the 2000m isobaths, for 47 wells drilled to date (PASA 2004). More than 75% of the prospective area is in water depths lower than 500m. However, these explorations have led to the discovery of two important gas fields (Kudu and Ibhubesi) and one oilfield.

❖ Source rocks

Source rocks in the Orange Basin are mostly located in shaly Cretaceous formations (figure 2.7). The productivity of shales is very low because of the high amount of muds which absorb most of the oil released, and the generation of gas prone is due to the dominance of woody organic matter.

❖ Reservoir rocks

Reservoir rocks are formed by fluvio-deltaic and lacustrine sandstones interbedded with conglomerates in the shelf deposited during the Early Cretaceous, while deep marine sandstones were formed during the post-rift succession (figure 2.8). The main oil-bearing reservoir is located within the Albian successions. It consists of thick and thin-bedded clay-silt and sand (3m-70m) sequences with the occurrence of thin and shaly beds. Gas reservoirs within

Albian successions are characterized by an association of coarsening upward, laminated and bioturbated mudstones to massive planar cross-bedded sandstones (Muntingh, 1993).

❖ Traps

According to Broad and Mills (1993), both structural and stratigraphic traps are encountered in the Basin. Pinchout and dome define stratigraphic traps while fault closures are structural traps.

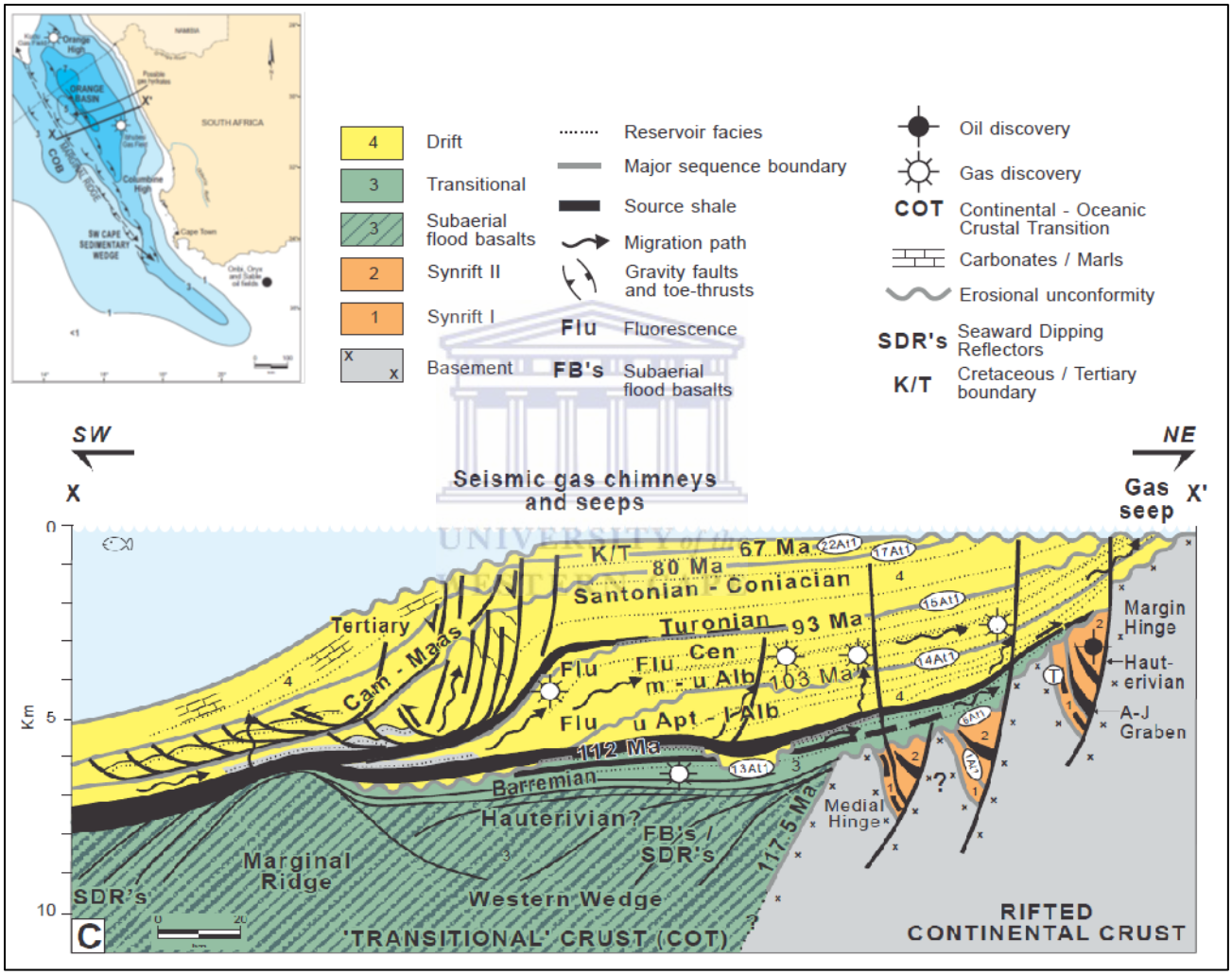

Figure 2.4: Schematic geological profile along the central Orange Basin (modified after Jungslager, 1999).

CHAPTER 3: FORMATION EVALUATION

In petrophysical studies, a formation refers to a stratigraphic unit of rocks generally deposited in the same environment, consisting of sedimentary strata usually of internal lithologic homogeneity and distinguish characteristic, in term of chemical composition and favorable physical properties (porosity and permeability) capable of bearing hydrocarbon in commercial quantity.

Nowadays, formation evaluation commonly known as reservoir characterization involves various techniques of analyzing and determining physical properties of the petroleum reservoir. Modern advances in seismic acquisition, processing and interpretation with powerful computer modeling software have significantly increased oil discovery and production.

Some of the useful tools in petroleum exploration including core samples and geophysical well logs will be described in this chapter.

3.1. Core samples

A core sample is a roughly cylindrical piece of subsurface formation brought to the surface for analyses purposes. During exploration, a core is obtained by substituting a conventional drill pipe core barrel and core bit for the drilling bit, as it penetrates the formation.

It is the only tool in the reservoir assessment that directly measures many important formation properties. It should be mentioned that these measurements are taken at surface so they do not represent exactly the subsurface conditions of the reservoir.

It aims to determine porosity, horizontal permeability, residual fluid saturation, grain size, density and other properties. It is also used for qualitative analysis to shape the lithology of the reservoir, infer the depositional history of an area. Furthermore, it can be applied to calibrate wireline logs.

The core barrel (figure 3.1) is a hollow cylindrical device between 3 m and 18 m in length, with a hollow drill bit which is attached to the bottom of the drill pipe for the purpose of recovering

continuous samples of the formation while the hole is being drilled, with the same length and approximately 0.08 m to 0.1 m in diameter. (Norman, 1991).

During laboratory test procedure, core handling, cleaning, drying, preparation and analysis procedure may introduce damage to the core if incorrectly performed (Sindouir and Duguiol, 1990). Therefore, destructive processes such as plugging may cause partial disintegration of formation and thus significantly damage the results of petrophysical property measurements. Likewise, some misidentification of minerals could be caused by highly drying the sample during laboratory procedure, which may drive off all the water in the clay particles and consequently modify petrophysical properties. The main consequence of errors during the core analysis procedure is that, core analysis results may be seriously different from geophysical logs data, and in such cases, predictions from geophysical logs are sometimes doubtful without consideration of laboratory analytical procedures.

Core analysis has evolved from qualitative geological description to the use of sophisticated analytical tools, such as Scanning Electron Microscope (SEM), X-Ray Diffraction (XRD), yet there are no uniform accepted experimental procedures or calibrating standards (Juhasz, 1990).

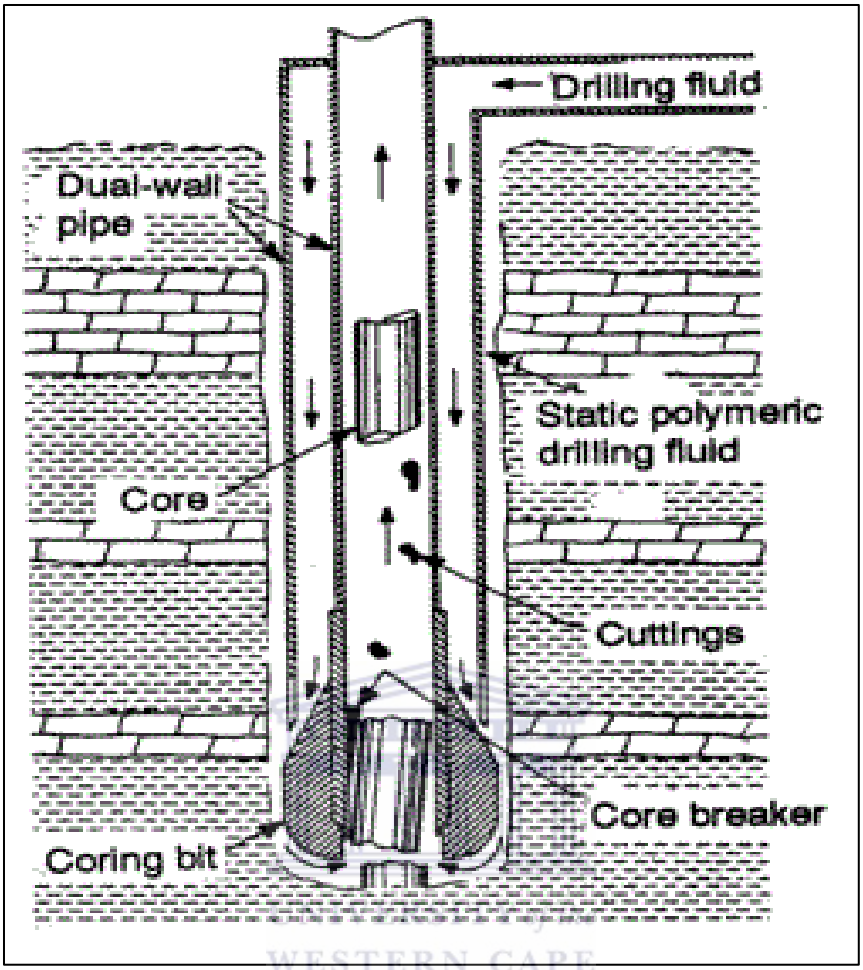

Figure 3.1: Core-drilling equipment (modified from www.globalsecurity/library/policy/army/fm/5-484/ch11.htm)

Other coring methods such as sidewall coring, could be carried out when additional rock samples are required after the well has been drilled and before it has been cased.

3.2. Well logs

A well log is the recording of the measurement of a geophysical parameter plotted continuously against depth in the well bore (Rider, 1996). It is used to identify and correlate underground rocks, determine their lithology, generate their physical properties and the nature of the fluids they contain.

Geological sampling during drilling ('cutting sampling') leaves a very imprecise record of the formations encountered. Likewise, entire formation samples can be brought to the surface by

mechanical coring, but this is both slow and expensive (Rider, 1996). Even though geophysical logs need interpretation to bring it to the level of geological or petrophysical experience, the strong points are in the precision and ability to bridge the gap between well cuttings and core samples.

Many different modern geophysical well logs exist. The most popular among other are wireline geophysical well logs. They are made using highly specialized equipment entirely separate from that used for drilling. They can be run as 'open-hole 'logs immediately after drilling and before casing, or as MWD (Measurement While Drilling) and LWD (Logging While Drilling) logs, simultaneously as the formation is drilled.

MWD are usually run to determine the deviation of a directional well, and LWD to reduce costs as they will refer to log-type measurements such as resistivity, density and so on (Rider, 1996).

To run 'open-hole' wireline logs (Figure 1.5), the hole is cleaned and stabilized and the drilling equipment extracted. The first logging tool is then attached to the logging cable (wireline) and lowered into the hole to the maximum drilled depth. Most of logs are run while pulling the tool up from the bottom of the hole and sampling the formation once every 15cm (Rider, 1996).

Necessary geophysical measurements are obtained to allow a quantitative evaluation of hydrocarbon in place. Therefore, it is imperative to get accurate, well calibrated and complete data.

3.3. Classification of geophysical wireline logs

Wireline logs can be classified based on either the principles of operations of logging tools or their usage i.e. measurable physical parameters and deductions that can be made from them (Serra, 1984).

- Classification based on operational principles:
    - Electrical logs: Spontaneous Potential (SP) and Resistivity logs.
    - Nuclear or Radioactive logs: Gamma-Ray (GR), Density and Neutron logs.
    - Acoustic logs: Sonic (DT) logs.

- Classification based on their usage:
    - Porosity logs: Sonic (DT), Density (RHOB) and Neutron (NPHI) logs.
    - Lithology logs: Gamma-Ray (GR) and Spontaneous Potential (SP) logs
    - Resistivity logs: Induction (ILD), Laterolog (LLS, LLD), Microresistivity (MSFL) logs.
    - Auxiliary logs: Caliper (CALI), Dipmeter etc.

3.4. Characteristics of selected wireline logs

3.4.1. Gamma-ray logs

A Gamma-ray log is a record of a natural formation's radioactivity. It measures the radiation of the combined elements of parent and daughter product, of the three main radioactive families: Uranium, Thorium and Potassium. It is used to identify lithology (shaliness) and to derive the shale volume of a formation.

The most modern Gamma-ray logging detector is the scintillation counter (figure 3.2). It has two basic components, a scintillating crystal and a photo multiplier tube. The transparent sodium-iodide crystal will give off a minute burst of light when struck by a gamma-ray. The light energy strikes a photo sensitive cell or cathode which causes electrons emission. The electrons so produced are drawn to an anode which, upon impact, releases additional electrons which are directed to another anode. There are several stages of such amplification which finally give a sufficient flow of electrons to be easily measured and recorded as an indication of the gamma radiation penetrating the detector (Baker Hughes Inteq, 1992).

In sediments, radioactive elements are borne by numerous minerals. Among other, Potassium is found in clay minerals, evaporates, carbonates and in low concentrations within the feldspars contained in sandstones. Thorium is a common constituent of the detrital fraction of minerals such as continental shale, certain beach-sands and placers. Uranium can be found in clay mineral containing organic matter of vegetable origin, clay particles, adsorptive material such as amorphous silica, alumina, coals (Serra, 1984). Therefore, shale have by far the strongest radiation; then sandstones, dolomite and finally limestone with weak radiation (Rider, 1996).

High gamma-ray may not imply shaliness, but a reflection of radioactive sands such as potassium rich feldspathic, glauconitic or micaceous sandstones. Gamma-ray log is usually preferred to spontaneous potential logs for correlation purposes in open holes nonconductive borehole fluids, for thick carbonates intervals, and to correlate cased-hole logs with open-hole logs. The standard unit of measurement of gamma-ray is API (American Petroleum Institute).

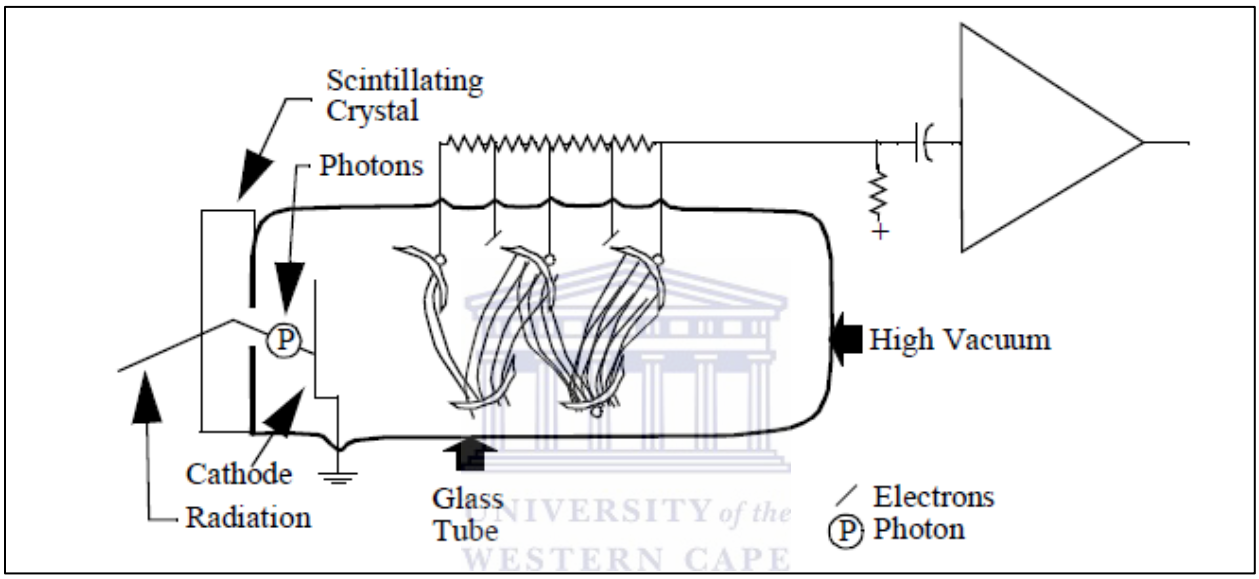

Figure 3.2: Scintillation counter (From Baker Hughes INTEQ, 1992).

3.4.2. Spontaneous Potential logs

Also known as self-potential log, it is a measurement of the natural potential differences between an electrode in the borehole and a reference electrode at the surface: no artificial current are applied. They originate from the electrical disequilibrium created by connecting formations vertically when in nature they are isolated.

The principal uses of the SP log are to calculate formation water resistivity and to indicate permeability. It can also be used to estimate shale volume, to indicate facies and in some cases for correlation.

Three factors are necessary to provoke an SP current: a conductive fluid in the borehole, a porous and permeable bed surrounded by an impermeable formation and a difference in salinity (or pressure) between the borehole fluid and the formation fluid. The principle of measurement is based on the difference in the diffusion potential of sodium chloride (figure 3.3), due to a variation of pore throws within the formation. The chloride ion is both smaller and more mobile than the larger, slower sodium. Therefore, because shale consist of layers with large negative surface charge, the negative chloride ions effectively cannot pass through the negatively charged shale layers, while the positive sodium ions pass easily. The shale (semi-permeable membrane) acts as a selective barrier. As sodium ions diffuse preferentially across a shale membrane, an overbalance of sodium ions is created in the dilute solution and hence a positive charge. A corresponding negative charge is produced in the concentrated solution. The shale potential is the larger of the two electrochemical effects. Consequently, the actual potential currents which are measured in the borehole are for the most part, a result of the combination of the two electrochemical effects described above. Likewise, the less saline solution opposite the sandstone bed (permeable membrane), the mud filtrate will become positively charged. As a result, the excess charge is negative next to the sand and positive next the shale (Rider, 1996).

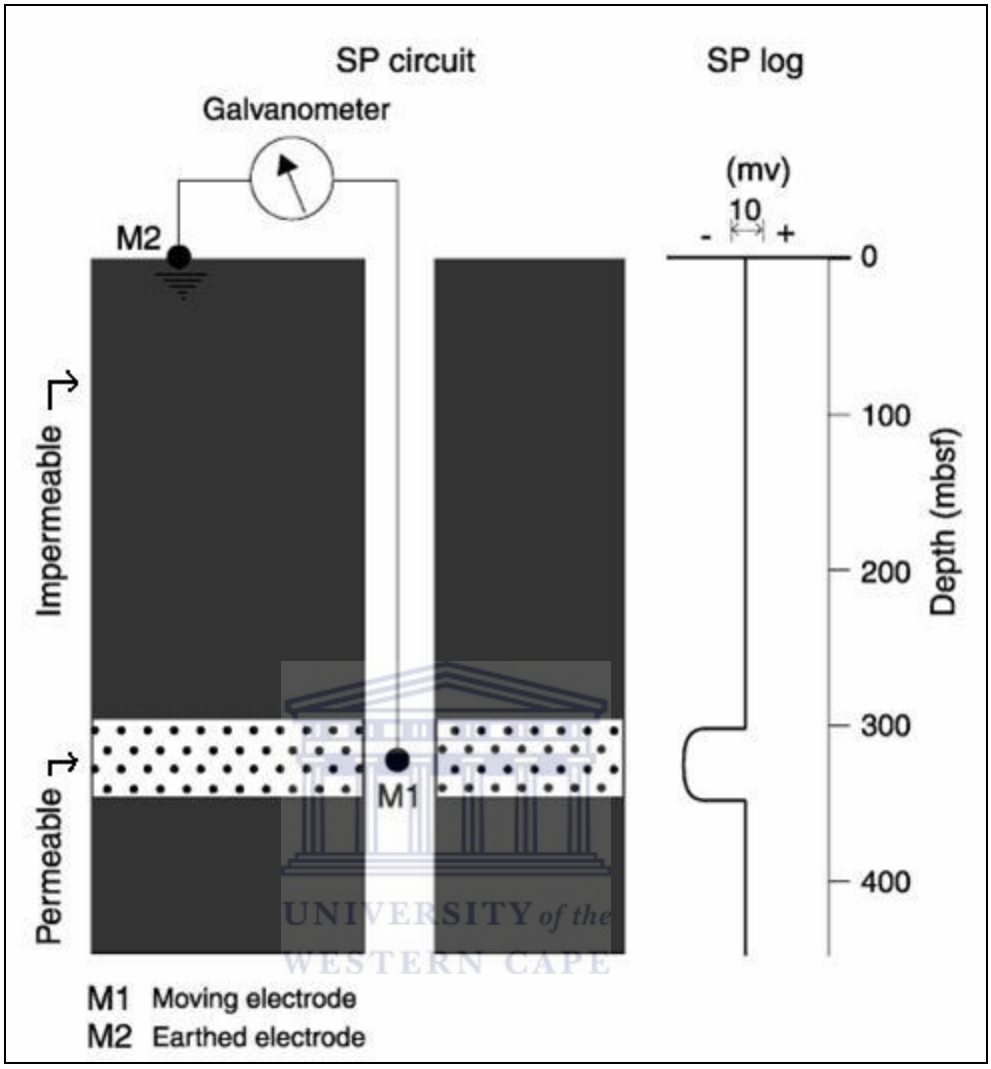

Figure 3.3: Illustration of the principle of the SP log (from Rider, 1996).

3.4.3. Density logs

The density log is a continuous record of a formation's bulk density. This is the overall density of a rock including the density of minerals (solid matrix) and the volume of free fluid enclosed in the pores (porosity).

Quantitatively, the density log is used to calculate porosity and indirectly, hydrocarbon density. Qualitatively, it is a useful lithology indicator (combined with Neutron logs); it can be used to identify certain minerals and may help to identify overpressure and fracture porosity.

The logging technique of the density tool is to subject the formation to a bombardment of medium-high collimated (focused) gamma rays, and to measure their attenuation due to their backscattering and absorption by the materials in the formation, between the tool source and detectors. The rate of absorption and the intensity of the backscattered rays depend on the number of electrons (electron density) that the formation contains, which in turn is closely related to the common density of the materials. Dense materials have more electrons per unit-volume (electrons/cm^3), with which the gamma particles can collide and loose energy. Hence, higher energy is absorbed in dense formations. In light materials with lower electron density, more gamma particles reach the detectors and are converted directly to bulk density for the log printout. However, although electron density as detected by the tool and real density are almost identical, there are differences when water (hydrogen) is involved. For this reason, the values presented on the density log are transformed to give actual values of calcite (2.71g/cm^3) and pure water (1.00g/cm^3).

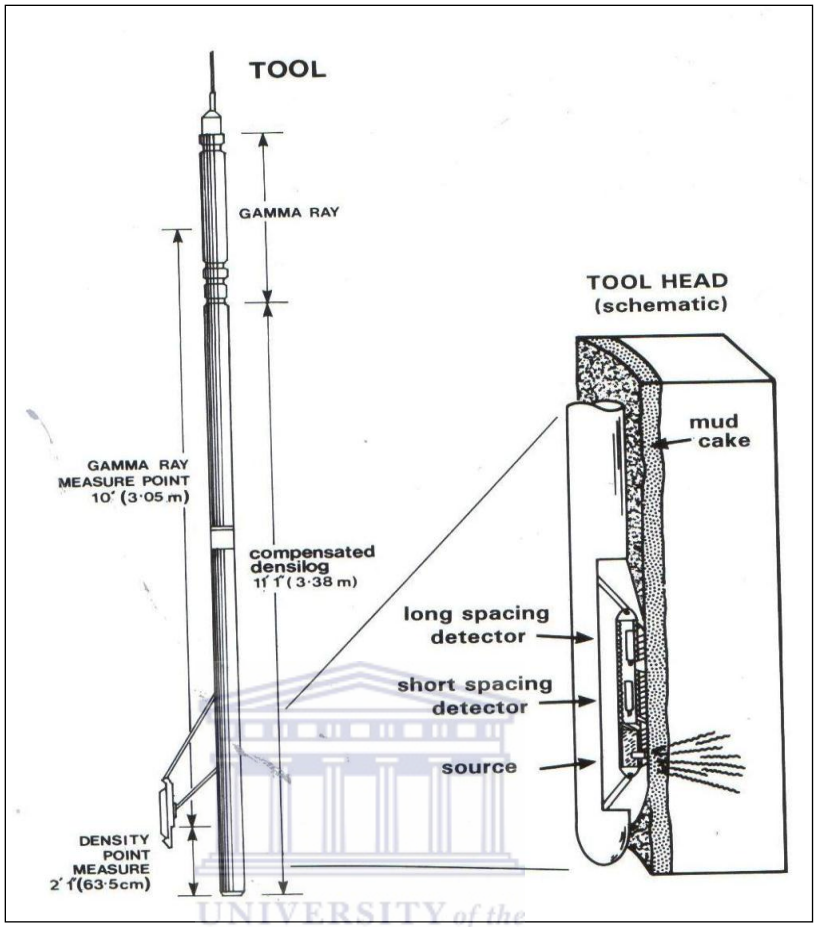

Figure 3.4: A density tool (from Rider, 1996).

An illustration of a density tool is provided in figure 3.4 above. It consists of a collimated gamma-ray source and two detectors (near and far) which allow compensation for borehole effects when their readings are combined and compared in calculated ratios. The source and the detectors are mounted on a plough-shaped pad which is pressed hard against the borehole wall during logging, to minimize the contribution of the drilling mud in the record signal. Density log therefore refers to only one sector on the borehole wall (Rider, 1996).

3.4.4. Neutron logs

The neutron log is a measurement of induced formation radiation produced by fast moving neutrons bombarding the formation. It is an indication to formation richness in hydrogen. A high neutron count rate indicates low porosity, while low neutron count rate indicates high porosity.

The principal uses of a neutron log are to measure porosity and to discriminate oil from gas saturations (the porosity will appear very low when gas is measured). It is a very good porosity indicator in limestones (figure 3.5.B) and can be used to identify gross lithology, evaporites, hydrated minerals and volcanic rocks. When combined with a density log, it is one of the best subsurface lithology indicators available.

The source (figure 3.5) used to produce neutrons is usually a mixture of Beryllium and Radium. As Radium decays, it emits alpha particles. The Beryllium responds to those alpha particles by emitting high energy neutrons through the formation. This energy will be slowed down by collisions with Hydrogen atoms, because of their masses approximately equal.

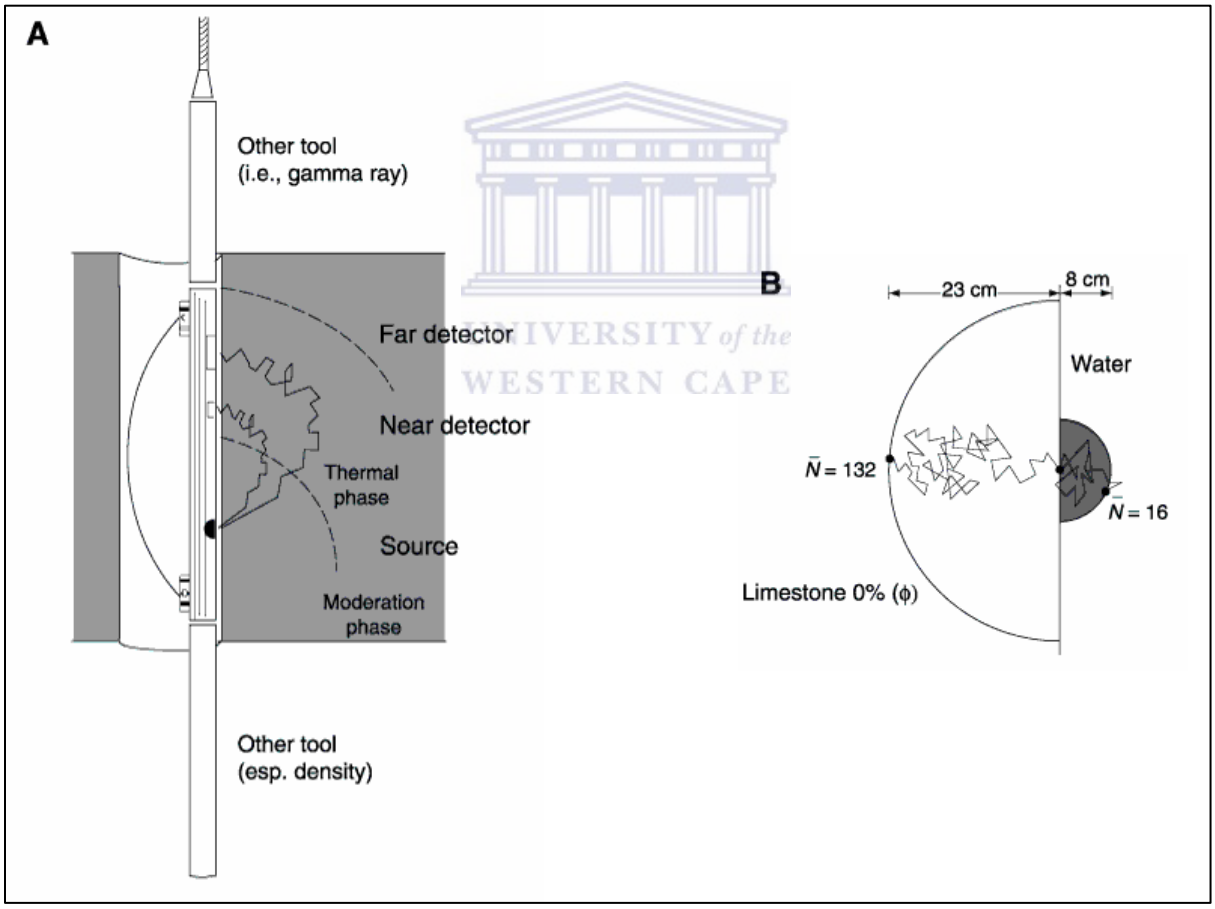

Figure 3.5: Compensated neutron tool drawing, B. Schematic trajectories of a neutron in a limestone with no porosity and pure water (modified from Rider, 1996).

Hence, the distribution of the neutrons at the time of detection is primarily determined by the Hydrogen concentration.

Neutron log responses vary, depending on: difference in detector types (Thermal, epithermal, and gamma-ray), spacing between source and detector (Near or far), and lithology (sandstone, limestone, and dolomites).

3.4.5. Sonic logs

A sonic log is a continuous record against depth of the specific time required (travel-time) for a compressed wave to traverse a given distance of formation adjacent to the borehole. It varies with lithology and rock texture, notably porosity. In general terms, the consolidated is a formation, the lower the travel-time.

Sonic logs are used quantitatively to evaluate porosity in liquid-filled holes. Cross-multiplied with the density, it is used to produce the acoustic impedance log, the first step in making a synthetic seismic trace. Qualitatively, the sonic log is sensitive to subtle textural variations in both sands and shales. It can also help to identify lithology and for correlations.

The acoustic tool (Figure 3.6) contains a transmitter and two receivers. When the transmitter is energized, the sound wave enters the formation from the mud column, travel through the formation and back to the receiver through the mud column. This travel-time or formation velocity is equal to the distance spanned by the two receivers. The system has circuits to compensate for borehole size changes or any tilting of the tool. The unit of measurement of this parameter is microsecond/foot. Travel-time is conventionally symbolized by delta-t (Δt).

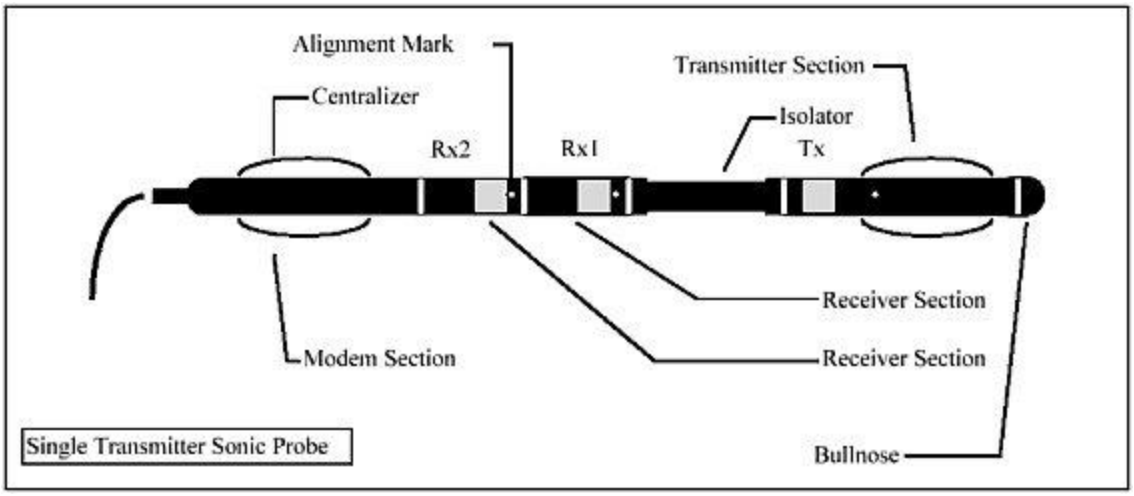

Figure 3.6: Sonic logging tool (modified from http://www.aegis-instruments.com/images/products/sonic.jpg).

3.4.6. Resistivity logs

The resistivity log is a measurement of a formation's resistivity, which is its resistance to the passage of an electric current. It can be measured directly by resistivity tools, or indirectly by conductivity tools. Conductivity data produced by induction tools measure a formation's conductivity or its ability to conduct an electrical current. These values are generally converted directly and plotted as resistivity on log plots.

Most rock materials are essentially insulators, while their enclosed fluids are conductors. Hydrocarbons are the exception to fluid conductivity, and on the contrary they are infinitely resistive. When a formation is porous and contains salty water, the overall resistivity will be very low. When this same formation contains hydrocarbons, its resistivity will be very high. It is this character that is exploited by the resistivity logs: high resistivity values may indicate a porous, hydrocarbon-bearing formation.

Resistivity logs were developed to find hydrocarbons. Their principal quantitative use is to furnish the basic numbers for petrophysical calculations such as the volume of oil in place.

Qualitatively, they can contribute to identify lithology, texture, facies, and overpressure of a formation.

An example of resistivity tool is Figure 3.7. Electrodes in the borehole (M, N) are connected to a power source (generator) and the current flows from the electrodes through the borehole fluid into the formation and then to the remote reference electrode (A).

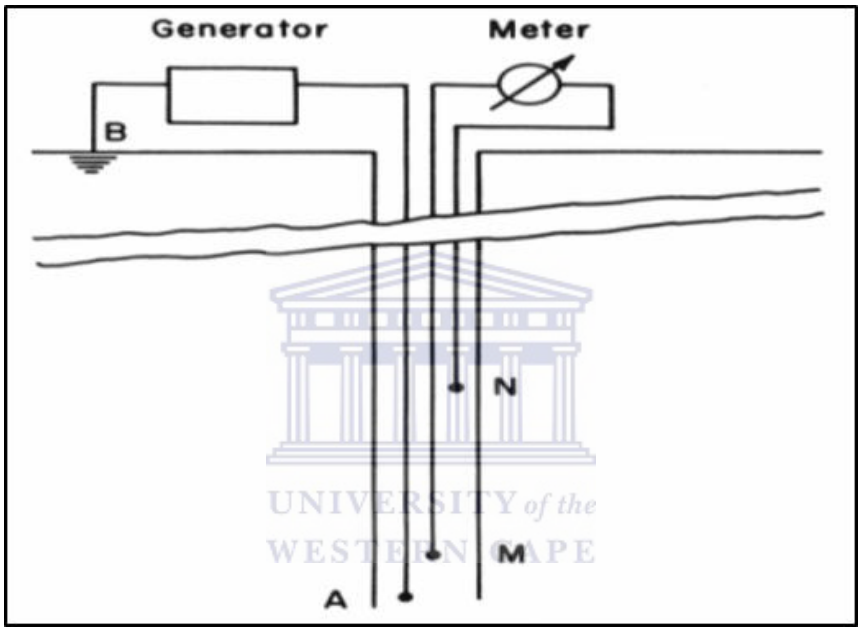

Figure 3.7: Electrode resistivity tool with electrodes M, N and A (modified from Schlumberger, 1972).

This tool can only function in borehole containing conductive muds mixed with salt water. They cannot be run in oil-based muds or freshwater based muds. Induction logs on the contrary, are most effective with non-conductive muds, oil-based or fresh water based and reasonably effective in salt water based muds (Rider, 1996).

3.4.7. Composite Log

This is a single log created by splicing together two logs of the same type run at different time in the well; or run at the same time (Schlumberger, 2002).

An example of common composite log is neutron-density log. It is a combination porosity log. Besides its uses as a porosity device, it is also used to determine lithology and to detect gas bearing zones.

3.5. Physical properties of rocks

The evaluation of a reservoir requires three basics data requirements: porosity, permeability and fluid saturation.

3.5.1. Porosity

Porosity is the first of the three essential attributes of a reservoir. It is a measure of the void space within a rock, expressed as a fraction (or percentage) of the bulk volume of that rock. It is conventionally symbolized by the Greek lowercase letter phi (ϕ). The general expression for porosity is:

$$\textbf{Porosity}\ (\boldsymbol{\varphi}) = \frac{\textbf{Volume of voids}}{\textbf{Total volume of rock}}$$

Volumes of voids or pores are of three morphological types: catenary, cul-de-sac and closed (Figure 3.8). Catenary pores are those that communicate with other by more than one throat passage. Cul-de-sac or dead-end pores have only one throat passage connecting with another pore. Closed pores have no communication with other pores.

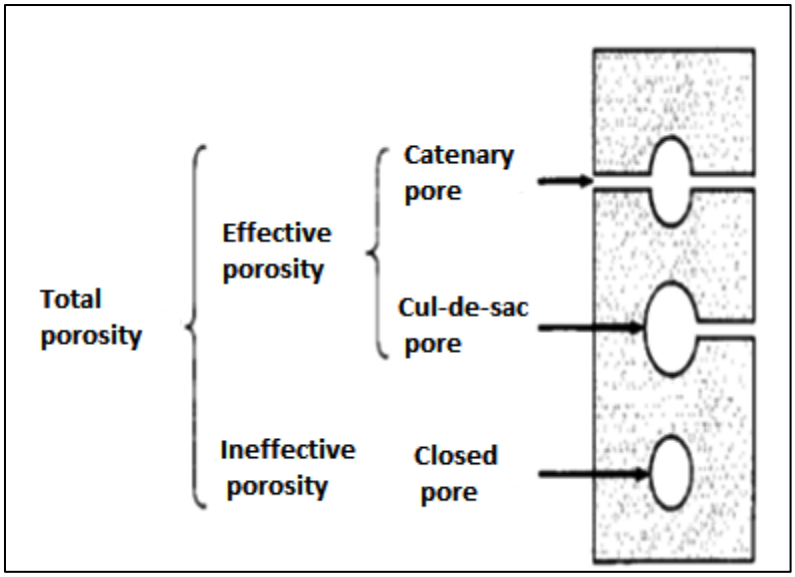

Figure 3.8: The three basic types of pores (Selley, 1998).

Catenary and cul-de-sac pores constitute effective porosity in that, hydrocarbons can emerge from them. It excludes pore volumes occupied by water adsorbed on clay minerals or other grains. In catenary pores, hydrocarbons can be flushed out by a natural or artificial water drive whereas cul-de-sac are unaffected by flushing, but may yield some oil or gas by expansion as reservoir pressure drops.

Closed pores are unable to yield hydrocarbons (such oil or gas having invaded an open pore subsequently closed by compaction or cementation) and constitute ineffective porosity.

The total (or absolute) porosity is all void space in a rock and matrix whether effective or ineffective. It includes porosity in isolated pores, adsorbed water on grains or particle surface and associated with clays.

During reservoir characterization, it is crucial to determine the size and geometry of the pores and the diameter and the tortuosity of the connecting throat passages, because they all affect the productivity of the reservoir. Hence, two main types of pore can be defined according to their time of formation:

- Primary pores are those formed when sediment is deposited. They are divided in two subtypes:
    - Interparticle (or intergranular) pores which are initially present in the sediment. They are often quickly lost in clays and carbonate sands because of the combined effect of compaction and cementation, but preserved in sandstone reservoirs.
    - Intraparticle (or intragranular) pores are generally found within the skeletal grains of carbonate sands and are thus often cul-de-sac pores.
- Secondary pores are those developed in a rock sometime after deposition. They represent additional pores resulting from fractures, vugs, solution channels, diagenesis, and dolomitisation. The three major types of secondary porosity are: solution-induced porosity, fracture porosity and intercrystalline porosity.

Porosity may be measured in three ways: directly from cores, indirectly from geophysical well logs, or from seismic data (Selley, 1998).

3.5.2. Permeability

The second essential requirement for a reservoir rock is permeability. Porosity alone is not enough, the pores must be connected. Permeability is the ability of fluids to pass through a porous material. It is controlled by the size of the available pores and the connecting passage between them.

The unit of permeability is the Darcy. Darcy's law is used to calculate permeability. It is defined as the permeability (symbolized by K), that allows a fluid of 1 centipoise (cP) viscosity to flow at a velocity of 1cm/s for a pressure drop of 1atm/cm. Because most reservoirs have permeabilities much less than a Darcy, the millidarcy (mD) is commonly used. The formula of Darcy's law is:

$$Q = \frac{K(P_1 - P_2)A}{\mu L}$$

Where:

Q = rate of flow

K = permeability

$(P_1 - P_2)$ = Pressure drop across the sample

A = cross-sectional area of the sample

L = length of the sample

μ = viscosity of the fluid

The absolute permeability is the ability of a rock to transmit a fluid 100% saturated with one fluid. It is when a single fluid flow through the formation. However, since petroleum reservoirs contain gas and/ or oil and water, the effective permeability for given fluids in the presence of others must be considered. It is the ability of a rock to transmit a fluid in the presence of another fluid when the two are immiscible.

The ratio of effective permeability of a fluid at partial saturation to its permeability at 100% saturation (absolute permeability) is the relative permeability. It is also defined as the ratio of the amount of a specific fluid that will flow at a given saturation, in the presence of other fluids, to the amount of the same fluid that will flow at a saturation of 100%, other factors remaining the same.

It should be noted that the sum of effective permeability will always be less than the absolute permeability. This is due to the mutual interference of the several flowing fluids.

The permeability of a reservoir can be measured in three ways: by means of drill-stem or production test, from wireline logs, and using a permeameter.

3.5.3. Fluid saturation

Porosity can be stated as the capacity to hold fluid. Fluid saturation is the fraction (or percentage) of the storage capacity of a rock occupied by a specific fluid. It is generally defined by:

$$\text{Fluid saturation } (S_f) = \frac{\text{Formation fluid occupying pores}}{\text{Total pore spaces in the rock}}$$

The fluid in the pore spaces of a rock may be wetting or non-wetting. In most reservoirs, water is the wetting phase while few reservoirs are known to be oil wet. The wetting phase exists as an adhesive film on the solid surface.

Water saturation (Sw) is the fraction of the pore volume occupied by a specific fluid; 1-Sw is the fraction of the pore volume occupied by hydrocarbons (Sh); it is measured in percentage.

Some of the fluids in the reservoir cannot be produced. This portion of the fluid is referred to as residual or irreducible saturation (Swirr). It is the water saturation, at which the water is absorbed on the grains in the rock, or held in capillaries by capillary pressure. At irreducible water saturation, water (wetting phase) will not move implying a zero relative permeability and the non-wetting phase is usually continuous and is producible under a pressure gradient of the well bore (Levorsen, 1967).

CHAPTER 4: LITHOLOGY INTERPRETATION

Lithology is the general physical characteristics of rocks in a particular area. Rider (1996) recommended that all the logs ran in the well should be taken into account during the manual interpretation of the reservoir rocks based on wireline logs. However, only gamma-ray or self-potential log may appear on the final lithological interpretation document.

The objective of lithology interpretation in this study is to evaluate the type of rocks (clean or tight sandstones, limestones) forming reservoir zones and their distribution within the reservoir in order to quantify gross zones, by relating the behavior of wireline logs signature based on horizontal and extensively vertical routine.

Digital wireline logs, petrography and well completion reports are used to reconstruct the reservoir lithology of each well. The analyzed interpretation interval varies from 20 m-150 m depending of the reservoir.

4.1. Methodology

The horizontal routine is often used during manual lithology interpretation. It consists of comparing and corroborating at the same depth, horizontally the gross lithology suggested by the well completion report to the gamma-ray log firstly, then through the other logs (resistivity, sonic and density-neutron). Extensively, a vertical routine should be applied for trends, baselines or absolute values and abrupt-peaks integrated with well reports for a quick interpretation of the depositional history and wireline logs correlation. According to Serra and Sulpice (1975), the shape of a gamma-ray log can be used to define it depositional environment. After much work in different fields, they identified three basic log shapes that corresponded to specific environments (figure 4.1):

- Bell shape consists of a regular increase in gamma-ray value upwards from a minimum value and corresponds to an increase in clay content upwards. It is associated with an alluvial or a fluvial channel, but also with a transgressive shelf sand which indicates a finning up sequence.

- Funnel shape characterizes a deltaic or shallow marine environment. It corresponds to a coarsening up succession materialized by a regular decrease in gamma-ray value upwards from a maximum value.
- Cylinder or block shape is more complex. It indicates a constant energy throughout the cycle.

Therefore, these interpretations will be confirmed with the well reports.

We also have a straight line shape which may indicate constant shale, clean sand or carbonate corresponding to a continuous deep marine environment.

Sedlog software is extensively used to digitize reservoir lithologies.

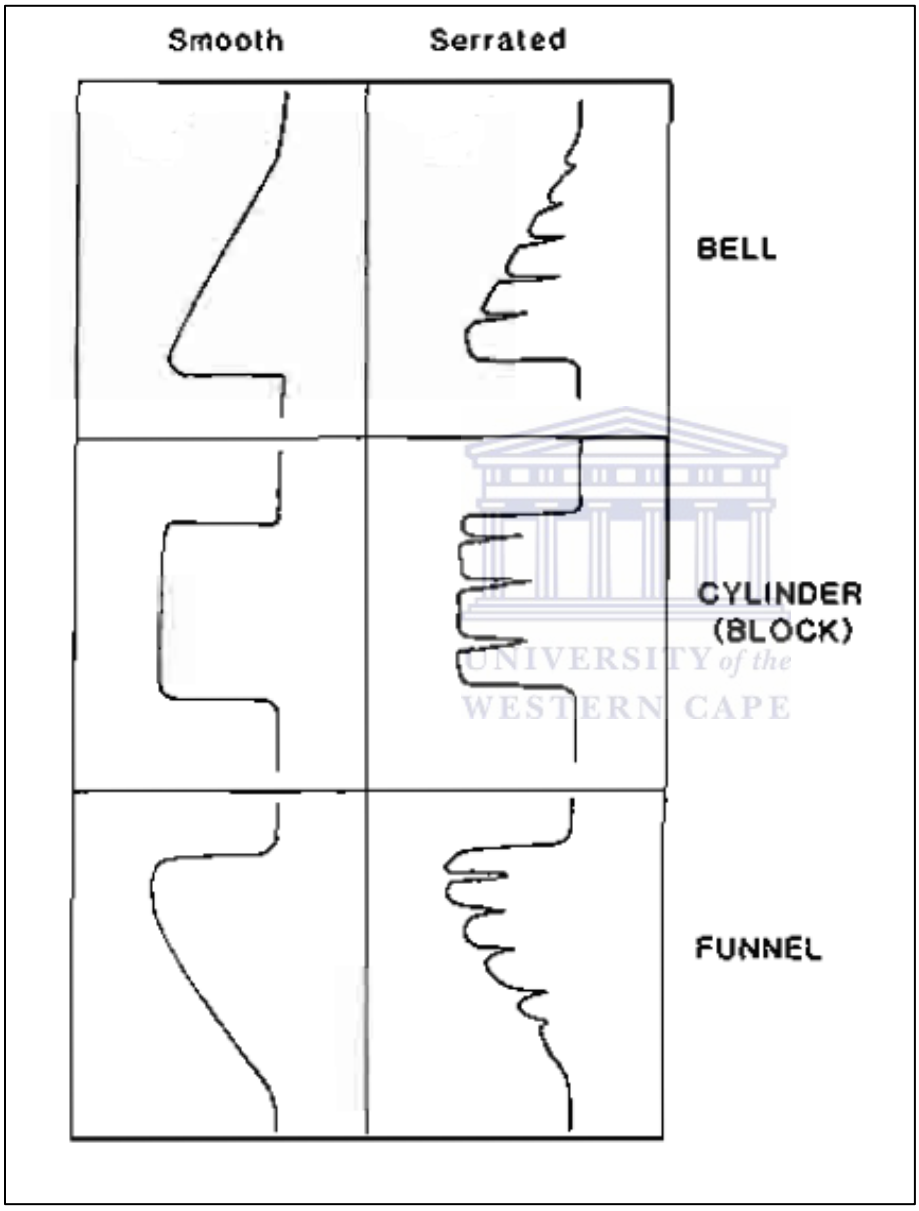

Figure 4.1 The basic geometrical shapes and description used to analyze Gamma-ray log curves.

Figure 4.2 is an example of the manual interpretation of reservoir 2 within well P-A1. On the left side of the figure, a summary of the lithology from the well report, four individual wireline logs and four composite logs are displayed. The composite logs of density-neutron and resistivity identify sandstone, while high gamma-ray value indicates shales and caliper log notifies when there is a change in formation. The result is represented on the left figure characterized by a coarsening up sequence. As a result from the above interpretation, the formation was deposited in a shallow marine environment and the well report indicates the presence of continental rocks. The lithology interpretations of the other reservoirs are shown in appendix A.

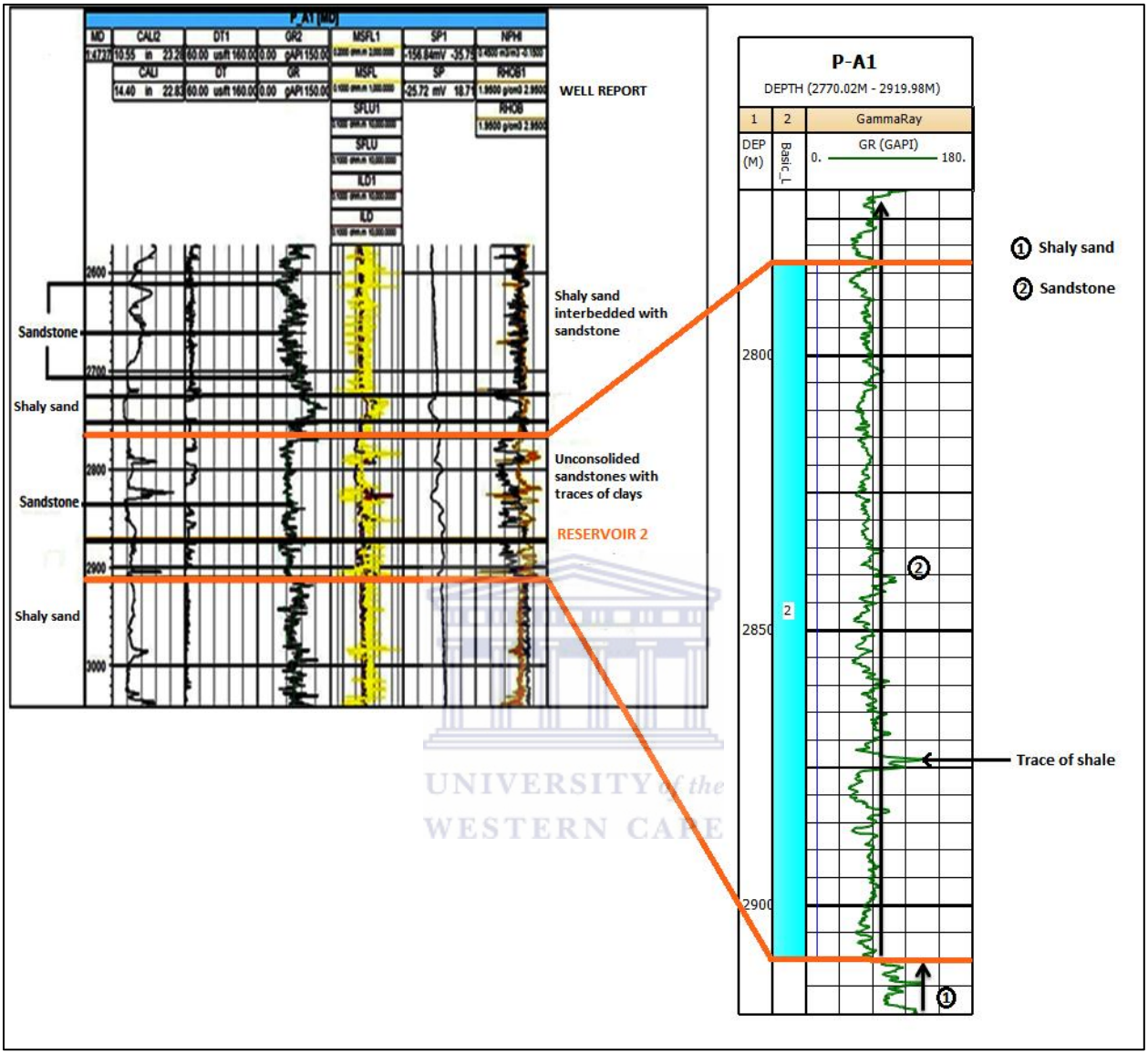

Figure 4.2 Manual interpretation of reservoir 2 within well P-A1.

4.2. Results

4.2.1. Well 0-A1

Figure 4.3 represents the lithology of reservoirs 1 and 2 within well 0-A1. Zone 1 is 11 m major sandstone mixed with minor shale interbedded. It is overlain by a sandy shale formation and is covered by shale. This sequence corresponds to a cylinder log shape, and the high presence of

clay indicates a low energy environment. Consequently, reservoir 1 was deposited in deep marine environment (well report).

Zone 2 is formed by shaly sand interbedded between sandy shale formations. Appendix A shows a gamma-ray log shape in block. This succession corresponds to a deep marine environment which is also confirmed by the well report.

Furthermore, a detailed study of the tabulated interpretative age information report and the lithology report results in the identification of unconformities 13At1, 9At1 and pre-9At1 respectively at 3793 m, 3933 m and 4185 m depths. By corroborating these results to the chronostratigraphy of the Orange Basin in figure 2.7, an estimation of the age of deposition of reservoirs 1 and 2 within well O-A1 was done. Figure 4.3 shows unconformity 13At1 on top of zone 1, and indicates that it was deposited during the Early Aptian. Reservoir 2 is interbedded between unconformity 9At1 above and Pre-9At1 below, which corresponds to Barremian in age.

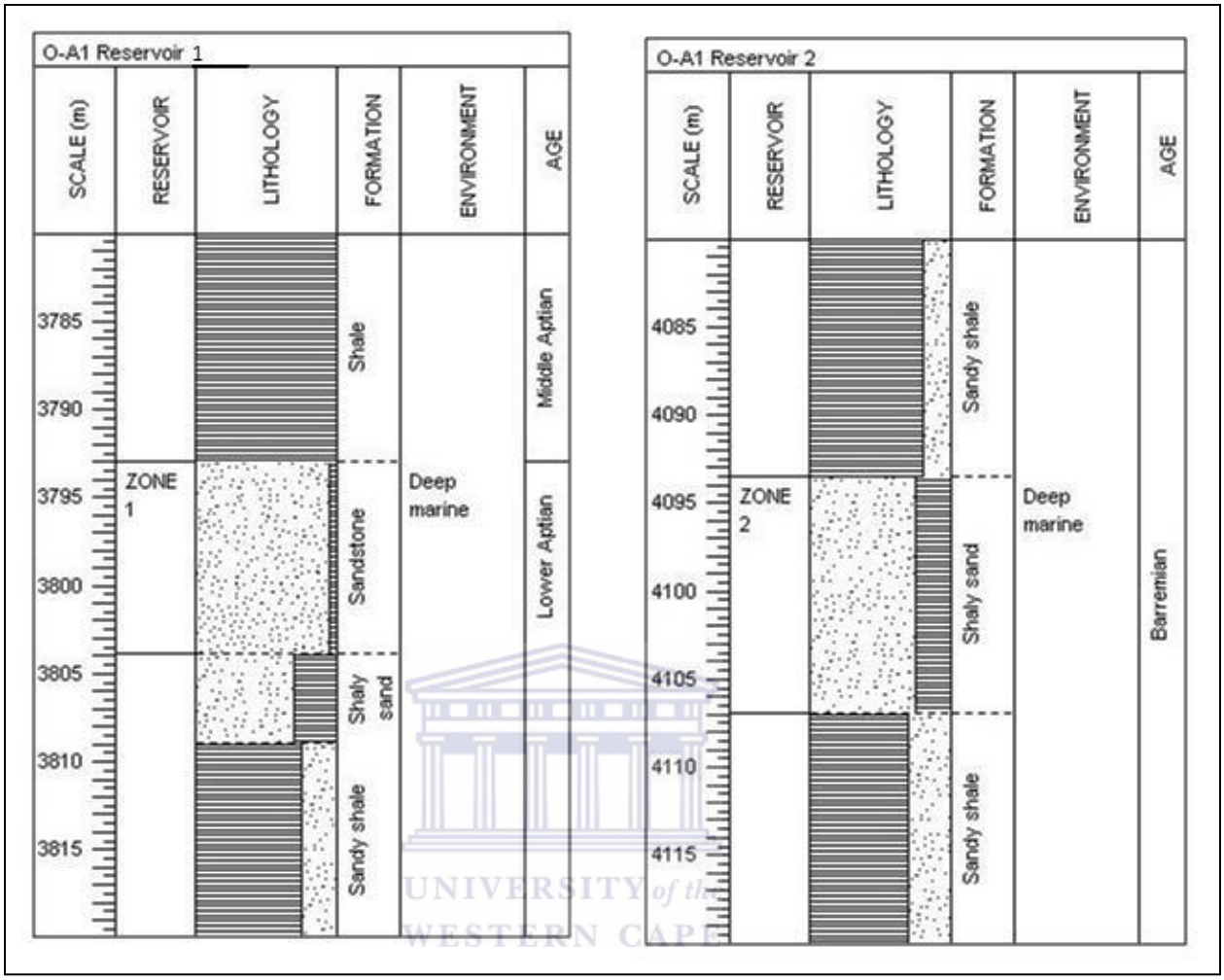

Figure 4.3 Lithology of reservoirs 1 and 2 within well O-A1.

4.2.2. Well A-N1

Reservoir targets comprise sandstones with clay content, deposited in deep marine environment during the Early Cretaceous (figure 4.4).

Zone 1 and 2 are shaly sand formations deposited respectively during Earlier Early Turonian and Middle Albian (well report).

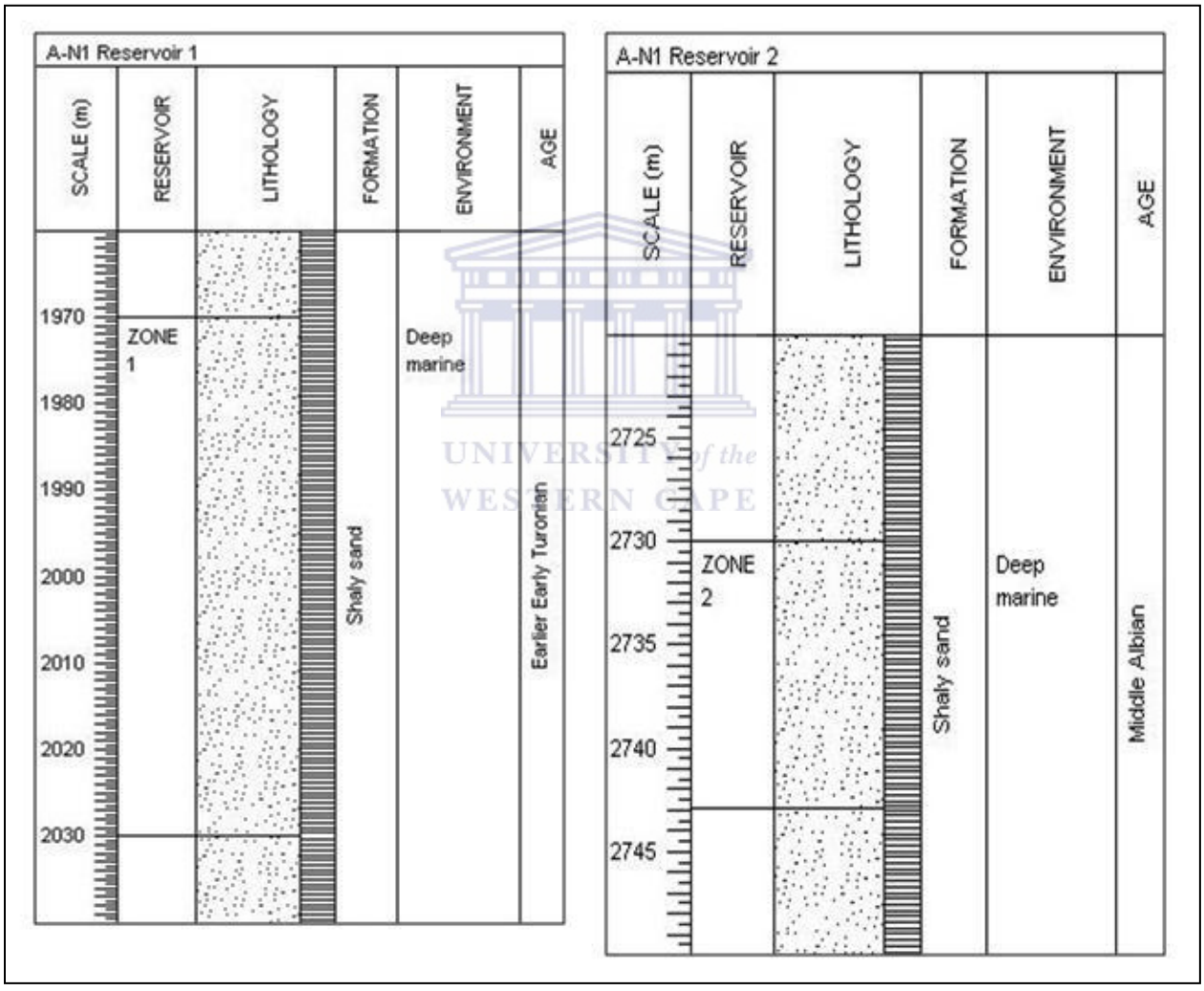

Figure 4.4 Lithology of reservoirs 1 and 2 of well A-N1.

4.2.3. Well P-A1

Well P-A1 comprises two reservoir zones deposited during Early Cretaceous. Their lithology is dominated by major sandstone.

Zone 1 consists of a tight sandstone formation with minor shale, described as a fining up sequence deposited in the transgressive shelf (figure 4.5). Zone 2 represents the biggest reservoir interval of this study. It is a coarsening up thick sandstone, interbedded with minor shale and forming part of the shallow marine environment. These interpretations are corroborated by the well report.

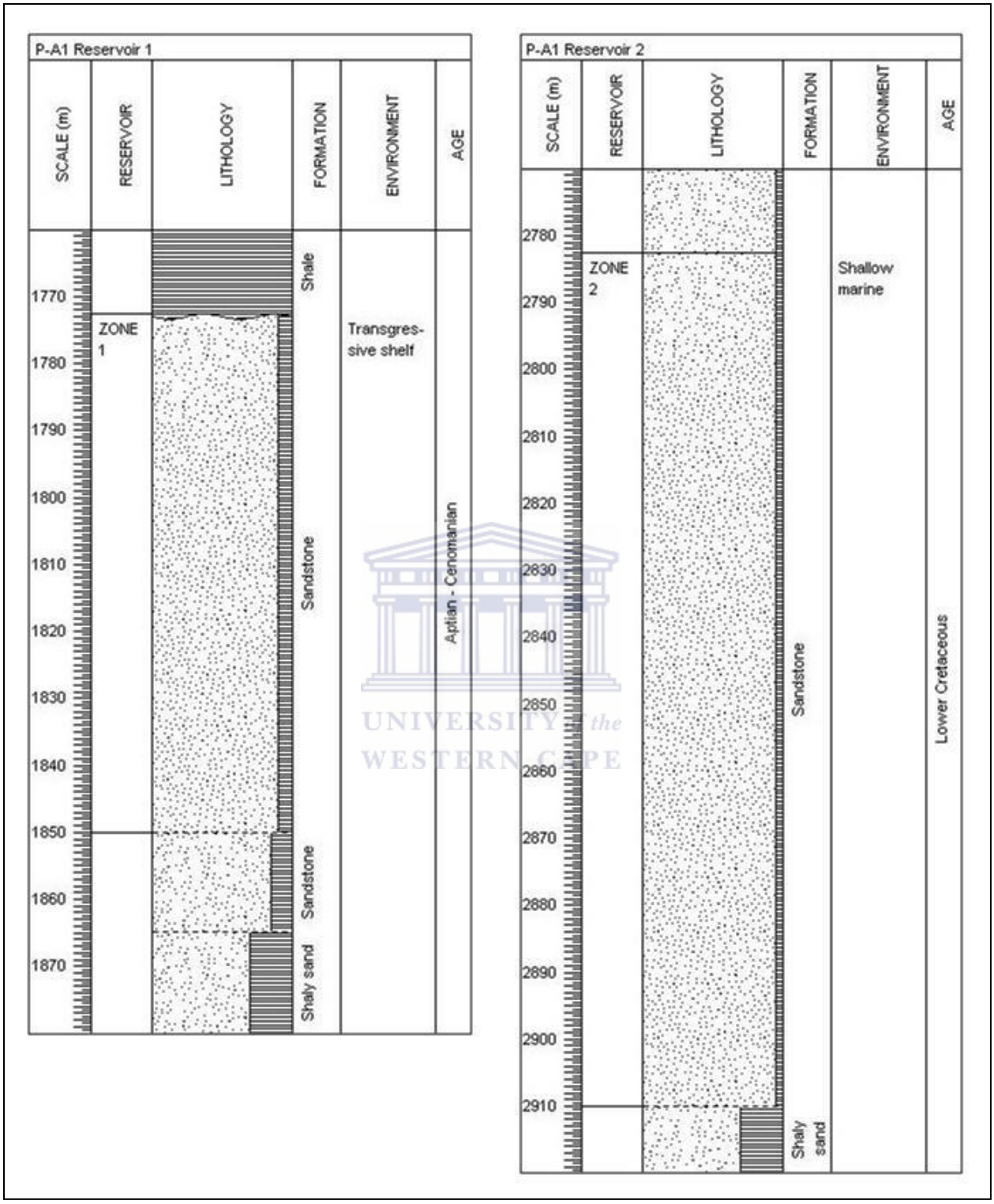

Figure 4.5 Lithology of reservoir zones 1 and 2 within well P-A1.

4.2.4. Well P-F1

Formations of reservoir zones within well P-F1 were deposited in the shallow marine environment during the Late Cretaceous. Results of the interpretation of reservoirs lithology are displayed in figure 4.6.

Zone 1 consists of major sandstone mixed with minor clay and overlying shale.

Zone 2 is characterized by a sandstone formation interbedded with clay in the upper zone (1379.0m – 1390.0m) and clean sandstone in the lower zone (1390.0m – 1400.0m).

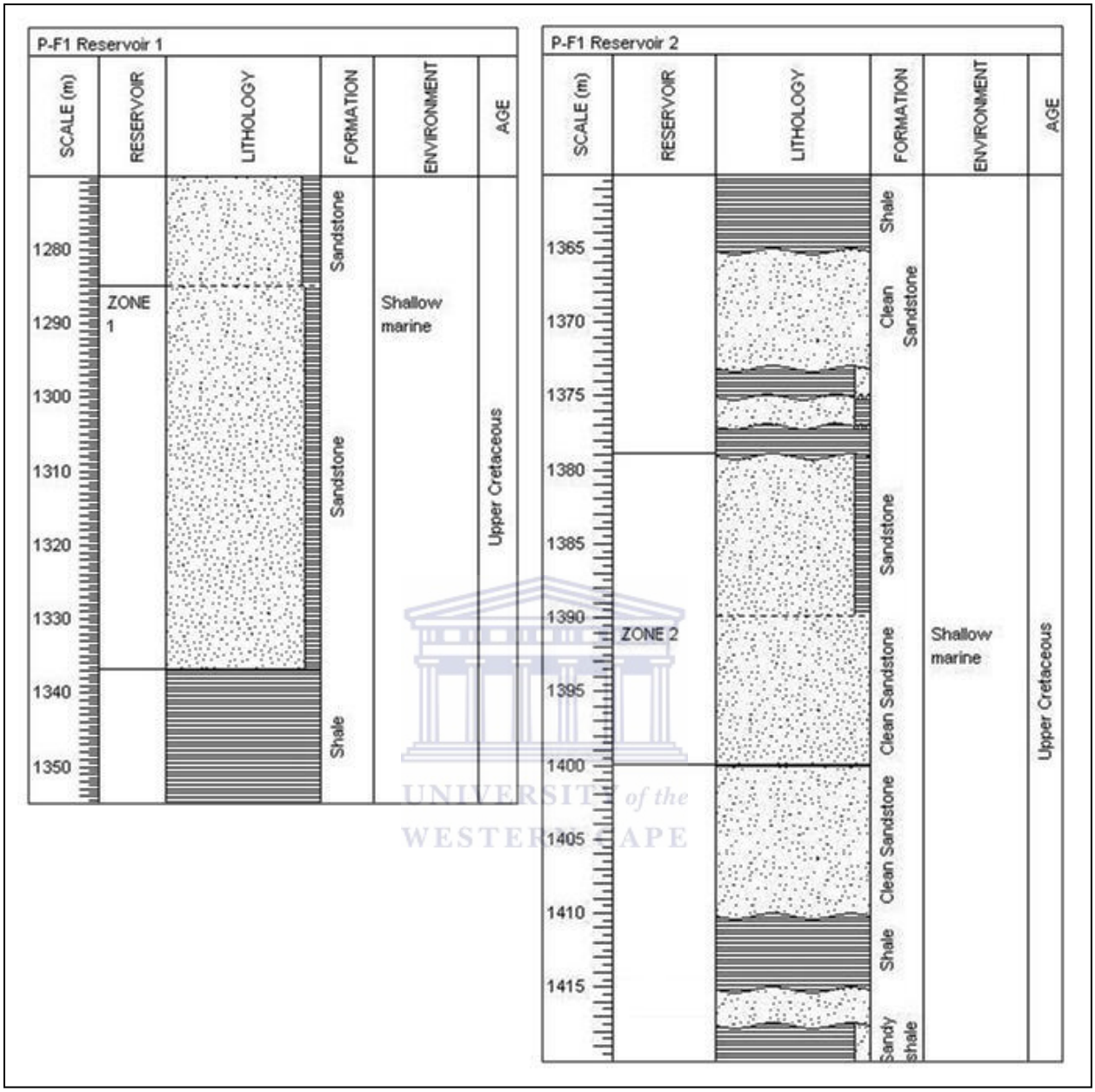

Figure 4.6 Lithology of reservoir zones within well P-F1.

4.3. Wireline log correlation

4.3.1. Definition

A wireline log correlation is the identification and linkage of similar marker horizons along different wells, which maybe a distinctive peak (unconformities), distinctive shape (stratigraphy) or distinctive lithology with unique log response (Rider, 1996). It is a combination of basic geological principles which include the understanding of depositional environment, concepts of logging tools and measurements, and qualitative log analysis.

Well log correlation is used in reservoir characterization to understand the lateral extent of sandstone reservoirs within a specific sequence. Therefore, the accuracy of a prepared geological interpretation is determined by the correctness of correlations undertaken.

Since the gamma ray log value in shale remains constant laterally at the same stratigraphic level and the gamma ray value of sandstone is rather constant vertically, wireline logs correlation is an appropriate method to understand the thickness of sandstone formations (Rider, 1996).

Based on the resulted lithologies, wireline logs of four wells within the interval in the study area have been correlated.

4.3.2. Results

The reservoir zones are correlated separately according to the wireline logs signatures, between O-A1 and A-N1 in the marine environment, and P-F1 and P-A1 in the margin.

Figure 4.7 is the wireline logs correlation of the reservoir intervals. It showscorrelations between wells O-A1 and A-N1, where reservoir zone 2 of both wells are related by their same wireline log behavior. Wells P-A1 zone 2 and P-F1 zone 1 are also similar and therefore linked. The absence of correlation between wells P-A1 and A-N1 might be explained by the long distance and the half graben separating them.

These results show the extension of the reservoir zones that could be considered for further explorations.

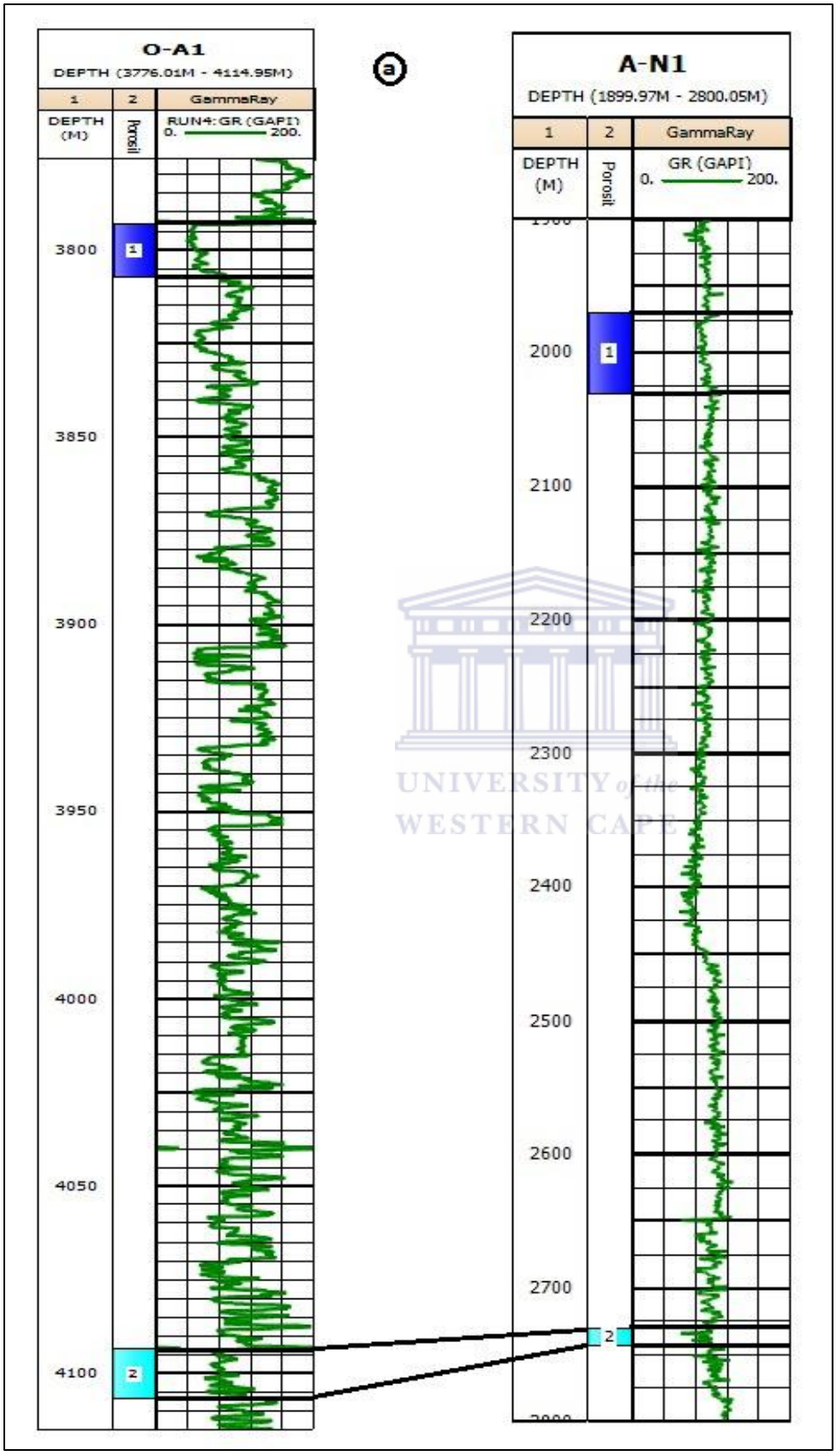

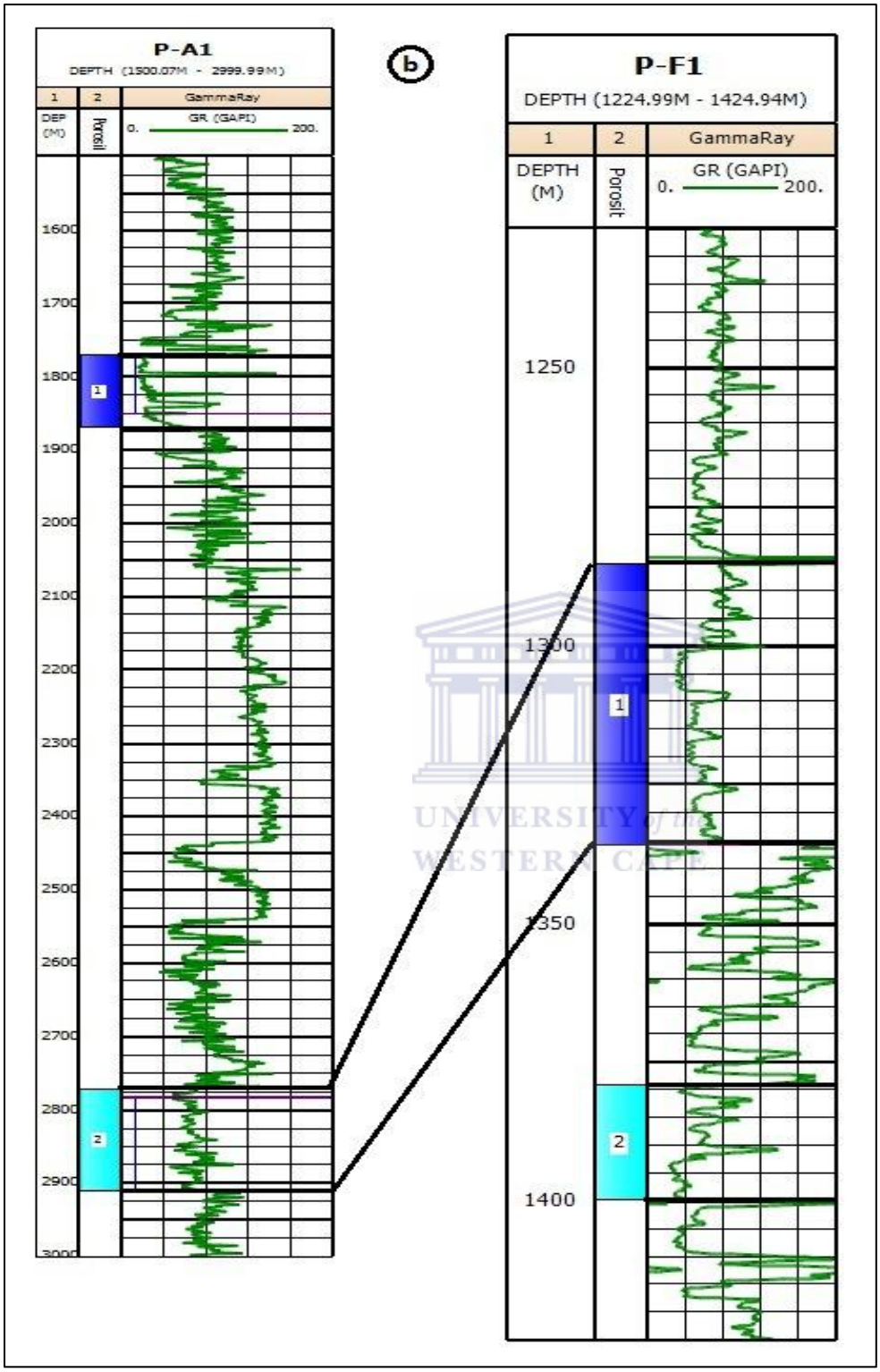

Figure 4.7: Wireline log correlation of the reservoir zones between: a. O-A1 and A-N1, b. P-A1 and P-F1.

CHAPTER 5: PETROPHYSICAL ANALYSIS

This chapter is built on the quantitative interpretation of wireline logs, within the potential reservoir intervals determined in chapter four.

The sorted digitized wireline log and geothermal data within the primary targets serve as input data into the Interactive Petrophysics (IP) software, in order to process and analyze them.

The input data are:

1. Depth (Reference to Kelly Bushy)
2. Gamma-ray log (GR)
3. Neutron log (NPHI)
4. Density log (RHOB)
5. Sonic log (DT)
6. Deep Laterolog (LLD)
7. Deep Induction Log (ILD)
8. Shallow Laterolog (LLS)
9. Spherically Focused log (SFLU)
10. Microspherically Focused Log (MSFL)
11. Photoelectric Effect Log (PEF)
12. Caliper log (CALI)

The above data are displayed as curves and gathered as a group in specific tracks during analysis, depending on their use. Thus, the combined NPHI - RHOB, LLD - LLS, ILD - MSFL or ILD - SFLU are made possible.

Petrophysical properties are derived from the input data for the selected interval along the studied wells and automatically calculated by the software. They are subsequently digitized as models to determine corresponding reservoirs quality.

The specific petrophysical parameters calculated are:

I. Volume of shale (V_{sh})
II. Total porosity (φ_T)
III. Effective porosity (φ_{eff})
IV. Water saturation (S_w)
V. Bulk volume of water (BVW)
VI. Hydrocarbon saturation (S_{hc})
VII. Irreducible water saturation (S_{wir})
VIII. Permeability (K)

5.1. Petrophysical characteristics of reservoir zones

Physical properties of rocks are estimated through quantitative analysis of the wireline logs. These properties are defined by their respective formula and depend on the change in geology of the reservoir with depth as recorded by geophysical tools.

Characterizing a reservoir also requires qualitative parameters which will depend on specific reservoir characteristics such as lithology (sandstone, limestone), reservoir fluid (oil, water, gas), rocks sorting (fine grained, coarse grained, medium grained, shaly, clean, porous, fractured) but also on materials used while drilling the well such as the type of drilling fluid (fresh water mud, saline water mud, or oil based mud).

In carrying out the detailed petrophysical analysis of Cretaceous reservoirs within the study area, applicable formulas were processed in IP to generate them.

5.1.1. Volume of shale (V_{sh})

The shale volume is needed to correct the porosity and water saturation, for their biased effects. It is considered as an indicator of reservoir quality in which the lower shale content usually reveals a better reservoir.

The value of clay content is derived from different shale indicators such as gamma-ray, neutron, and resistivity. The following methods are the most common used depending on the correctness of the parameter.

5.1.2. Gamma-ray method

It is one of the best methods used for identifying and determining shale volume, principally due to its sensitive response to radioactive minerals normally concentrated in the shaly formation.

According to figure 5.1, considering the maximum average gamma ray log value to be pure 100% shale (shale line) and lowest value to indicate no shale at all (sand line), a scale from 0-100% shale can be constructed. If the scale is considered to be linear, any value (GR) of the gamma-ray log will give the gamma-ray index from the linear equation:

$$\mathrm{IGR} = \frac{\mathrm{GR\ (log)} - \mathrm{GR(min)}}{\mathrm{GR(max)} - \mathrm{GR(min)}} \qquad (1)$$

Where:

IGR = Gamma-ray Index

GR (log) = Gamma-ray reading from the log

GR (min) = Gamma-ray sand line

GR (max) = Gamma-ray shale line

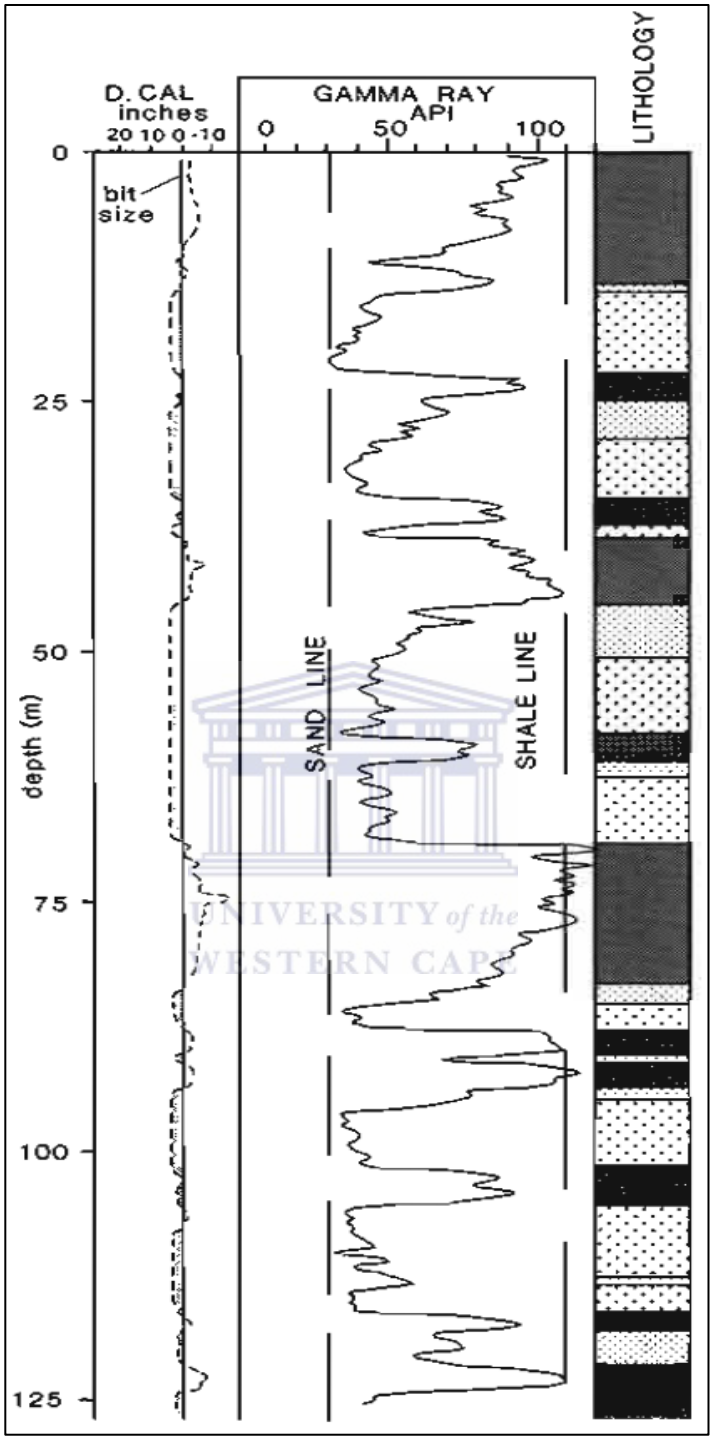

Figure 5.1: Sand line and shale line defined on a gamma-ray log. These baselines are for the quantitative use of the log (Rider, 1996).

Generally, the value IGR is not very accurate and tends to give an upper limit to the volume of shale. Moreover, there is no scientific basis for assuming that the relationship between

gamma-ray value and shale volume should be linear. Thus, Dresser Atlas (1982) proposed a new approach as a result of empirical correlation where the relationship changes according to the age or volume content of the formation.

1. Older rocks (Paleozoic and Mesozoic), consolidated:

$$Vsh = 0.33\ (2^{2IGR} - 1) \quad (2)$$

2. Younger rocks (Tertiary), unconsolidated:

$$Vsh = 0.083\ (2^{3.7IGR} - 1) \quad (3)$$

Steiber also suggested an empirical equation:

$$Vsh = 0.5\ (IGR / (1.5 - IGR)) \quad (4)$$

Where:

Vsh = Volume of shale

5.1.3. Neutron Method

The use of neutron logs to calculate the volume of shale is mostly effective in case of high clay content and low effective porosity. It measures the Hydrogen content of a formation and can be determined using the following equation:

$$Vsh \leq \frac{\Phi neulog}{\Phi neushale} \quad (5)$$

Where:

Vsh = Volume of shale

Φneulog = neutron log reading for each studied zone

Φneushale = neutron log reading in front of a shaly zone

5.1.4. Spontaneous Potential Method

The shale content could also be determined from the spontaneous potential log based on the following relationship:

$$\mathrm{Vsh} = \frac{\mathrm{SPclean} - \mathrm{SPlog}}{\mathrm{SPclean} - \mathrm{SPshale}} \quad (6)$$

Where:

Vsh = Volume of shale

SPlog = SP log reading for study zone

SPclean = maximum SP deflection from a nearby clean wet zone

SPshale = SP value within a shale formation

5.1.5. Resistivity Method

This method can be utilized to calculate the volume of shale in case of high clay content and low deep resistivity (Rt) value from the relation below:

$$\mathrm{Vsh} \leq \frac{\mathrm{Rsh}}{\mathrm{Rtlog}} \quad (7)$$

If this ratio is less than 0.5 (i.e. Vsh ≤ 0.5) then:

$$Z = \frac{\mathrm{Rclay}}{\mathrm{Rt}} \times \frac{(\mathrm{Rclean} - \mathrm{Rt})}{(\mathrm{Rclean} - \mathrm{Rclay})} \quad (8)$$

In the case Rt> 2Rclay, then

$$\mathrm{Vsh} = 0.5 \times (2 \times Z)^{0.67 \times (Z+1)} \quad (9)$$

Otherwise, Vsh = Z.

Where:

Rclay =Resistivity of a shaly zone

Rclean = Resistivity log reading for a clean formation

Rsh = Resistivity of the adjacent shale unit

5.1.6. Correction of shale Volume

The value Z or Vsh obtained previously have to be corrected by valid formula, to determine the optimum value usable in the log interpretation.

1. Clavier correction formula (clavier et al, 1971):

$$Vsh = 1.7\ (3.38 \times (Z + 0.7)^2)^{0.5} \quad (10)$$

2. Larionov (tertiary rocks):

$$Vsh = 0.33\ (2^{2\times Z} - 1) \quad (11)$$

3. Steiber method (1973):

$$Vsh = \frac{0.5 \times Z}{1.5 - Z} \quad (12)$$

However, different formations were classified into clean, shaly and shale zones according to the following bases:

- If Vsh ≤ 10 % we are in a clean zone
- If 10 % <Vsh ≤ 35 % We are in a shaly zone
- If Vsh> 35 % we are in a shale zone

5.1.7. Porosity (φ) and effective porosity (φ_{eff})

Porosities in the reservoir rocks usually range from 5 % to 48 % depending of the arrangement (cubic or rhombohedral), size and sorting of the rock. In general, porosities tend to be lower in deeper and older (consolidated) formations, due to cementation and overburden pressure stress on the rock. Likewise, the porosity of shale decreases rapidly with depth than sand (Rider, 1996).

As emphasized in chapter three, there are many descriptions of porosity, but the two common are the total and the effective porosity.

Total porosity can be estimated from a single log (sonic, density and neutron) or the combination of two logs (neutron – density), while effective porosity involves subtraction between total porosity and volume of shale.

- **Sonic porosity (Φ_S, φ_{eff})**

The porosity estimated from the sonic log does not see fractures and vugs; therefore it only reacts to primary porosity.

i. The determination of porosity depends on Wylie's et al. (1958) equation:

$$\Phi_S = \frac{\Delta T\log - \Delta Tma}{\Delta Tf - \Delta Tma} \qquad (13)$$

In the case the compaction factor is considered, the equation became:

$$\Phi_S = \frac{\Delta T\log - \Delta Tma}{\Delta Tf - \Delta Tma} \times \frac{1}{CP} \qquad (14)$$

With: $CP = \frac{\Delta Tsh}{100}$

ii. The effective porosity formula derived was suggested by Dresser Atlas (1979):

$$\Phi_{Seff} = \left(\frac{\Delta T\log - \Delta Tma}{\Delta Tf - \Delta Tma} \times \frac{1}{CP}\right) - \left(\frac{\Delta Tsh - \Delta Tma}{\Delta Tf - \Delta Tma}\right) \qquad (15)$$

Where:

Φ_S = Sonic porosity

Φ_{Seff} = effective porosity

$\Delta T\log$ = Formation of interest sonic log reading

ΔTma = Matrix travel-time

ΔTf = Mud fluid travel-time

ΔTsh = Transit time within shale material

CP = Compaction factor

Vsh = Volume of shale.

The mud fluid travel time used in this study is water saline and corresponds to ΔTf = 189 μs / ft.

- **Density porosity (Φ_D, φ_{Deff})**

Density tool reads extremely high porosity values.

i. Density porosity can be determined from the relationship below:

$$\Phi_D = \frac{\rho ma - \rho b}{\rho ma - \rho f} \quad (16)$$

ii. The effective porosity derived is expressed as follows:

$$\Phi_{Deff} = \left(\frac{\rho ma - \rho b}{\rho ma - \rho f}\right) - Vsh \left(\frac{\rho ma - \rho sh}{\rho ma - \rho f}\right) \quad (17)$$

Where:

Φ_D = Density porosity

ϕ_{Deff} = Effective porosity

ρma = Matrix density

ρb = Bulk density measured by the tool

ρsh = Shale zone density

Vsh = Volume of shale

ρf = Fluid density.

Fluid density ρf and matrix density ρma (table 5.1) varies respectively according to the fluid injected during drilling and the lithology of the formation.

For:

Fresh water mud, ρf = 1.0 g/cm^3

Salt water mud, ρf = 1.1 g/cm^3

Gas mud, ρf = 0.7 g/cm^3.

Table 5.1 Densities of common lithologies (Rider, 1996).

Lithology	Range (g/cm^3)	Matrix (g/cm^3)
Shale	1.8 – 2.75	Varies (Av. 2.65 – 2.70)
Sandstone	1.9 – 2.65	2.65
Limestone	2.2 – 2.71	2.71
Dolomite	2.3 – 2.87	2.87

- **Neutron porosity (Φ_N)**

Neutron logs give directly the porosity values on the log track in a clean formation. It is different from the density and sonic tools because it can read extremely low porosity within a formation. However in shaly formations, the effect of clays must be corrected through the following formula:

$$\Phi N_c = \Phi N_{log} - Vsh \times \Phi N_{sh} \quad (18)$$

Where:

ΦN_c= Neutron porosity corrected

ΦN_{log} = Formation of interest neutron log reading

ΦN_{sh} = Neutron shale zone

Vsh = Volume of shale.

- **Neutron – Density porosity ($\varphi_{N\text{-}D}$, $\varphi_{N\text{-}Deff}$)**

The combination of a neutron log which measures the Hydrogen Index (fluid content) of a formation, and bulk density log which reads both the matrix and fluid content of a formation is considered as a good approach for determining porosity.

i. The total porosity is calculated from the method below:

$$\phi_{N\text{-}D} = 0.5\ (\phi_N - \phi_D) \quad (19)$$

ii. The effective porosity is:

$$\phi_{N\text{-}Deff} = (0.5 \times (\phi_{NC}^2 + \phi_{DC}^2))^{0.5} \quad (20)$$

Where:

$$\phi_{NC} = \phi_N - \left(\frac{\phi Nsh}{0.45}\right) \times 0.30 \times Vsh$$

$$\phi_{DC} = \phi_D - \left(\frac{\phi Nsh}{0.45}\right) \times 0.13 \times Vsh$$

5.1.8. Formation water resistivity (Rw)

The formation water resistivity is the resistivity value of the water, uncontaminated by the drilling mud and that saturates the porous formation.

It is estimated during reservoir core analysis, from clean non-shaly water filled sandstone using the relationship between formation factor and shale free, water filled rock defined by Archie in 1942.

The method consists of saturating cores of different porosities with varieties of brines. The resistivity of the water (Rw) and the resistivity of the 100 % water saturated rock (Ro) are measured. Then, the results are plotted and the series of straight lines of slopes are referred to as the electrical formation factor F (Bateman, 1985).

Archie also discovered from other experiments that the rock formation factor could be related to the porosity of the rock . Therefore, the rock formation factor F is defined as the resistivity of a rock sample completely saturated with water (Ro) to the resistivity of the water (Rw). The relationship derived is:

$$F = \frac{Ro}{Rw} \quad (21) \qquad \text{Related to} \qquad F = \frac{1}{\Phi^m} \quad (22)$$

Where:

F = Rock formation factor

Ro = Resistivity of a rock 100 % water saturated

Rw = Resistivity of water

Φ = Porosity

m = Cementation exponent.

Few years later, Winsauer and McCardell (1953) also conducted some experimental measurements on cores, and this resulted in another equation relating F and Φ of the form:

$$F = \frac{a}{\Phi^m} \quad (23)$$

Where:

F = Rock formation factor

a = Tortuosity factor

Φ = Porosity

m = Cementation exponent.

By rearranging (21) = (23)

$$Rw = \left(\frac{\Phi^m}{a}\right) \times Ro \qquad (24)$$

In shaly zones, Crain (2004) recommended the following parameters:

For tight sandstones, a = 0.81 and m = 2.00 (F < 15 %)

For porous sandstones, a = 0.062 and m = 2.15 (F > 15 %)

For carbonates, a = 1 and m = 2.

The water resistivity can also be estimated from Spontaneous Potential log in water bearing clean sandstone, from the following relationship:

$$RwSP = - Tf \log (Rmfe / Rwe) \qquad (25)$$

Where:

RwSP = Static SP in mV

Tf = Temperature of the formation

Rmfe = Equivalent resistivity of mud filtrate

Rwe = Resistivity of formation water

This equation may not be used to wells drilled with an oil based mud because SP measurements will not be generated. Likewise, SP readings are reduced in shaly formations and oil bearing zones (Bateman, 1985).

Another equation used to estimate the water resistivity of a formation is below:

$$Rw = (Rmf \times Rt) / Rxo \qquad (26)$$

Where:

Rt = Resistivity of the uninvaded zone

Rxo = Resistivity of the flushed zone

Rmf = Resistivity of the mud filtrate

Rw = Resistivity of the water formation.

5.1.9. Formation resistivity (Rt, Rxo)

The formation resistivity Rt and Rxo are taken directly from the logs. Rxo represents the invaded or flushed zone resistivity and is directly read from Spherically Focused Log (SFLU), Microspherically Focused Log (MSFL) and Shallow Laterolog (LLS), while Rt refers to the uninvaded zone resistivity or true formation resistivity recorded by Deep Induction Log (ILD) and Deep Laterolog (LLD).

5.1.10. Water saturation (S_w)

Different methods can be used to evaluate the water saturation of a reservoir formation:

- The Archie method which involves clean sandstone formations.
- The shaly sand method comprising the resistivity approach (Simandoux model, Poupon and Leveaux model, Schlumberger model, Indonesian model) and the conductivity approach (Waxman-smith model, Dual-water model, Juhasz model).

In this study, only Archie and resistivity (Poupon and Leveaux, Simandoux, Schlumberger) methods will be developed, because only resistivity tools were ran.

Archie developed an equation resulting from his experiment on voids saturation. He found that water saturation of the rocks could be related to their resistivity. The formula showed that increasing porosity will reduce the water saturation for the same resistivity in a clean (homogenous) formation. Thus, the relationship between those parameters was mathematically expressed as:

$$Sw = \left(\frac{a}{\Phi^m} \times \frac{Rw}{Rt}\right)^{1/n} \qquad (27)$$

Where:

Sw = Water saturation

a = Tortuosity factor

m = Cementation factor

n = Saturation exponent

Φ = Porosity of the formation

Rt = Deep resistivity of the formation.

Later on, Simandoux (1963) and Schlumberger (1972) developed adequate equations for shaly (heterogeneous) formations, shown as follow:

- Simandoux equation

$$\frac{1}{\mathrm{Rt}} = \frac{\mathrm{Vsh} \times \mathrm{Sw}}{\mathrm{Rsh}} + \frac{\mathrm{S_w^n} \times \Phi^{\mathrm{m}}}{\mathrm{a} \times \mathrm{Rw}} \qquad (28)$$

- Schlumberger equation

$$\frac{1}{\sqrt{\mathrm{Rt}}} = \mathrm{S_w^{n/2}} \times \left(\frac{\mathrm{Vsh}^{\left(1-\frac{\mathrm{Vsh}}{2}\right)}}{\sqrt{\mathrm{Rsh}}} + \frac{\Phi^{\mathrm{m/2}}}{\sqrt{(\mathrm{a} \times \mathrm{Rw})}} \right) \qquad (29)$$

Where:

Rsh = Resistivity of a thick shale unit.

Poupon and Leveaux (1971) proposed an empirical model based on characteristic of fresh water and high degree of shaliness that were present in many oil reservoirs in Indonesia:

$$\frac{1}{\sqrt{\mathrm{Rt}}} = \mathrm{S_w^{n/2}} \times \left(\frac{\sqrt{\Phi \mathrm{e}^{\mathrm{m}}}}{\mathrm{a} \times \mathrm{Rw}} + \frac{\mathrm{Vsh}^{\left(1-\frac{\mathrm{Vsh}}{2}\right)}}{\sqrt{\mathrm{Rsh}}} \right) \qquad (30)$$

5.1.11. Bulk volume of water (BVW)

It is the product of water saturation (Sw) and porosity (Φ). The formula used to determine BVW is:

$$BVW = Sw \times \Phi \quad (31)$$

5.1.12. Hydrocarbon saturation (S_{hc})

The hydrocarbon saturation can be deduced from water saturation by the following relationship:

$$Shc = 1 - Sw \quad (32)$$

It is normally differentiated into the non-exploitable or residual hydrocarbon (S_{hr}) and the exploitable or movable hydrocarbon (S_{hm}), as follow:

$$Shc = Shr + Shm \quad (33)$$

5.1.13. Irreducible water saturation (S_{wir})

It is the residual water around the grain of rocks that cannot be moved out of the reservoir with oil or water.

- In a clean formation,

$$Swir = \Phi_e \times Sw \quad (34)$$

- In shaly formation,

$$Swir = \frac{\Phi T \times Sw}{1 - Vsh^2} \times \Phi_e \quad (35)$$

Where:

Swir = Irreducible water saturation

Φ_T = Total porosity

Sw = Water saturation

Vsh = Volume of shale

Φ_e= Effective porosity

5.1.14. Permeability (K)

The permeability can be predicted from different models:

- The Wyllie and Rose equation:

$$\sqrt{K} = C \times \Phi^3 / Swir \quad (36)$$

Where:

K = Permeability

C = Factor that depends on the density of the hydrocarbon.

Φ = Porosity

Swir = Irreducible water Saturation

- The Morris and Biggs (1967) as model modified by Timur in 1968 and Schlumberger in 1972 as follows:

$$K = a \times (\Phi^b / Swir^c) \quad (37)$$

Where:

K = Permeability

Φ= Porosity

Swir = Irreducible water saturation

The constants a, b and c for Timur, Morris-Biggs, and Schlumberger models are given below:

Morris-Biggs for gas:	a= 6241; b = 6 and c = 2
Timur:	a = 8581; b = 4.4 and c = 2
Schlumberger:	a = 10000; b = 4.5 and c = 2

- In the case where laboratory measurements are available, a function can be estimated from the crossplot of core porosity against core permeability, and then applied to the non-core wells for permeability prediction.

5.2. Results

Interactive Petrophysics software was used to generate composite models of lithology, resistivity tools and calculated petrophysics properties within potential hydrocarbon bearing zones, derived from probable reservoir zones.

All the petrophysical parameters estimated were exclusively determined from the wireline logs provided because no special core analysis, no drillstem testing, no repeating formation factor were conducted, and a conventional core analysis was performed only in well O-A1.

5.2.1. Volume of shale

The volume of shale was calculated based on the gamma-ray method because reservoir zone within the field of study are not high clay content, they all fall within sandstone dominating reservoirs.

The parameters used to determine the volume of shale are presented in table 5.2.

Table 5.2: Summary of parameters used for volume of shale calculations.

Well	GRmin (API)	GRmax (API)
O-A1	14.70	196.25
A-N1	44.53	139.13
P-A1	13.06	198.00
P-F1	9.93	253.50

The Steiber corrected method was used for evaluation because of its advantage of deleting likely initial high responses of a GR log to a small amount of shale.

The resulted average volume of shale is presented in table 5.3, indicating a clean sandstone reservoir within well O-A1 zone 1(Vsh ≤ 10.0 %). The table also shows shaly sandstone

reservoirs (If 10.0 % <Vsh ≤ 35.0 %) as the most common in all the wells, with the volume of shale increasing with depth.

Table 5.3: Average resulted volume of shale

WELL	RESERVOIR	DEPTH (m)	Vsh
O-A1	Zone 1	3793.0 – 3807.0	8.4
	Zone 2	4093.6 – 4106.7	17.0
A-N1	Zone 1	1970.0 – 2030.0	16.3
	Zone 2	2730.0 – 2743.0	33.6
P-A1	Zone 1	1772.8 – 1865.5	10.6
	Zone 2	2783.0 – 2910.0	17.0
P-F1	Zone 1	1284.0 – 1335.0	10.5
	Zone 2	1378.0 – 1400.0	12.9

An example model of the volume of shale is shown in figure 5.2 below, indicating the trend of the volume of shale in blue, within track 4 of reservoir zone 2 of well O-A1.

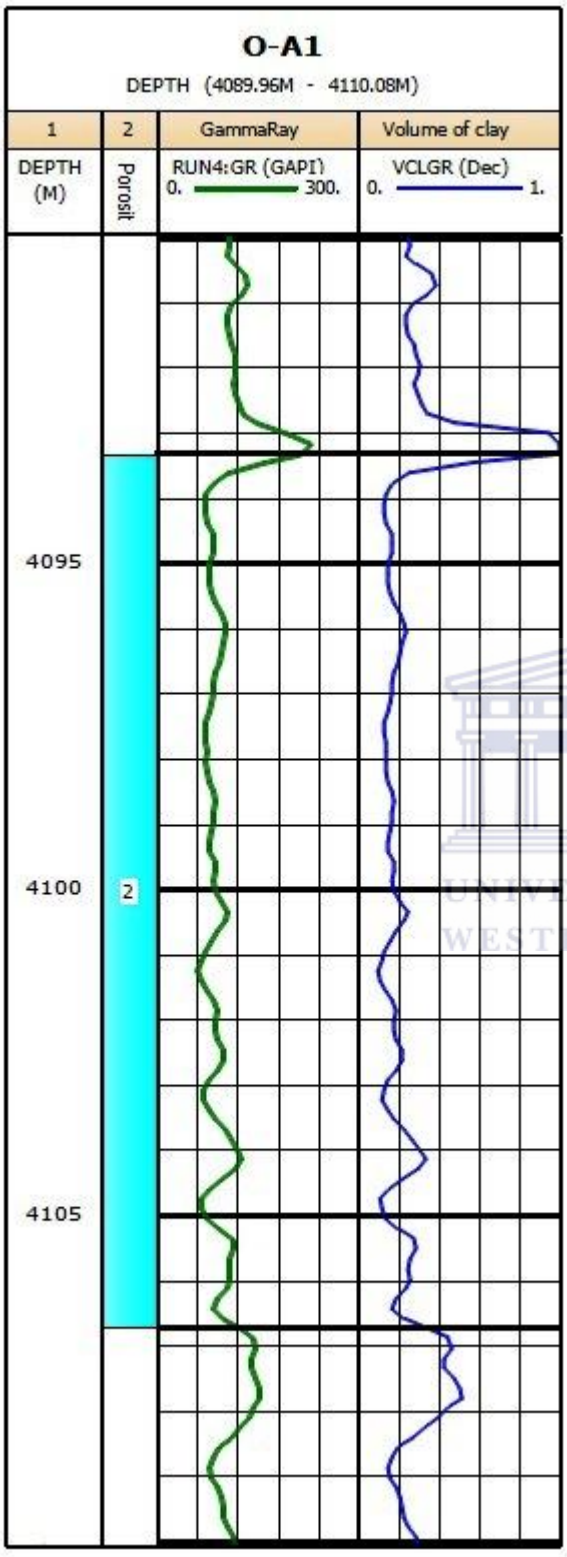

Figure 5.2: Volume of clay model of well O-A1 zone 2.

5.2.2. Porosity

A summary of parameters inputted to perform porosity models is tabulated below (table 5.4). It consists of: volume of shale, neutron clay, shale density, matrix density, sonic matrix and sonic clay.

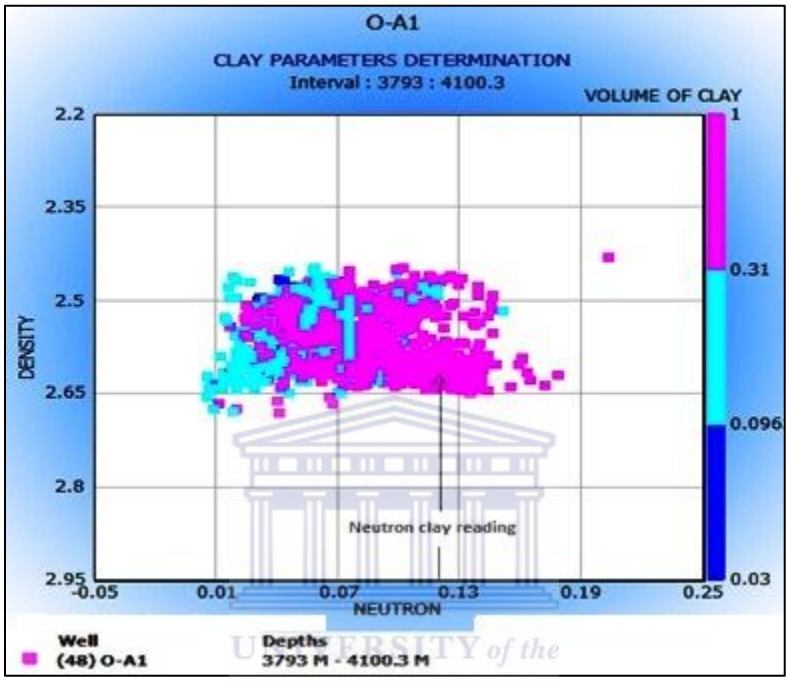

Figure 5.3: Example of neutron clay parameters determination in well O-A1.

Matrix density was chosen from table 5.1 because it was not measured for technical reasons according to well reports. Neutron and density clays were estimated from the crossplot of density volume of shale against neutron. Sonic matrix and sonic clay were estimated from the crossplot of density and volume of shale against sonic.

No neutron tool was run in well A-N1, therefore no neutron data was available and density clay was deduced from density-volume of shale against sonic plot.

An example of neutron-volume of shale against density plot is shown in figure 5.3 above, the other plotting can be found in appendix B.

Density porosity was executed in two of the studied wells: in O-A1 because it correlates well with the porosity values determined from the conventional core analysis from well O-A1 as shown by figure 5.4 below, where sonic porosity in black (PhiSon), neutron-density porosity in green (PhiND) and density porosity in red (PhiDen), are compared to the core porosity (black squares) respectively in track 3, 4 and 5.Density porosity is also used in well P-F1 because the density tool was the most reliable device geophysical data collection, according to the well report.

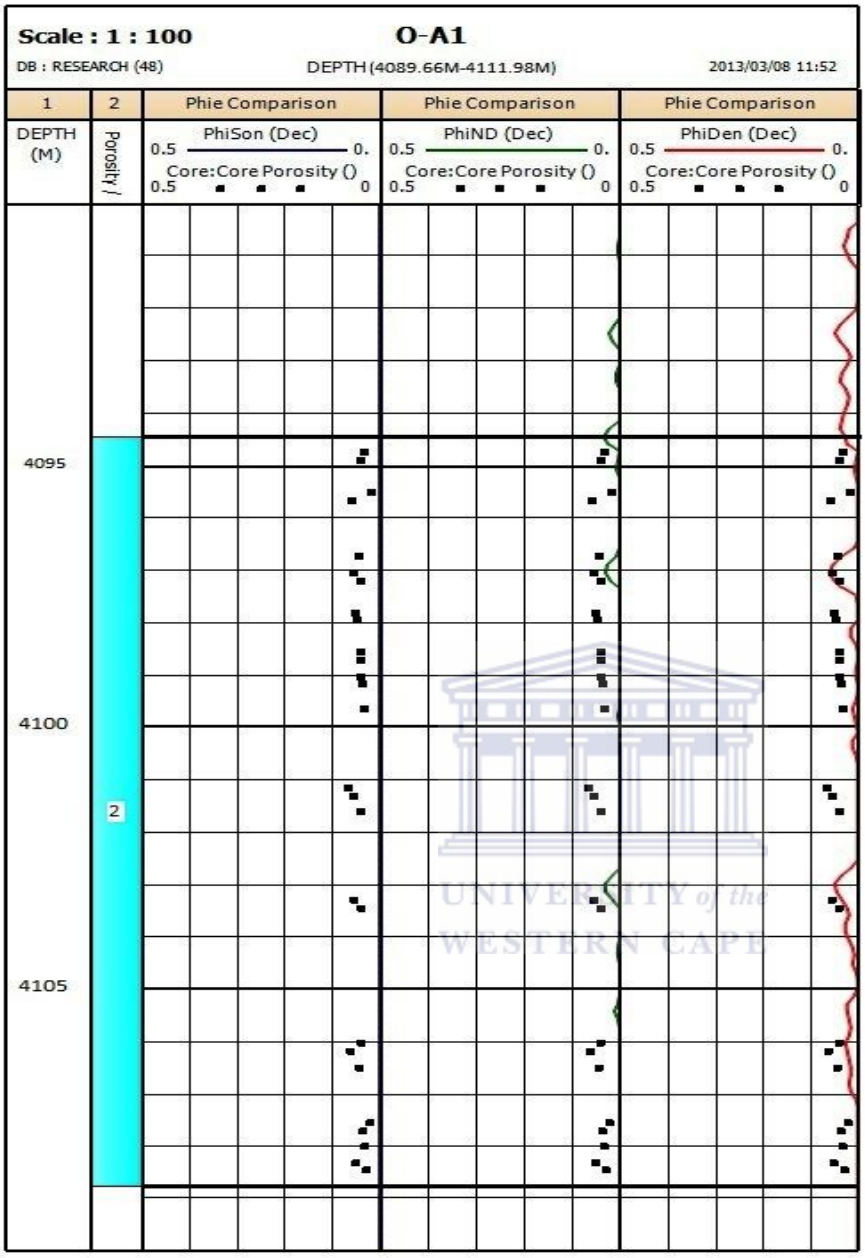

Figure 5.4: Comparison of log porosities with core porosity in well O-A1 reservoir zone 2.

Sonic porosity was selected in well A-N1 because no neutron tool was ran in the well and the high content of shale within reservoir zones could be neglected by density porosity, and the density porosity was also used in well P-A1 because the neutron tool was partly ran along the well and sonic did not yield satisfactory results.

Table 5.4: Summary of parameters used for porosity calculations.

WELL	RESERVOIR	DEPTH (m)	Vsh	NPHIclay (v/v)	RHOB clay (g/cc)	RHOB matrix (g/cc)	DTmatrix	DTclay
O-A1	Zone 1	3793.0 – 3807.0	8.4	0.12	2.6	2.65	66	73
	Zone 2	4093.6 – 4106.7	17.0					
A-N1	Zone 1	1970.0 – 2030.0	16.3					
	Zone 2	2730.0 – 2743.0	33.6	_	2.54	2.65	65	94
P-A1	Zone 1	1772.8 – 1865.5	10.6					
	Zone 2	2783.0 – 2910.0	17.0	0.20	2.50	2.65	64	78
P-F1	Zone 1	1284.0 – 1335.0	10.5	0.32	2.43	2.65	54	103
	Zone 2	1378.0 – 1400.0	12.9					

Table 5.5 corresponds to the average porosity calculated within the reservoir intervals of each well. Porosity decreases with depth within all the corresponding wells. P-F1 shows very good porosity, while O-A1 porosity is low.

Table 5.5: Average porosity results.

WELL	RESERVOIR	DEPTH (m)	Phi
O-A1	Zone 1	3793 – 3807.0	6.8
	Zone 2	4093.6 – 4106.7	5.5
A-N1	Zone 1	1970.0 – 2030.0	17.0
	Zone 2	2730.0 – 2743.0	6.6
P-A1	Zone 1	1772.8 – 1865.5	19.2
	Zone 2	2783.0 – 2910.0	6.0
P-F1	Zone 1	1284.0 – 1335.0	26.2
	Zone 2	1378.0 – 1400.0	25.5

5.2.3. Effective porosity

The effective porosity is obtained from the corresponding formulas in section 5.1.2 (equations 15, 17 and 20). The effective porosity of reservoir zones of well O-A1 and P-A1 was calculated with equation (17), while well P-F1 effective porosity was evaluated from model (20) and well A-N1 used relationship (15).

Effective porosity excludes all the bound water connected with shale, but implies all the voids linked in the pore system and that can contribute to flow. Table 5.6 below presents the parameters used to calculate effective porosity.

Table 5.6: Summary of parameters used for effective porosity calculations.

WELL	RESERVOIR	DEPTH (m)	Vsh	Phi
O-A1	Zone 1	3793.0 – 3807.0	8.4	6.8
	Zone 2	4093.6 – 4106.7	17.0	5.5
A-N1	Zone 1	1970.0 – 2030.0	16.3	17.0
	Zone 2	2730 – 2743	33.6	6.6
P-A1	Zone 1	1772.8 – 1865.5	10.6	19.2
	Zone 2	2783.0 – 2910.0	17.0	6.0
P-F1	Zone 1	1284.0 – 1335.0	10.5	26.2
	Zone 2	1378.0 – 1400.0	12.9	25.5

The respective average effective porosity results are displayed in the following table.

Table 5.7: Results of the average effective porosity calculations.

WELL	RESERVOIR	DEPTH (m)	Phi_{eff}
O-A1	Zone 1	3793.0 – 3807.0	6.2
	Zone 2	4093.6 – 4106.7	4.3
A-N1	Zone 1	1970.0 – 2030.0	14.8
	Zone 2	2730.0 – 2743.0	4.5
P-A1	Zone 1	1772.8 – 1865.5	19.0
	Zone 2	2783.0 – 2910.0	5.2
P-F1	Zone 1	1284.0 – 1335.0	25.4
	Zone 2	1378.0 – 1400.0	24.6

Figure 5.5 below represents the effective porosity model of well O-A1 reservoir zone 2. It trend is displayed in black within track 3.

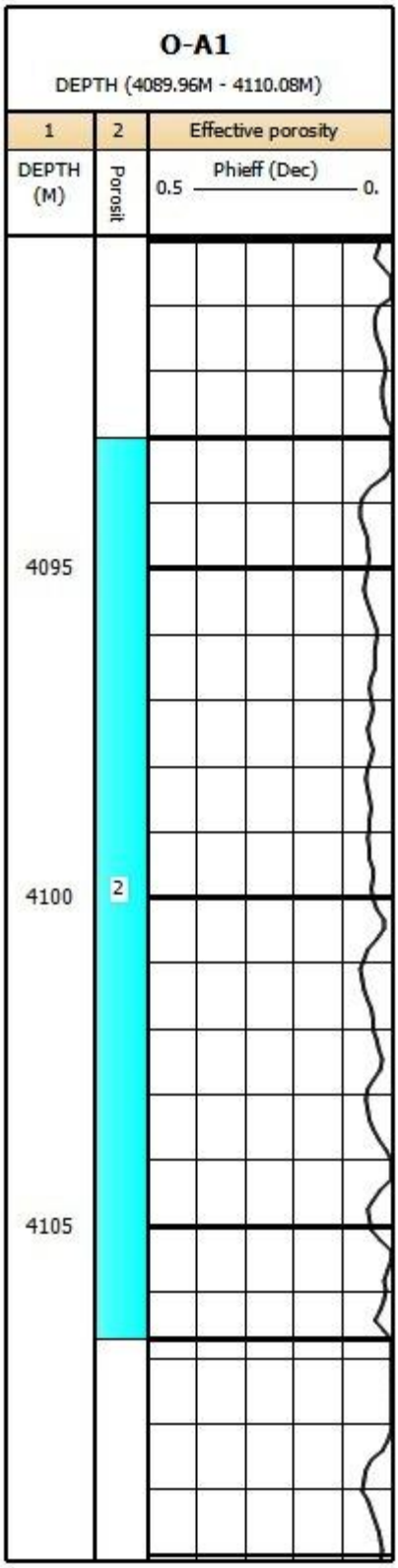

Figure 5.5: Effective porosity model of well O-A1 reservoir zone 2.

5.2.4. Water saturation, bulk volume of water and irreducible water saturation

Prior to fluid saturation calculations, resistivity and temperature parameters were determined.

- The formation temperature

It was deduced from the surface temperature, the log depth, the bottom hole temperature and the total depth by the following equation:

$$T_2 = \frac{L_D(T_{BH} - T_1)}{TD} + T_1 \qquad (38)$$

Where:

T_2 = Formation temperature

L_D = Log depth

T_{BH} = Bottom hole temperature (estimated from the geothermal gradient)

TD = Total depth

T_1 = Surface temperature.

- The resistivity of mud filtrate (Rmf)

The resistivity of mud filtrate was calculated at formation temperature, using the surface temperature in the log header information well. Therefore, the following relationship was applied:

$$Rmf_2 = Rmf_1 \frac{(T_1 + 6.77)}{(T_2 + 6.77)} \qquad (39)$$

Where:

Rmf_1 = Resistivity of mud filtrate at surface temperature

Rmf_2 = Resistivity of mud filtrate at formation temperature

- Resistivity of formation water (Rw)

The resistivity of formation water was determined by equation (26) and the parameters a, m and n were recommended fixed by Crain (2004), as no special core analyses were conducted. Likewise, the SP method could not be used because most of the reservoir intervals are shaly.

Table 5.8 is a summary of the average parameters estimated and used to calculate fluid saturation of reservoir zones.

Table 5.8: Summary of the parameters used to estimate fluid saturation.

WELL	RESERVOIR	DEPTH (m)	T_2 (^{o}c)	Rmf_2 (Ω)	Rt (Ω)	Rxo (Ω)	Rw (Ω)
O-A1	Zone 1	3793.0 – 3807.0	97.8	0.10	15.5	11.9	0.24
	Zone 2	4093.6 – 4106.7	106.8	0.20	30.7	26.7	0.40
A-N1	Zone 1	1970.0 – 2030.0	93.8	0.21	1.7	1.8	0.41
	Zone 2	2730.0 – 2743.0	120.1	0.12	5.9	7.3	0.13
P-A1	Zone 1	1772.8 – 1865.5	57.0	0.13	1.3	1.6	0.04
	Zone 2	2783.0 – 2910.0	93.6	0.05	13.2	18.9	0.08
P-F1	Zone 1	1284.0 – 1335.0	39.8	0.14	0.9	2.2	0.06
	Zone 2	1378.0 – 1400.0	42.2	0.17	1.1	2.4	0.08

The Simandoux equation was extensively used to estimate the water saturation within all targets because they were considered as shaly sandstone reservoir zones, while model (35) was applied for irreducible water saturation. The average fluid saturation of each of the reservoir zones is summarized in table 5.9 below. Only well O-A1 reservoir zone 2 and well P-A1 zone 2 show reasonable water saturation for further interest.

Figure 5.6 below is a representation of the saturation models within reservoir zone 1 of well O-A1. It displays in track 3 the trends of water saturation in blue (Swsim), irreducible water saturation in red (Swir) and bulk volume of water in green (BVW).

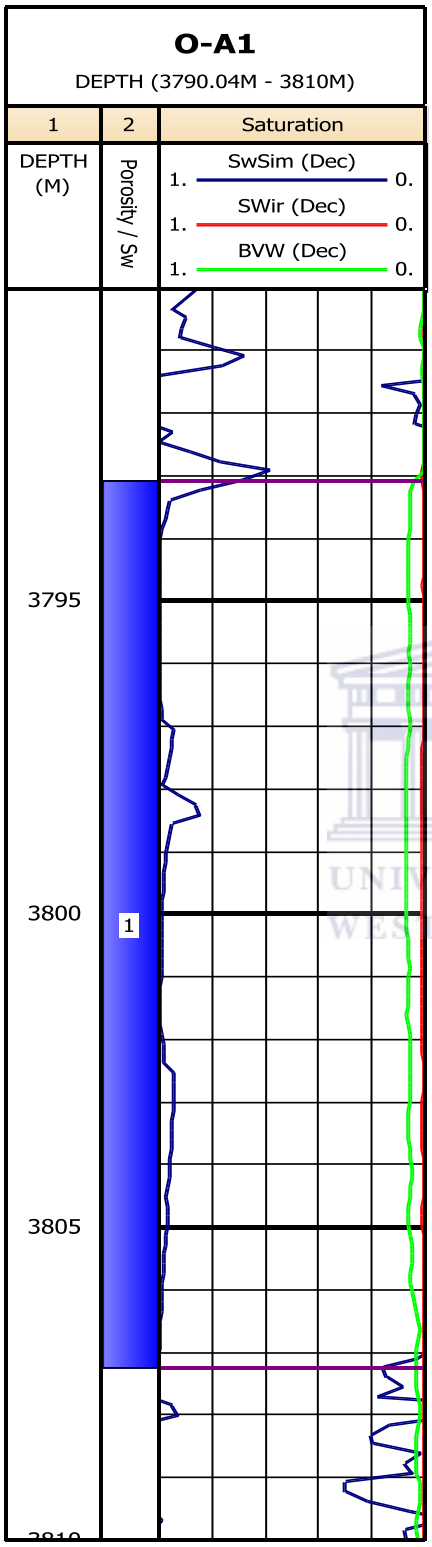

Figure 5.6: Fluid saturation trends of well O-A1 reservoir zone 1.

Table 5.9: Summary of the average fluid saturation calculated.

WELL	RESERVOIR	DEPTH	Sw	BVW	Shc	Swir
O-A1	Zone 1	3793.0 – 3807.0	89.1	6.4	10.9	0.4
	Zone 2	4093.6 – 4106.7	64.4	3.5	35.6	0.2
A-N1	Zone 1	1970.0 – 2030.0	89.8	17.6	10.2	8.8
	Zone 2	2730.0 – 2743.0	79.2	5.6	20.8	0.3
P-A1	Zone 1	1772.8 – 1865.5	87.3	23.6	12.7	4.1
	Zone 2	2783.0 – 2910.0	56.1	2.7	43.9	0.3
P-F1	Zone 1	1284.0 – 1335.0	89.6	31.8	10.4	8.3
	Zone 2	1378.0 – 1400.0	90.1	28.5	9.9	7.5

5.2.5. Predicted permeability

A function was derived from the core permeability-porosity crossplot of well O-A1, and was then extensively applied to the other wells.Figure 5.8 shows the regression line used to determine the relationship.

Figure 5.7 presents the trend of Morris-Biggs model (Kcomp) in red within track 3, compared to the core permeability (black squares) of well O-A1 reservoir zone 2; and in track 4 the comparison of K predicted (blue trend) which is the function derived from the core permeability-porosity crossplot of well O-A1, with the core permeability model (black squares). As a result, k predicted model best match the core permeability trend. It will be used to predict the permeability of the other wells.

Wyllie and Rose model could not be used because C was missing, while Timur and Schlumberger model gave very high results.

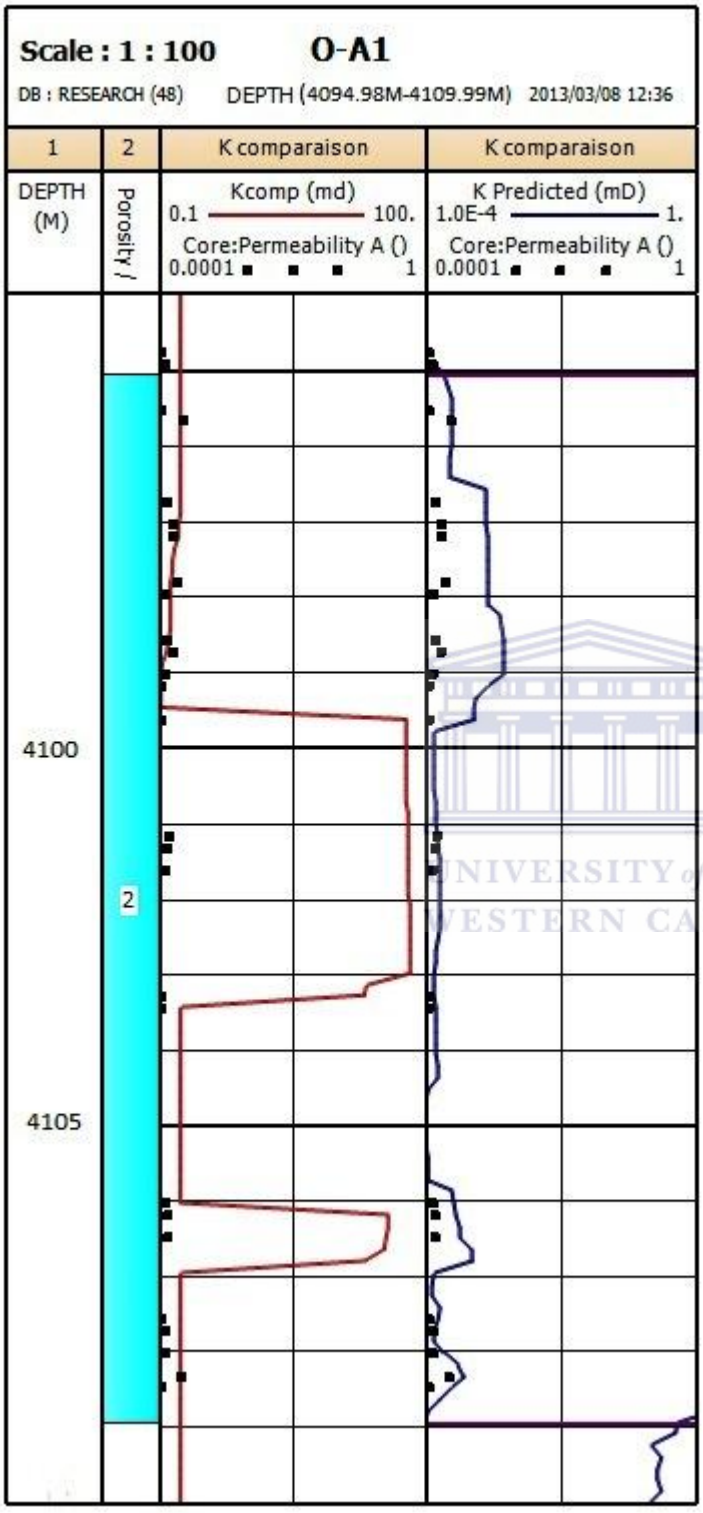

Figure 5.7: Comparison of core permeability with predicted permeability.

The function estimated is:

$$\text{Log } K = (-3.38 + 40.04) \times \phi \qquad (40)$$

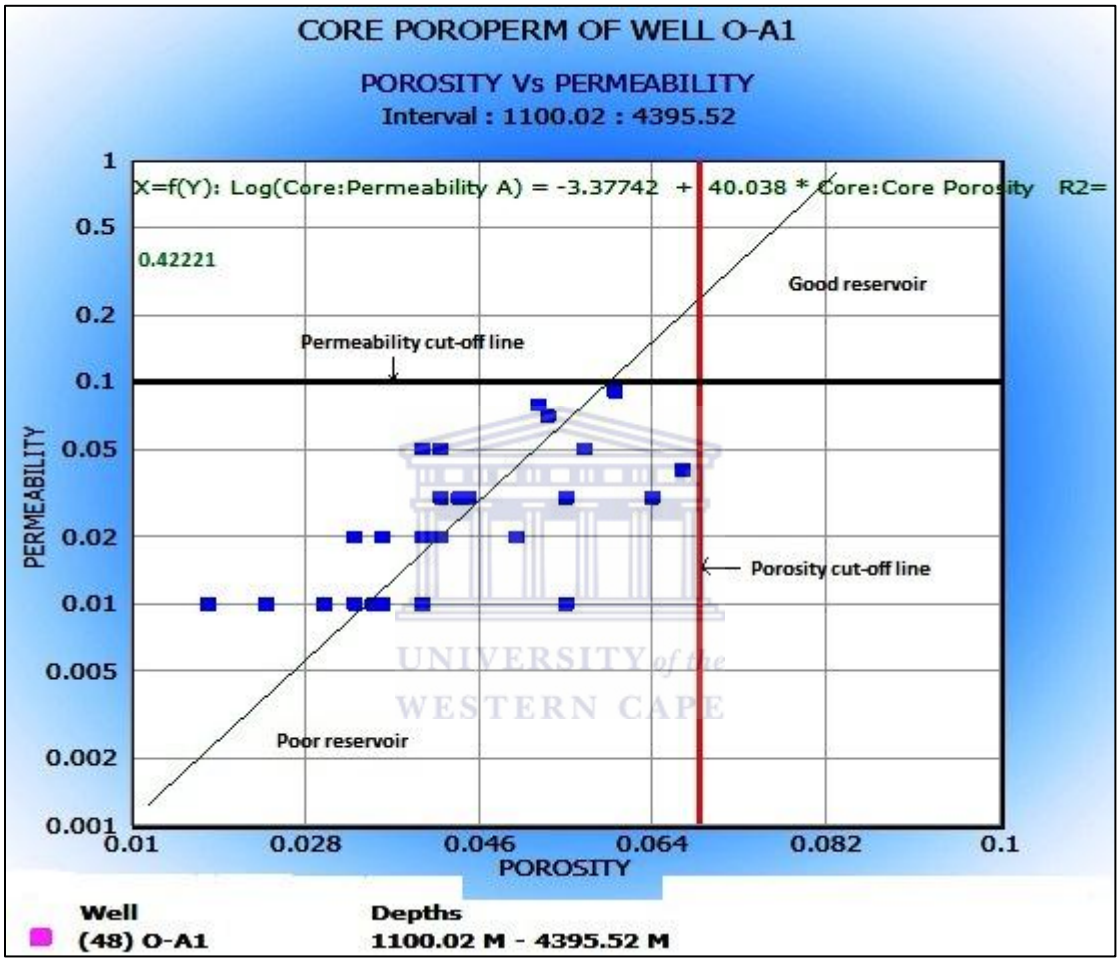

Figure 5.8: Crossplot of core poroperm of well O-A1.

The average predicted permeabilities for corresponding reservoir zones are tabulated below. As we can observe, good permeabilities are found in well P-A1 and P-F1.

Table 5.10: Average predicted permeability of the corresponding reservoir zones.

WELL	RESERVOIR	DEPTH (m)	$K_{Predicted}$
O-A1	Zone 1	3793.0 – 3807.0	0.35
	Zone 2	4093.6 – 4106.7	0.09
A-N1	Zone 1	1970.0 – 2030.0	0.69
	Zone 2	2730.0 – 2743.0	0.05
P-A1	Zone 1	1772.8 – 1865.5	0.95
	Zone 2	2783.0 – 2910.0	0.61
P-F1	Zone 1	1284.0 – 1335.0	1.60
	Zone 2	1378.0 – 1400.0	0.82

5.3. Interpretation

The resulted physical parameters and logging tool responses are digitized and displayed in respective well interpretation sections as:

- Depth (m)
- Reservoir zone
- Gamma-ray (API)
- Composite Deep – Shallow Resistivities (ohm)
- Predicted permeability (mD)
- Fluid saturation (fraction)
- Composite Porosity – Effective porosity (fraction)
- Lithology

This section of the study focuses on the application of petrophysical properties determined from geophysical well data. After identifying a potential reservoir based on its lithology, the next step consists of evaluating its quality. Hence, some petrophysical parameters calculated above will be interpreted to characterize potential and non - potential reservoirs. An appropriate approach to relate physical properties and reservoir quality is the application of the cut-off concept.

According to Worthington and Cosentino (2005), there is no single applicable method for determining a cut-off. The starting point in estimating a cut-off is to recognize reference parameters that will allow us to separate a good reservoir from a poor reservoir. The next step consists of evaluating the hydrocarbon potential and the flow rate of the reservoir in order to delineate a net pay zone that will produce hydrocarbon at a commercial rate.

A net pay zone represents any interval within the gross zone (reservoir zone) that contains sufficient producible hydrocarbons; it is controlled by a satisfactory permeability. In this research work, only absolute permeability has been considered and will be applied to a single fluid, since it does not take into account the reservoir fluid characteristics (Georges and Stiles, 1978).

Thereafter, minimum values need to be set for each property according to the type of rock and the field studied.

The reference parameters chosen for reservoir quality are: volume of shale, water saturation and porosity. A cut-off of permeability can be used later when a net pay zone is defined within a well, in order to evaluate the flow rate of hydrocarbon that will be extracted. The volume of shale and water saturation cut-offs are selected from Opuwari's (2010) studies in the same field, who set his reference values after identifying a dry well containing non-potential reservoir zones. Porosity and permeability cut-offs are derived from the conventional core analysis performed in well O-A1, based on the fact that the well was concluded to be dry and the target evaluated was a non-potential reservoir with a maximum core porosity ϕ = 7.0% and a maximum core permeability K = 0.09mD (figure 5.4). Table 5.11 below summarizes the respective cut-off values.

Table 5.11: Average cut-off values for gas reservoirs characterization.

Vsh	Phi	Sw	K_{Gas}
< 40.0 %	> 7.0 %	< 65.0 %	>0.09 mD

5.3.1. Reservoir zones of Well O-A1

The log analysis of well O-A1 was divided into two zones of interest with each zone being chosen to correlate with lithology. They are part of an aggradational sequence within supersequence II (figure 2.7). Zone 1 was chosen as the interval 3793.0 m – 3807.0 m corresponding to major sandstones interbedded with minor shales deposited during the Late Aptian, highly affects porosity (table 5.5) while zone 2 is a Barremian sandstone formation mixed with claystone extending from 4093.6 m to 4106.7 m (figure 5.9).

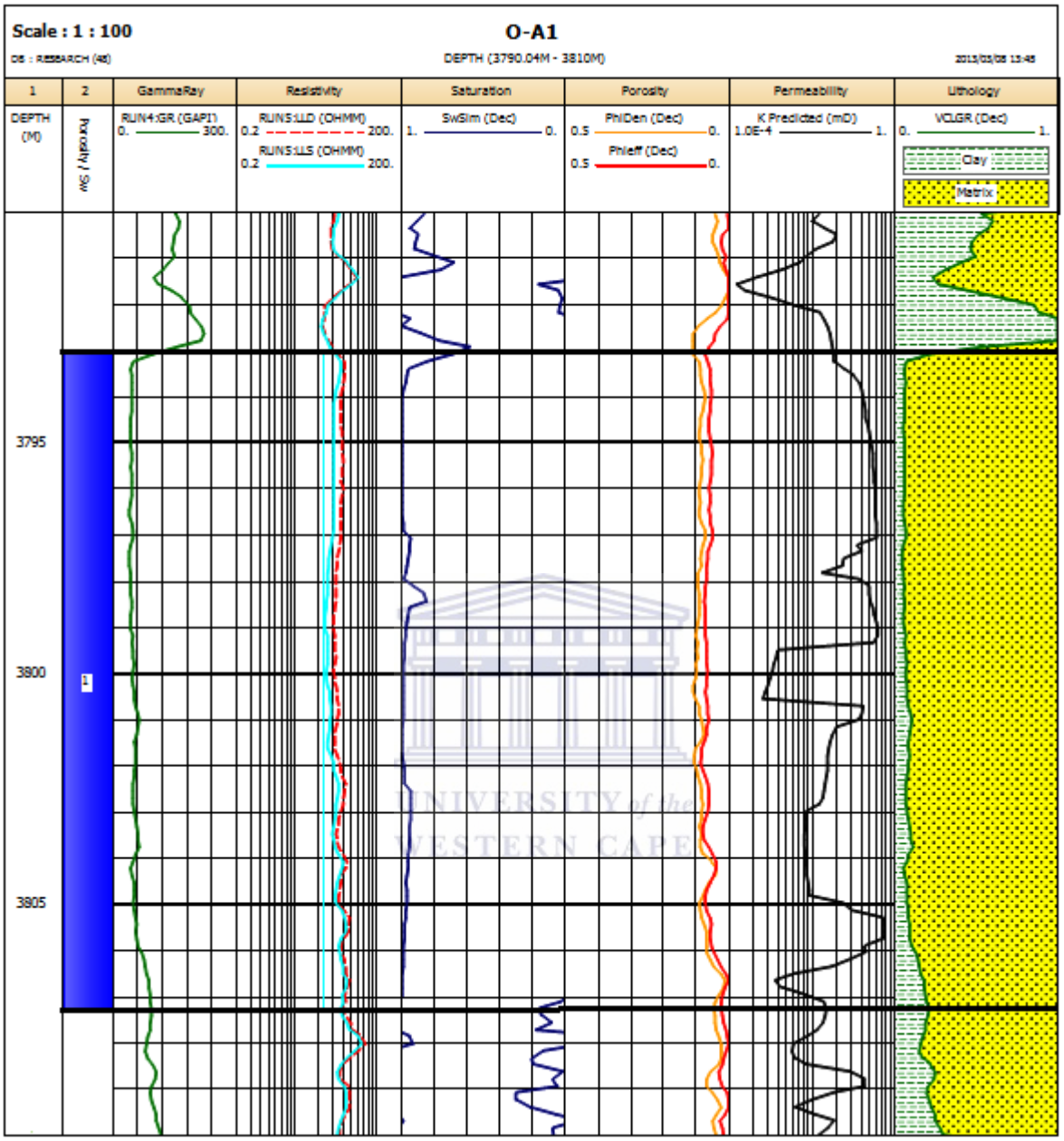

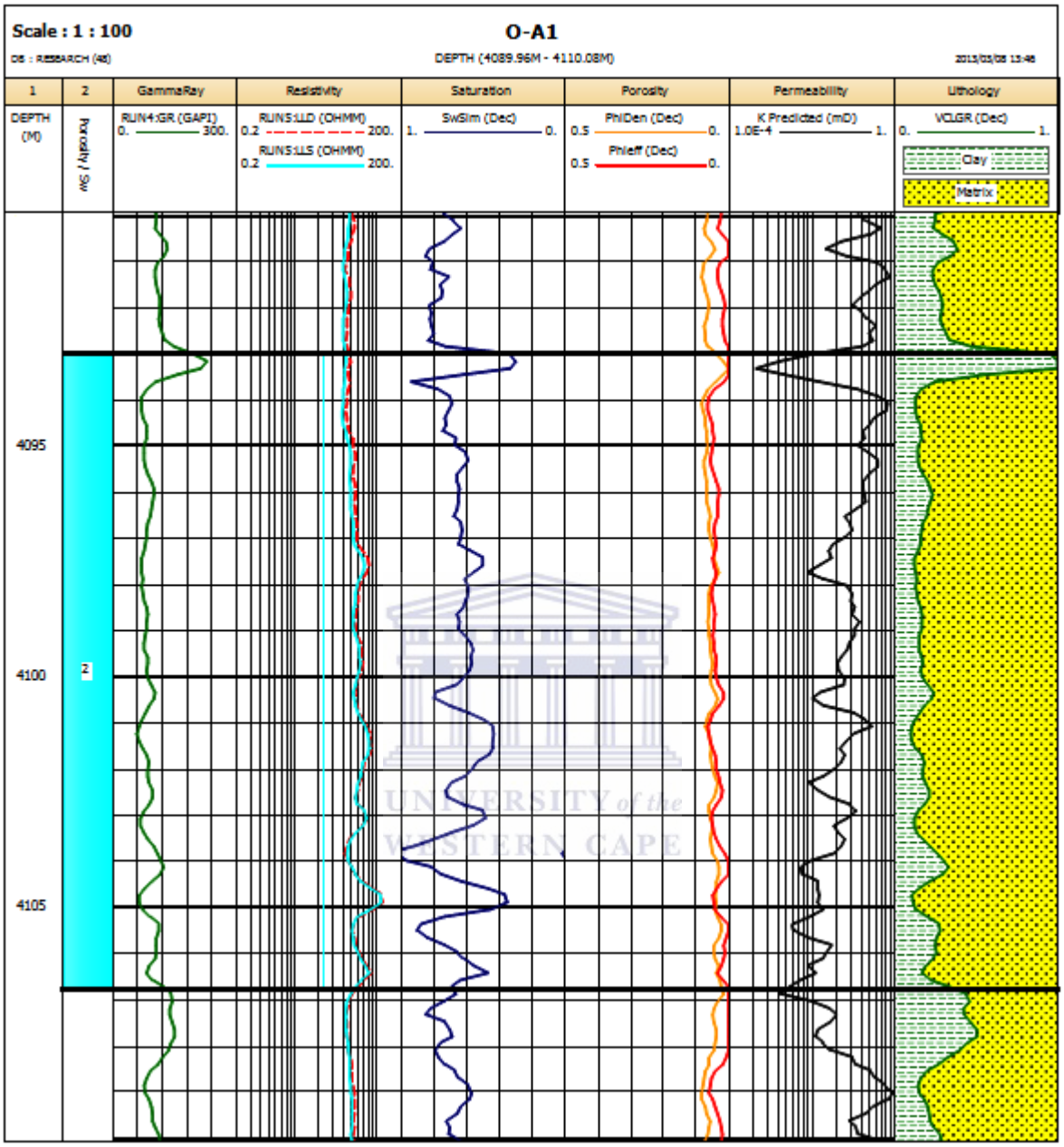

Figure 5.9: Digitized petrophysical properties, gamma-ray, resistivity and lithology models of well O-A1 reservoir zones 1 and 2.

The density porosity method was used to estimate the porosity of reservoir zones because it was the best model that fitted the conventional core porosity. The SP response tool was affected by the oil based mud filtrate between 3180.0 m – 4398.0 m which restricted the

formation water resistivity (Rw) calculations to equation (26), with an average resistivity mud filtrate Rmf_1 = 0.10 Ω for zone 1 and Rmf_2 = 0.20 Ω for zone 2.

An average Rw_1 = 0.24 Ω and Rw_2 = 0.40 Ω respectively for zone 1 and 2, were used for fluid saturation determination at temperature T_1 = 97.8^{o}c and T_2 = 106.8^{o}c, with the tortuosity factor, cementation factor and saturation exponent respectively a, m and n recommended by Crain (2004) as follow:

For tight sandstones, a = 0.81 m = 2.00 n = 2.00

The invaded and uninvaded zones' resistivity were deduced from average Shallow and Deep Laterolog within the corresponding zones as Rxo_1 = 11.9 Ω, Rxo_2 = 26.7 Ω and Rt_1 = 15.5 Ω, Rt_2 = 30.7 Ω.

Table 5.12 presents the summary of calculated pay zone parameters evaluated along well O-A1.

Table 5.12: Summary of calculated pay parameters for well O-A1.

RESERVOIR	TOP	BOTTOM	Gross	Net	Net/Gross	Av Phi	Av Sw	Av Vsh
ZONE 1	3793.0	3807.0	14.0	0.0	0.0	6.8	89.1	8.4
ZONE 2	4093.6	4106.7	13.1	0.0	0.0	5.5	64.4	17.0

An application of the cut-off concept on petrophysical properties within well O-A1 shows unsatisfactory results. Zone 1 bears an average water saturation too high to store sufficient hydrocarbons for economic production, and zone 2 is characterized by a low average porosity below the cut-off.

In summary, no net pay zone was identified within well O-A1.

5.3.2. Reservoir zones of well A-N1

Two targets were identified along well A-N1 and correlated according to chronostratigraphy. The first reservoir zone corresponds to 50.0 m fine grained sandstone interbedded with clay. It falls within the Earlier early Turonian. It is the result of a passive margin caused by an aggradational sequence. The second target is part of a succession of aggradation and progradation resulting in an accelerated subsidence along the shoreline, deposited during the Middle Albian. Its lithology is dominated by major sandstone and minor shale. Figure 5.10 below displays the models of physical properties and lithology for well A-N1.

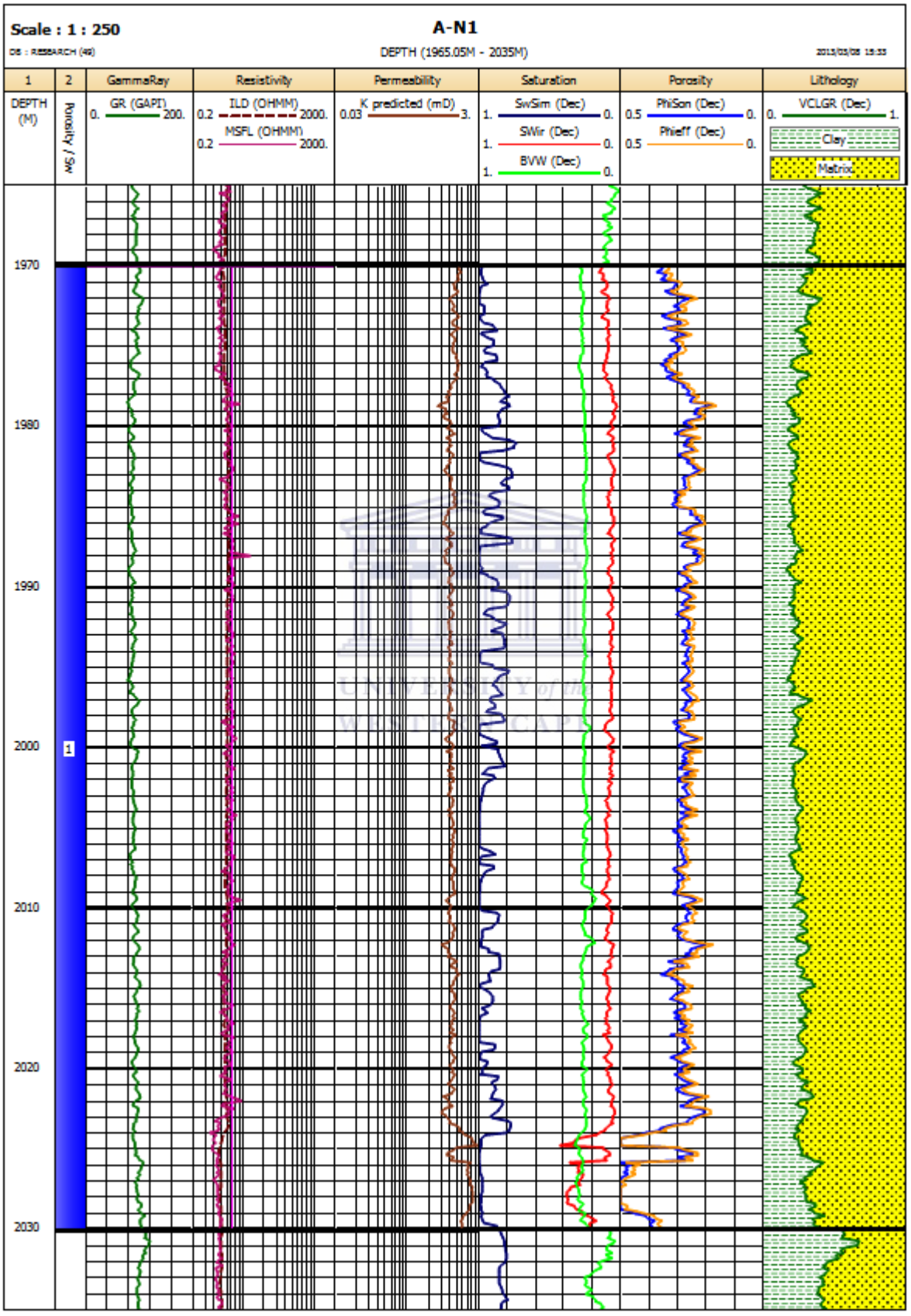
Scale : 1 : 250
A-N1
DEPTH (1965.05M - 2035M)
1
2
GammaRay
Resistivity
Permeability
Saturation
Porosity
Lithology
DEPTH (M)
Porosity / SW
GR (GAPI) 0. 200.
ILD (OHMM) 0.2 2000.
MSFL (OHMM) 0.2 2000.
K predicted (mD) 0.03 3.
SwSim (Dec) 1. 0.
SWir (Dec) 1. 0.
BVW (Dec) 1. 0.
PhiSon (Dec) 0.5 0.
Phieff (Dec) 0.5 0.
VCLGR (Dec) 0. 1.
Clay
Matrix
1970
1980
1990
2000
2010
2020
2030

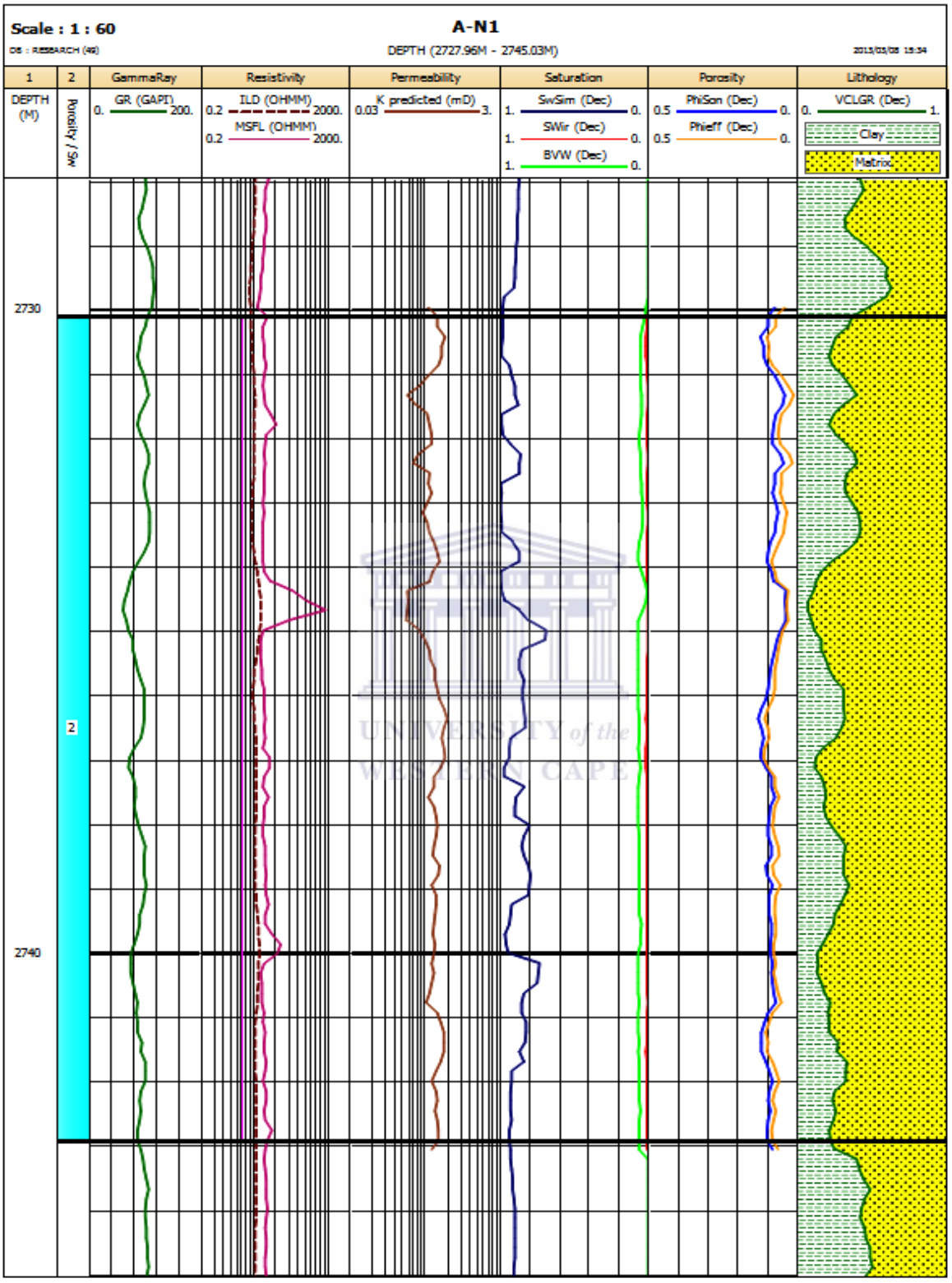

Figure 5.10: Digitized petrophysical properties, gamma-ray, resistivity and lithology models of well A-N1 reservoir zones 1 and 2.

The sonic porosity model was applied in well A-N1 to determine the total porosity of each of the reservoir zones because it was the only successful wireline. Equation (26) was the only appropriate method to estimate Rw, due to poor response to SP reading along shaly formations and the fact that no conventional core was drilled. The average resistivity values are summarized in table 5.8, with deep resistivity inferior to shallow resistivity in both zones. The formation water resistivity Rw was calculated at temperature $T_1 = 93.8^oc$ $T_2 = 120.1^oc$ for zone 1 and 2 respectively.

A summary of evaluated pay parameters for each reservoir zones is tabulated below.

Table 5.13: Evaluated pay zone parameters for well A-N1.

RESERVOIR	TOP	BOTTOM	Gross	Net	Net/Gross	Av Phi	Av Sw	Av Vsh
ZONE 1	1970.0	2030.0	50.0	0.0	0.0	17.0	89.8	16.3
ZONE 2	2730.0	2743.0	13.0	0.0	0.0	6.6	79.2	33.6

Reservoir zones are water bearing despite the fairly good average volume of shale within zone 1, and the satisfactory average porosity of zone 2.

In summary, there is no net pay zone identifiable within reservoir intervals of well A-N1.

5.3.3. Reservoir zones of well P-A1

The analysis of petrophysical properties of well P-A1 reservoirs was done in two sections of interest separated according to depositional environment. Section 1 was chosen as the interval 1350.0 m-2060.0 m consisting of transgressive shelf environment. It consists of coarsening upward sequence that shallows from upper slope at the base, to outer shelf higher up in the sequence deposited during the Aptian-Cenomanian period. A first target is identified in this section and corresponds to a thick sandstone formation interbedded between massive shale and modeled in figure 5.11.

The second section is chosen as the interval 2060.0 m-3200.0 m; it comprised interbedded, coarse, shallow marine sandstone formed during Lower Cretaceous. It also bears reservoir zone

2 located at depth 2783.0 m-2910.0 m and is composed of fine grained sandstone mixed with clay (figure 5.8).

Porosity was calculated using the density relationship because an attempt to run the neutron tool failed from 500.0 m-1400.0 m and its reading was non-consistent in the rest of the well. The sonic log was very constant along the reservoir zones and could not be used.

The same equation (26) that performs in the other wells was applied to estimate the formation water saturation due to no significant SP response. An average Rw_1 = 0.04 Ω and Rw_2 = 0.08 Ω was calculated at T_1 = 57.0^{o}c and T_2 = 93.6^{o}c, later used with a, m and n parameters recommended by Crain (2004) for tight sandstones to determine the fluid saturation. It is also noted that shallow resistivity is greater than deep resistivity along both zones. The results of reservoir zones' physical properties are gathered in table 5.14 below.

Table 5.14: Summary of pay parameters used to characterize the quality of reservoir zones within well P-A1.

RESERVOIR	TOP	BOTTOM	Gross	Net	Net/Gross	Av Phi	Av Sw	Av Vsh
ZONE 1	1772.8	1865.5	92.7	0.0	0.0	19.2	87.3	10.6
ZONE 2	2783.0	2910.0	127	0.0	0.0	6.0	56.1	17.0

Despite the good average porosity and satisfactory average volume of shale of zone 1, average high water saturation indicates a water bearing reservoir interval.

The reference petrophysical parameters of reservoir zone 2 are fairly good. Nonetheless, no net pay zone was identified.

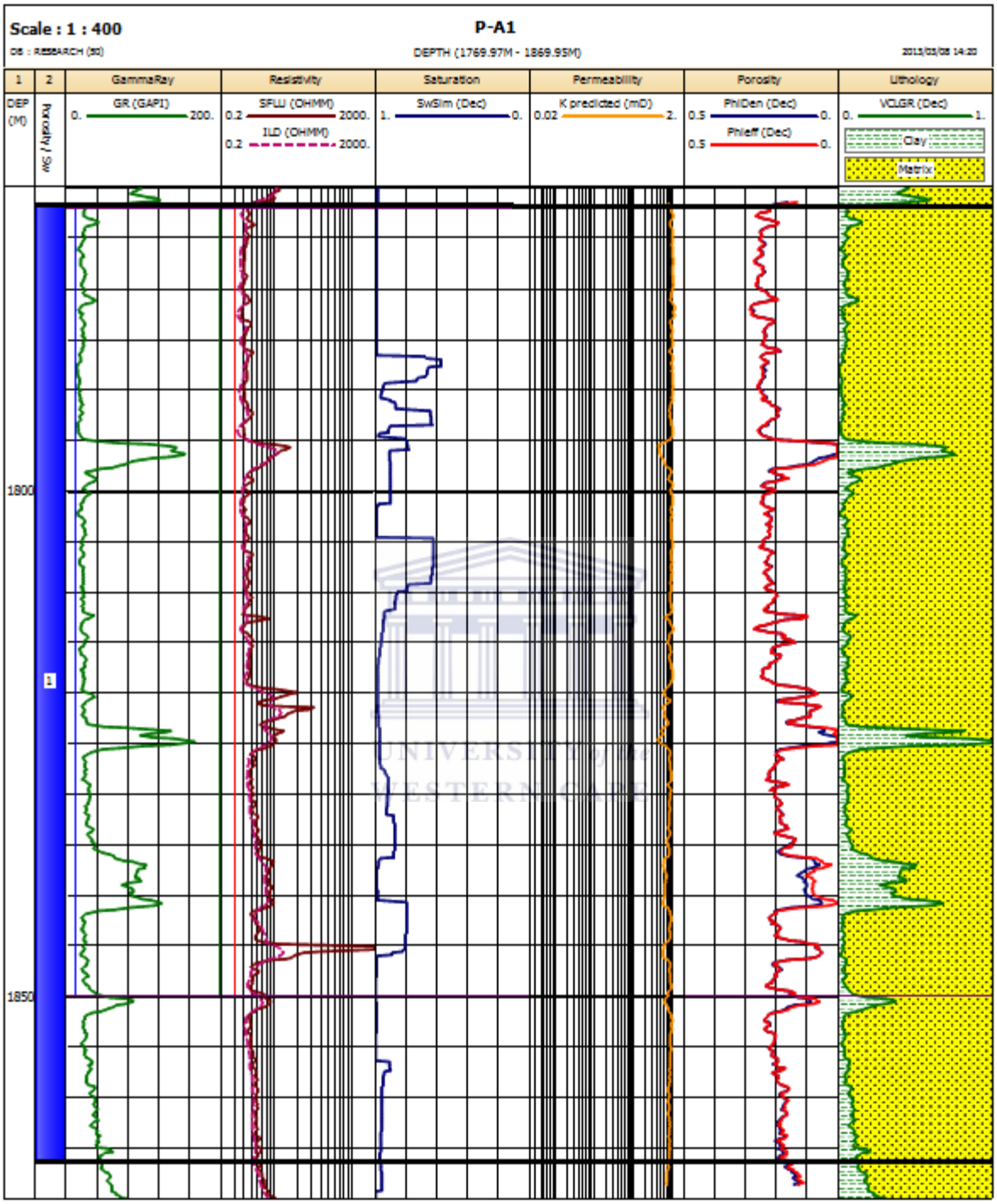
Scale : 1 : 400
P-A1
DEPTH (1769.97M - 1869.95M)
1
2
GammaRay
Resistivity
Saturation
Permeability
Porosity
Lithology
DEP (M)
Porosity / Sw
GR (GAPI)
0.
200.
SFLU (OHMM)
ILD (OHMM)
0.2
2000.
SwSim (Dec)
1.
0.
K predicted (mD)
0.02
2.
PhiDen (Dec)
PhiEff (Dec)
0.5
VCLGR (Dec)
Clay
Matrix
1800
1850

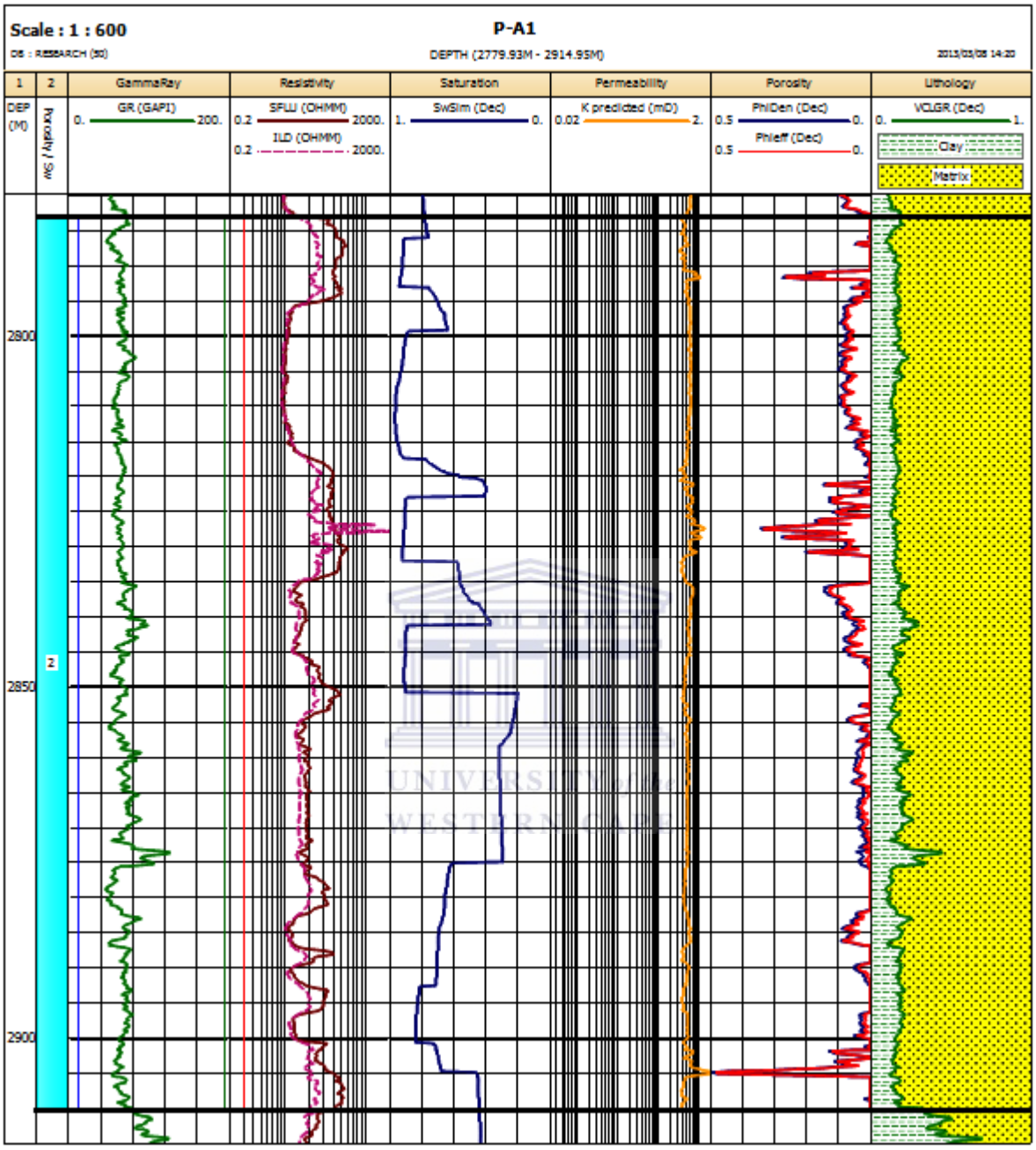

Figure 5.11: Digitized petrophysical properties, gamma-ray, resistivity wireline logs and lithology models of well P-A1 reservoir zones 1 and 2.

5.3.4. Reservoir zones of well P-F1

Well P-F1 was drilled through a succession of shallow-marine shelf complex consisting of sandstones deposited within the southern Orange Basin. Two potential reservoir zones were delineated: Zone 1 corresponding to a shallow-marine clean sandstone formation interbedded with thin claystones (figure 5.12) deposited during the Late Aptian, while zone 2 is a marine shaly sandstone formation of Middle-Aptian age.

Formation water resistivity was calculated from resistivity mud filtrate $Rmf_1 = 0.14\ \Omega$ and $Rmf_2 = 0.17\ \Omega$ at $T_1 = 39.8^{o}c$ and $T_2 = 42.2^{o}c$. The resulted average water resistivity $Rw_1 = 0.06\ \Omega$ and $Rw_2 = 0.08\ \Omega$ deduced from equation (26) were then used to estimate fluid saturation.

The neutron-density porosity method was used to determine the porosity of well P-F1 because it was the most suitable method and the only consistent tool run through the well.

Table 5.15: Result of the pay parameters used to characterize the quality of reservoir zones within well P-F1.

RESERVOIR	TOP	BOTTOM	Gross	Net	Net/Gross	Av Phi	Av Sw	Av Vsh
ZONE 1	1284.0	1335.0	51.0	0.0	0.0	26.2	89.6	10.5
ZONE 2	1378.0	1400.0	22.0	0.0	0.0	25.5	90.1	12.0

Table 5.15 summarizes the computed result of petrophysical properties of well P-F1 reservoir intervals. They display zero net pay intervals and high water saturation average values.

In conclusion, no net pay zones were identified from the corroboration of reference petrophysical properties of reservoir zones of each well with predefined cut-off values.

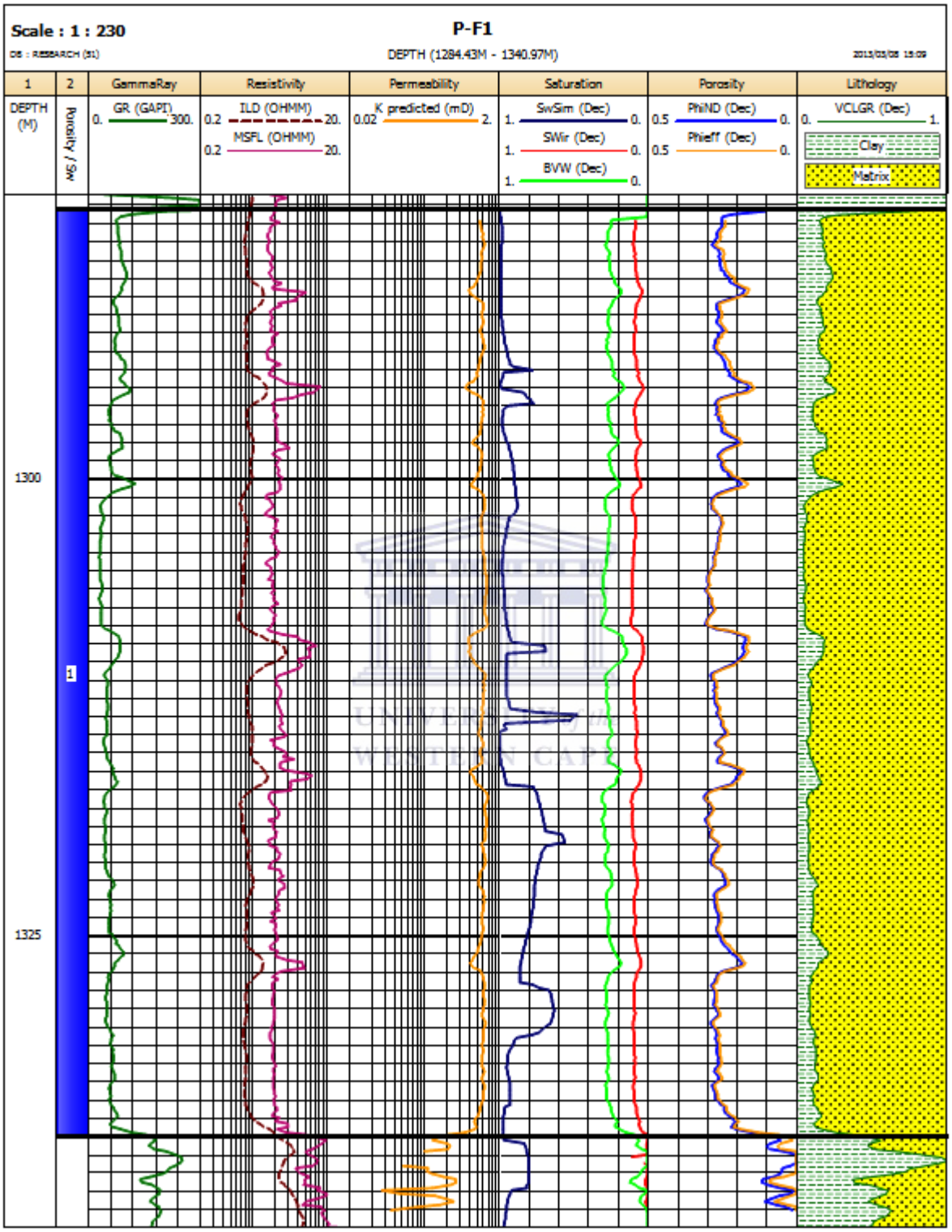
Scale : 1 : 230
P-F1
DEPTH (1284.43M - 1340.97M)
1
2
GammaRay
Resistivity
Permeability
Saturation
Porosity
Lithology
DEPTH (M)
Porosity / Sw
GR (GAPI)
0.
300.
ILD (OHMM)
MSFL (OHMM)
0.2
20.
K predicted (mD)
0.02
2.
SwSim (Dec)
SWir (Dec)
BVW (Dec)
1.
0.
PhiND (Dec)
Phieff (Dec)
0.5
VCLGR (Dec)
Clay
Matrix
1300
1325

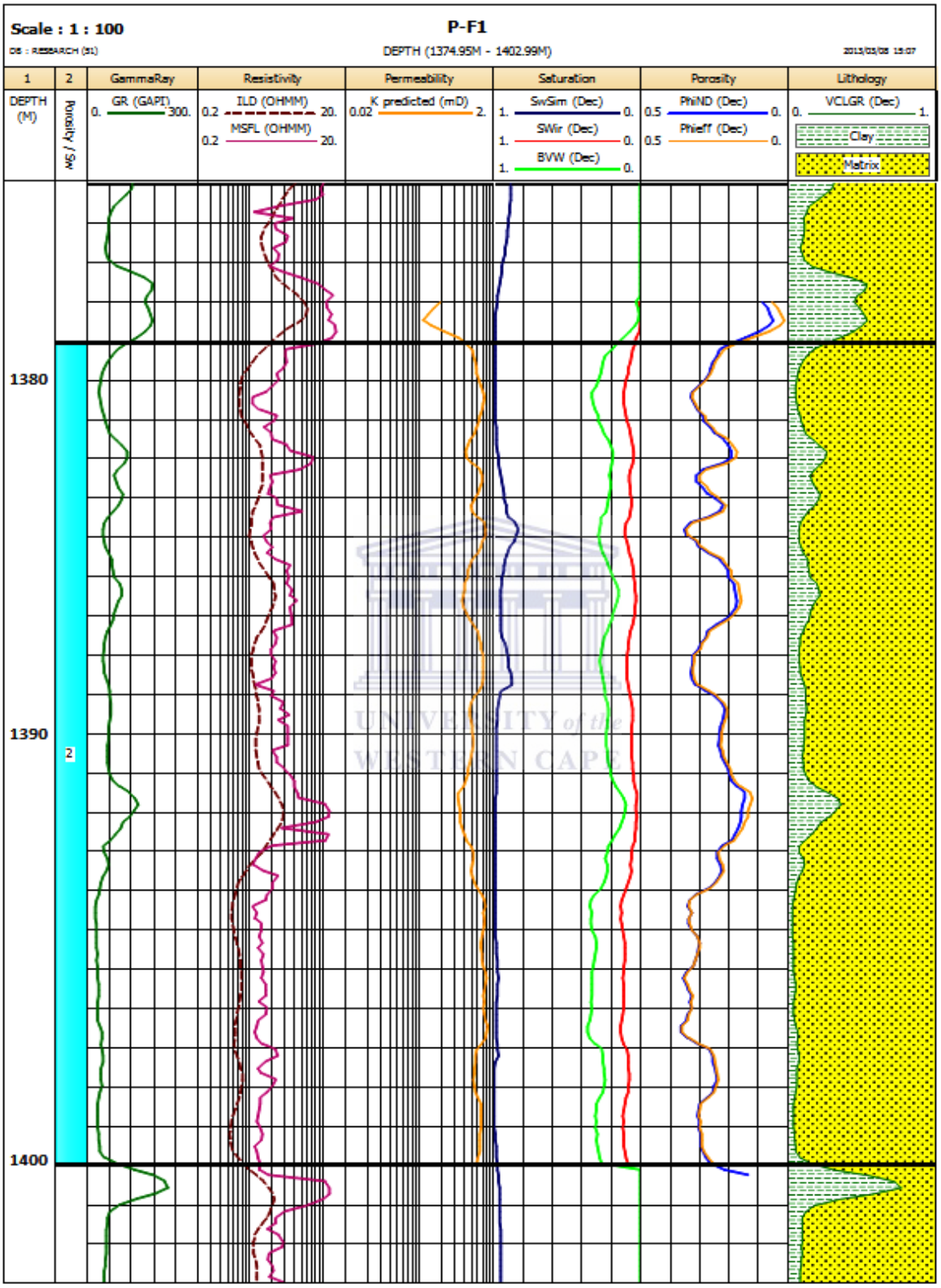

Figure 5.12: Digitized petrophysical properties, gamma-ray, resistivity wireline logs and lithology models of well P-F1 reservoir zones 1 and 2.

CHAPTER 6: CONCLUSIONS

Extensive petrophysical evaluation of four wells within Cretaceous gas-bearing sandstone reservoirs along blocks 4 and 5 in the Orange Basin has been carried out in this research, within the limit of the amount and quality of data available. Necessary editing and corrections have been applied to resolve errors related to environment and depth shifting. Though some previous studies have been conducted within the area; no detailed petrophysical evaluation was done before. Therefore, it is hoped that this report will help for future explorations in the field. The study was organized in three main sections which are: (1) formation evaluation, (2) interpretation of reservoirs lithology based on wireline logs and (3) determination of petrophysical properties of reservoir rocks.

- The first section summarizes the physical properties of rocks, the principles and uses of wireline logs. The geophysical wireline logs were classified based on their usage or their operational principle. The first group helps to determine physical and chemical properties of reservoir rocks; this includes porosity logs (sonic, density and neutron), lithology logs (gamma-ray and spontaneous potential), resistivity logs (induction, laterolog and microresistivity) and auxiliary logs (caliper, dipmeter). The second group is based on the method of measurement and corresponds to electrical logs (spontaneous potential and resistivity), radioactive or nuclear logs (gamma-ray, neutron and density) and acoustic logs (sonic).

- The second section focuses on the reservoir zones lithology of studied wells. This part of the research consisted of evaluating the type of rocks (clean or tight sandstones) forming the reservoir intervals and their distribution in order to quantify gross zones, by relating the behavior of wireline logs signature based on horizontal routine. Extensively, a vertical routine was used to estimate their lateral distribution by correlating the gamma-ray logs of the corresponding wells, but also to identify their depositional environments (shallow to deep marine).

- The last section deals with the petrophysical evaluation of the identified potential reservoirs. Eight parameters were calculated and three of them were used as reference for reservoir characterization. The volume of shale was estimated in all the wells using the corrected Steiber method because it rectifies gamma-ray reading errors. Density porosity was performed in wells O-A1 and P-A1, while sonic porosity was applied in well A-N1 and neutron-density porosity in well P-F1 with the purpose of having reasonable results. Equation (26) was used to determine formation water resistivity, and water saturation was calculated based on the Simandoux relationship with Crain's recommended parameters. Furthermore, a predicted permeability function was derived from the crossplot of core porosity against core permeability, and matched best with the core permeability of well O-A1. This function was also used to predict permeability in the other wells.

As a result, average volumes of shale 12.7%, 24.9%, 13.8% and 11.7% were determined respectively for wells O-A1, A-N1, P-A1 and P-f1, showing a decrease from the west of the field towards the east; while average porosities increase from the south-west through the east with the following average values: 6.15%, 11.8%, 12.6% and 25.8% respectively corresponding to wells O-A1, A-N1, P-A1 and P-F1. Likewise average water saturations increase from well O-A1, toward wells A-N1 and P-F1 with respective values 76.7%, 84.5% and 89.5%, despite the abnormal value 71.7% of well P-A1.

Subsequently, a cut-off value was applied to the reference parameters with the aim of determining net pay zones. The parameters and cut-offs selected were respectively: volume of shale less than 40.0%, porosity more than 7.0% and water saturation less than 65.0%. Despite a good volume of shale content, a satisfactory porosity and the presence of hydrocarbon traces in wells O-A1 and A-N1 according to the well reports, no pay zone was identified.

In view of deductions made above, the following suggestions need to be considered:

- Basic core analysis of reservoir zones of wells A-N1, P-A1 and P-F1 needs to be done to confirm the results of this study.

- A fluid flow modeling along the study area, based on the interpretation of seismic data ran in the field and integrated with the results of this report.
- Additional exploration wells are required to understand the extent of Late Aptian gas-bearing sandstone reservoirs between wells O-A1 and A-N1.

REFERENCES

Archie, G. E., (1942): The Electrical resistivity log as an aid in determining some reservoir characteristics. Transaction of AIME 146; 54.

Baker Hughes Inteq, (1992): Advanced Wireline & MWD Procedures Manual. Technical Publication paper, number: 80459H Rev. A, procedure manual.

Bateman, R., (1985): Open-hole log analysis and formation Evaluation: Boston, International Human resources Development Corporation; 647.

Baum G. R., and Vail, P. R., (1988): Sequence stratigraphic concepts applied to Paleogene outcrops, Gulf Atlantic basins. In: sea level changes: an integrated approach. (Eds) Wilgus, C. K., Hastings, B. S., Kendall, C. G. St. C., Posamentier, H. W., Ross, C. A. and Van Wagoner, J. C. S.E.P.M Sp. Pub. 42, 309-327.

Ben-Avraham, Z., Smith, G., Reshef, M. and Jungslager, E., (2002): Gas hydrate and mud volcanoes on the southwest African continental margin off South Africa. Geology, Vol. 30, pp. 927- 930.

Broad, D.,(2004): South Africa Activities and Opportunities, an unpublished Power Point Presentation to PetroChina.

Broad, D.S., Jungslager, E.H.A., McLachlan, I.R., Roux, J., (2006): Offshore Mesozoic Basins. In: Johnson, M.R., Anhaeusser, C.R., Thomas, R.J. (Eds.), The Geology of South Africa. Geological Society of South Africa, Johannesburg/Council for Geosciences, Pretoria, pp. 553–571.

Broad, D. S. and Mills, S. R. (1993): South Africa offers exploratory potential in variety of basins: Oil & Gas Journal, vol. 91, (December 6, 1993), p. 38–44.

Brown, L. F, Jr., Benson, J.M., Brink, G.J., Doherty, S., Jollands, A., Jungslager, E.H.A.,Keenan, J.H.G, Muntingh, A., & Van Wyk, N.J.S., (1995): Sequence stratigraphy in offshore South African divergent basins. An Atlas on Exploration for Cretaceous Lowstand traps. Tulsa, Oklahoma: In American Association of Petroleum Geologists, Studies in Geology, vol. 14, pp. 0-183.

Brown, L.F., Brown, L.F, Jr., Benson, J.M., Brink, G.J., Doherty, S., Jollands, A., Jungslager, E.H.A., Keenan, J.H.G., Muntingh, A., Van Wyk, N.J.S., (1996): Sequence stratigraphy in offshore South Africa divergent basins. An atlas on exploration for cretaceous lowstand traps by SOEKOR (Pty) Ltd. American Association of Petroleum Geologists (AAPG) Studies in Geology, vol. 41, pp. 0-184.

Catuneanu, O., (2002): Sequence stratigraphy of clastic systems: concepts, merits,and pitfalls, Journal of African Earth Sciences, Volume 35, Issue 1, pp. 1-43.

Clavier, C., Huyle W. R., Meunier D., (1971): Quantitative Interpretation of T.D.T Logs; Part 1 and 11, Journal of Petroleum Technology, No. 6.

Crain, E.R., (2004): Crain's Petrophysical Handbook: Canada, Spectrum 2000 Mindware, 3rd Millennium Edition. URL: http://www.spec2000.net/lcmain.htm.

Demaison, G. and Huizinga, B. J., (1994): Genetic classification of petroleum systems using three factors: charge, migration and entrapment, In: Magoon, L. B. and Dow, W. G., (Eds.) the petroleum system from source to trap: AAPG memoir 60, pp. 73-89.

De Wit, M.J., and Ransome, I.G.D., (Eds.) (1992): Inversion Tectonics of the Cape Fold Belt, Karoo and Cretaceous Basins of Southern Africa. Proc. Conf. of Inversion Tect. of the Cape Fold Belt, Cape Town, 2-6 Dec. 1991. A.A. Balkema, Rotterdam/Brookfield, 266.

De Wit, M.J, Stankiewicz, J., (2007): Restoring Pan African-Brasiliano connections: more Gondwana control, less Trans-Atlantic corruption, EGU 2007-A-06500, Vienna, Austria.

Dingle, R.V, Siesser, W. G., and Newton, A.R., (1983): Mesozoic and Tertiary Geology of Southern African. A.A. Balkema/Rotterdam. pp. 99-106.

Dresser Atlas (1979): Log Interpretation Charts; Houston, Dresser Industries Inc.

Dresser Atlas (1982): Well logging and interpretation techniques. The course for home study. Dresser Atlas Publication.

Ellis, D., and Singer, J.M., (2008): Well logging for Earth Scientists, 2nd edition. Springer, Dordrecht, 699p.

George, C. J., Stiles,L. H., (1978): Improve techniques for evaluating carbonate waterfloods in West Texas, Journal of Petroleum Technology, vol 30, no 6; 1547 -1554.

Gerald, I., and Smith, G. C., (1982): Post-Paleozoic Succession and structure of the South Western African continental margin: Rifted Margins: Field Investigations of Margin Structure and Stratigraphy. In: Studies in Continental Margin Geology. AAPG Special volumes, A110, pp. 49-74.

Hirsch, K. K., Scheck-Wenderoth, M., van Wees, J.-D., Kuhlmann, G. (2010): Tectonic subsidence history and thermal evolution of the Orange Basin. - Marine and Petroleum Geology, Vol.27, issue 3, pp. 565-584.

Juhasz, I., (1990): core analysis opportunity and challenges in the 1990's. Europe core analysis symposium, pp. 1-15.

Jikelo, N. A., (1999): The natural gas resources of southern Africa: Journal of African Sciences, 31(1), 34.

Jungslager, E. H. A., (1999): Petroleum habitats of the Atlantic margin of South Africa. Special publications, Geological Society: Oil and Gas Habitats of the South Atlantic, pp. 153-168.

Leeder, M. R., and Gawthorpe, R. L., (1987): Sedimentary models for extensional tilt-block/half graben basins. Special Publication, geological society. Vol.28, pp. 139-152.

Levorsen, A. I., (1967): The geology of petroleum. Freeman, San Francisco, second edition, 724p.

Macdonald, D., Gomez-Pereza, I., Franzeseb, J., Spallettib, L., Lawverc, L., Gahaganc, L., Dalzielc, I., Thomasd, C., Trewind, N., Holed, M., and Patona, D., (2003): Mesozoic break-up of SW Gondwana: implications for regional hydrocarbon potential of the southern South Atlantic. Marine and Petroleum Geology, vol. 20, pp. 287 – 308.

Morris, R. L., and Biggs, W. P., (1967): Using log derived values of water saturation and Porosity. Trans; SPWLA, Annual logging Symposium.

Muntingh, A. (1993): Geology, prospect in Orange Basin offshore western South Africa: Oil and Journal, January 25 P. pp. 106 – 108.

Muntingh, A. and Brown Jr., F. L., (1993): Sequence Stratigraphy of Petroleum Plays, Post Rift Cretaceous Rocks (Lower Aptian to Upper Maastrichtian) Orange Basin, Western Offshore, South Africa. In: Weimer, P., and Posamentier, H., (editors), Siliciclastic Sequence Stratigraphy, Recent Developments and Applications. AAPG memoir 58, pp. 71 – 98.

Norman, J. H., (1991): Dictionary of Petroleum exploration, drilling and production. Penn Well publishing company, 107p.

Nummedal, D., and Swift D. J. P., (1987): Transgressive stratigraphy at sequence bounding unconformities: some principles derived from Holocene and Cretaceous examples. In: sea level

fluctuations and coastal evolution. (Eds) Nummedal, D., Pilkey, O.H. and Howard. J.D. soc. Econ. Paleontol. Mineral. Spec. Pub. 41, 241-260.

Opuwari, M., (2010): Petrophysical evaluation of the Albian age gas bearing Sandstone reservoirs of the o-m field, orange Basin, South Africa. Unpublished Phd thesis. University of Western Cape, South Africa.

Paton, D.A., Di Primio, R., Kuhlmann, G., Van der Spuy, D. and Horsfield, B., (2007): Insights into the Petroleum System Evolution of the southern Orange Basin, South Africa. South African Journal of Geology, Geological Society of South Africa, Volume 110, pp. 261-274.

Petroleum Agency of South Africa (PASA), (2003a/2004/2006/2007/2008): Exploration Opportunities in the Deepwater Orange Basin, off the West Coast of South Africa. Petroleum Agency of South Africa online brochure: www.petroleumagencysa.com.

Petroleum Agency of South Africa (PASA), (2010): Petroleum Exploration in South Africa Information and Opportunities. Petroleum Agency of South Africa online brochure. Url: http://www.petroleumagencysa.com/files/PetExplOpp2010web.pdf.

PetroSA Report (2003): Ibhubesi field Geological Evaluation Orange Basin, Block 2 South Africa.

Poupon, A., and Leveaux, J., (1971): Evaluation of water saturation in shaly formations; Trans. SPWLA 12th Annual Logging Symposium; 2.

Rider, M. H., (1996): The geological interpretation of well logs, 2nd edition. Rider – French consulting limited, 280p.

Schlager, W., (1992): Sedimentological and Sequence Stratigraphy of Reef and Carbonate Platform: American Association of Petroleum Geologists Cont. Educ. Course Note Ser., 34, 71.

Schlumberger (1972): Log interpretation principles, volume I, Schlumberger Ltd.

Schlumberger (2002): Schlumberger Oil Field Glossary: Where the Oil Field
Meets the Dictionary. URL: http://www.glossary.oilfield.slb.com.

Selley, R. C., (1998): Elements of petroleum geology, 2nd edition. Academic press, California, 497p.

Serra, O., (1984): Fundamentals of Well Log Interpretation (Vol. 1): The Acquisition of Logging Data: Dev. Pet. Sci., 15A: Amsterdam (Elsevier).

Serra, O., and Sulpice L., (1975): Sedimentological analysis of sand shale series from well logs. SPWLA 16th Ann. Symp. Trans., paper W. 1-23.

Simandoux, P., (1963): Dielectric Measurements on Porous Media: Application to measurement of water saturation. Study of the behaviour of argillaceous formation. SPWLA, Houston, vol.2; 97-124.

Sindouir, G., and Duguiol, S. J., (1990): Laboratory induced damage – A review of the problem: European core analysis symposium, pp. 95-109.

Steiber, R. G., (1973): Optimization of Shale Volumes in Open Hole Logs. Journal of Petroleum Technology.

Timur, A., (1968): An investigation of Permeability, Porosity, and Residual water Saturation Relationships for Sandstone Reservoirs. Log Analyst, 9, 4; 8-17.

Vail, P. R., Mitchum, R. M., Thomsom, S. III., (1977): Seismic stratigraphy and global changes in sea level, part 3: relative change of sea level from coastal onlap. In: seismic stratigraphy-

application to hydrocarbons exploration. (Ed) payton C.E. bull. Amer. Assoc. pet. Geol. Mem. Vol.26. pp.63-97.

Van der Spuy, D., (2003): Aptian source rocks in some South African Cretaceous basins. In: Arthur, T.J., MacGregor, D.S & Cameron, N.R. (Eds.), Petroleum Geology of Africa: New Themes and Developing Technologies. Geol. Soc., London, Spec. Publ. The Geological Society of London.

Van der Spuy, D., (2005): Prospectivity of the Northern Orange Basin, Offshore South Africa. In 18th World Petroleum Congress.

Van Wagoner, J.C., Mitchum Jr., R.M., Campion, K.M., Rahmanian, V.D., (1990): Siliciclastic sequence stratigraphy in well logs, core, and outcrops: concepts for high-resolution correlation of time and facies. American Association of Petroleum Geologists Methods in Exploration Series 7, pp. 55.

Winsauer, W. O., and McCardell, W. M. (1953): Ionic double layer conductivity in reservoir rocks. Transactions of AIME,vol 198,p.129.

Worthington, P. F., Cosentino (2005): The role of Cut-Offs in Integrated Reservoir Studies. SPE Reservoir Evaluation and Engineering (4). SPE 84387.

Wyllie, M. R. J., Gregory, A. R., Gardner, G. H. F., (1958): An experimental Investigation of factors affecting elastic wave velocities in porous media. Geophysics, vol.23.

Wyllie, M. R. J., Rose, W. D., (1950): Some theoretical considerations related to the Quantitative Evaluation of Physical Characteristics of reservoir Rock from Electrical log Data. Trans; AIME, 189.

Related websites

www.globalsecurity.org/military/library/policy/army/fm/5-484/ch11.htmfig111.1.

http://www.aegis-instruments.com/images/prod`ucts/sonic.jpg.

APPENDICES

Appendix A: Lithology interpretation of reservoir zones within respective wells**.**

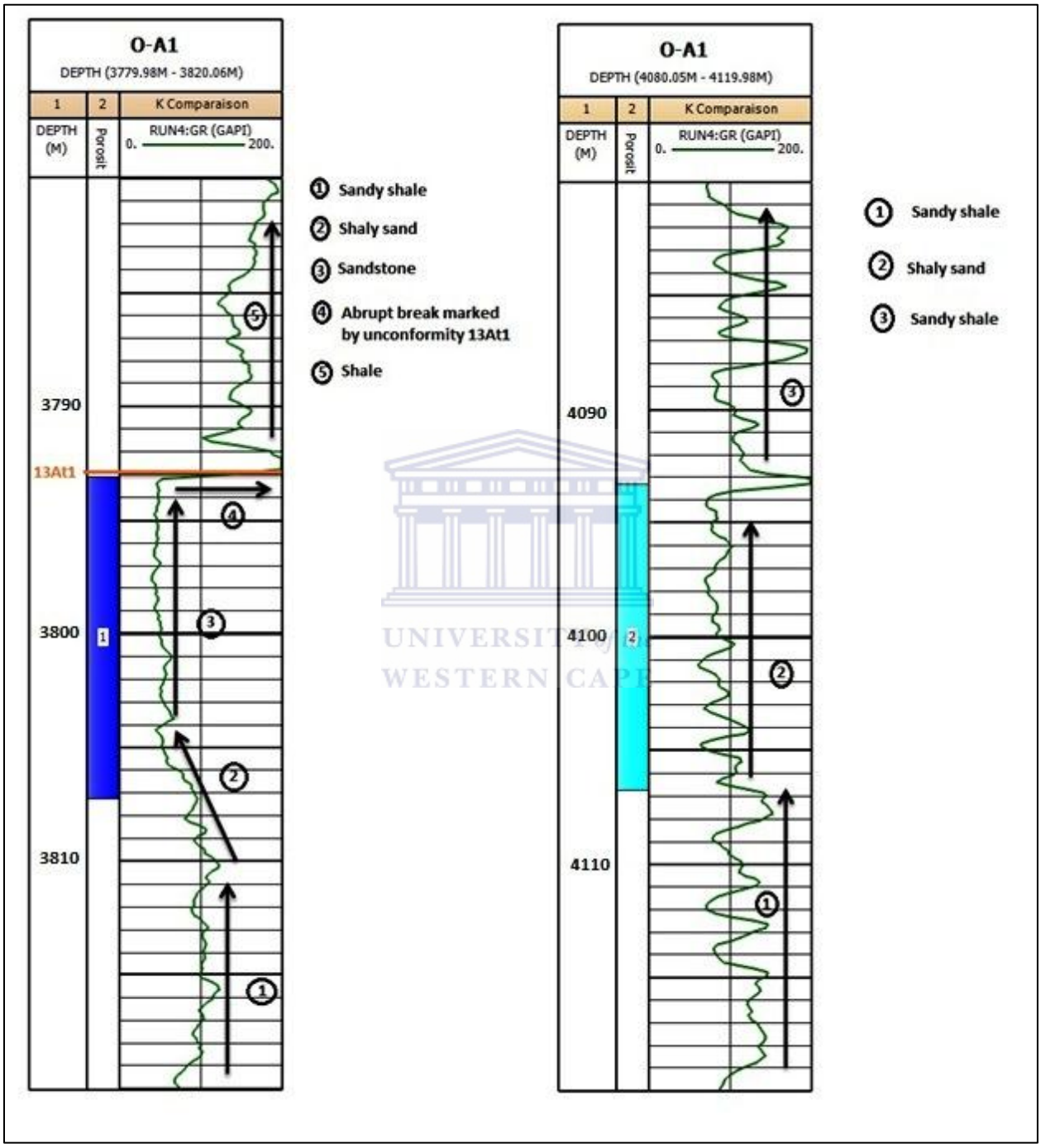

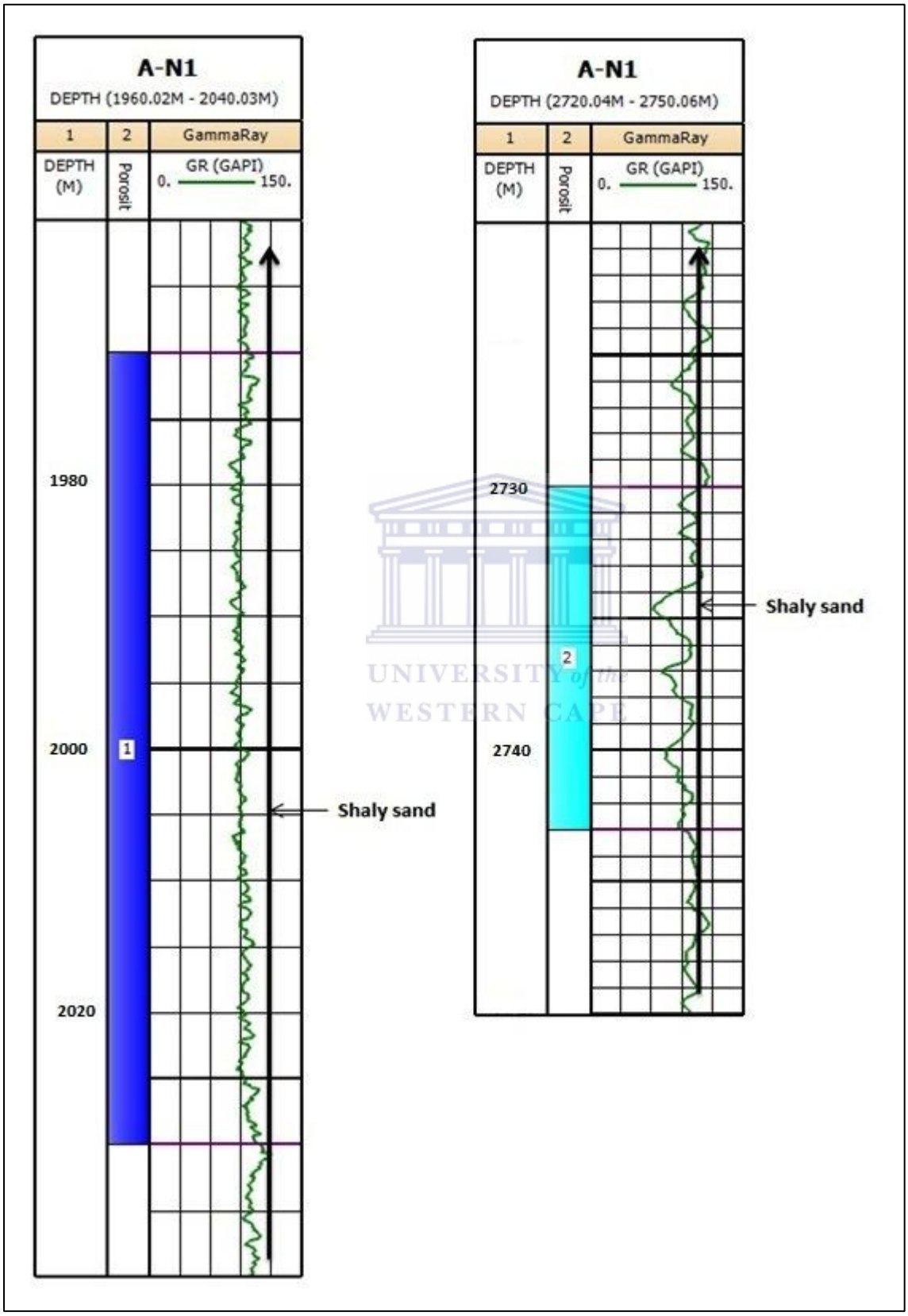

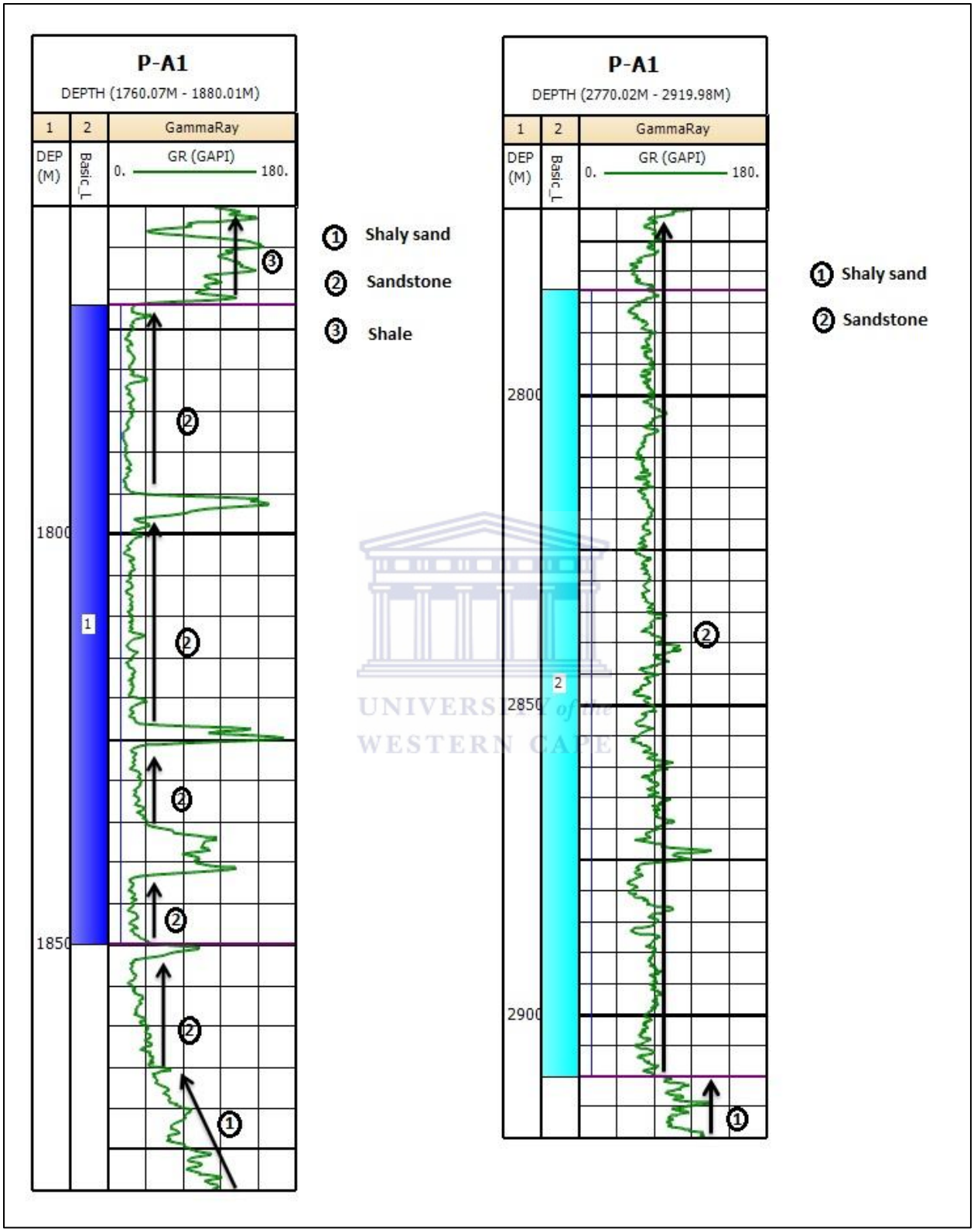

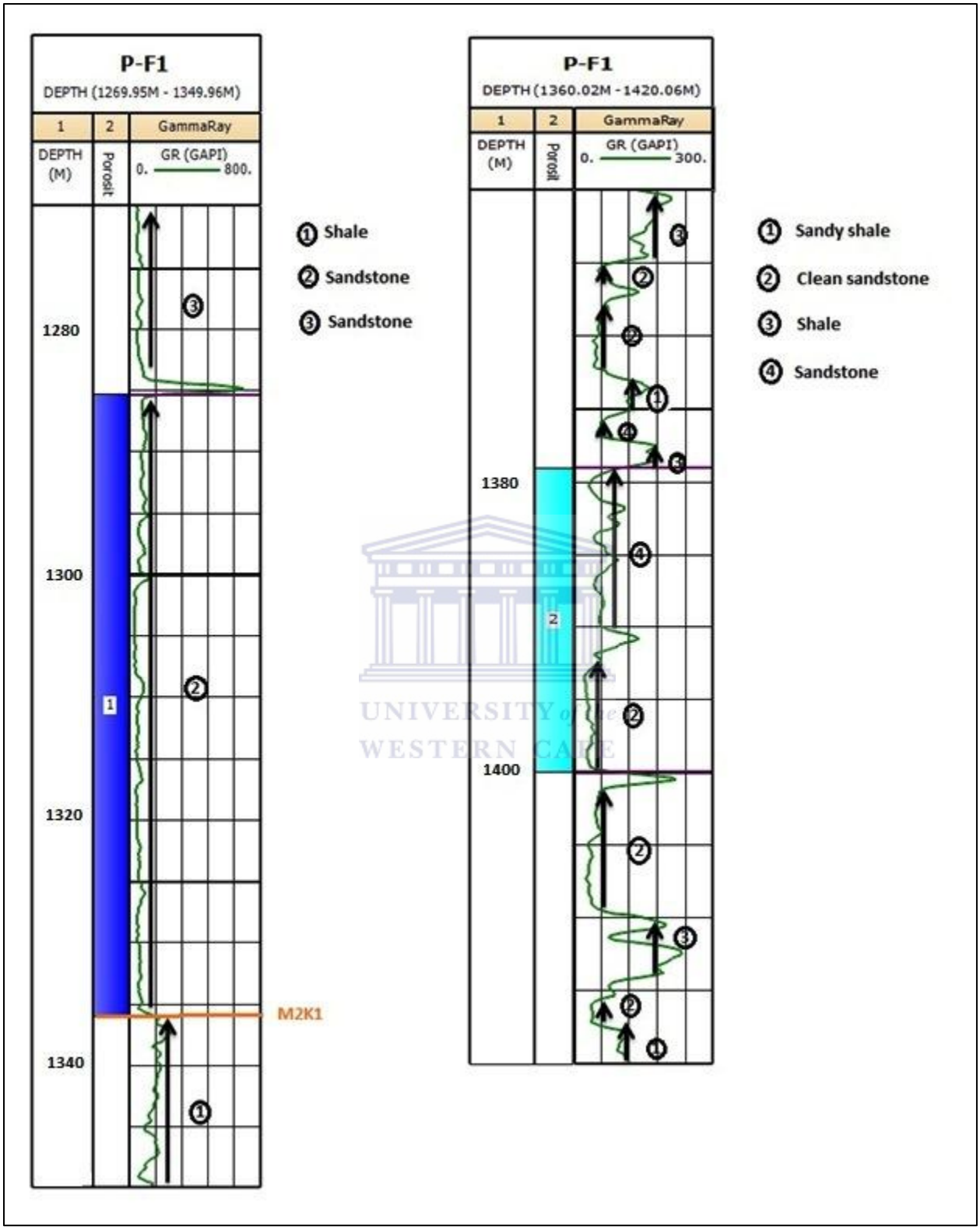

Appendix B: Clay parameters determination**.**